

12-14-2015

Vulnerable Species in a Changing Climate: The Genomic Response of Antarctic Notothenioid Fishes to Predicted Oceanic Conditions as a Model of Physiological Plasticity and Adaptive Capability

Troy James Huth

University of South Carolina - Columbia

Follow this and additional works at: <http://scholarcommons.sc.edu/etd>



Part of the [Biology Commons](#)

Recommended Citation

Huth, T. J. (2015). *Vulnerable Species in a Changing Climate: The Genomic Response of Antarctic Notothenioid Fishes to Predicted Oceanic Conditions as a Model of Physiological Plasticity and Adaptive Capability*. (Doctoral dissertation). Retrieved from <http://scholarcommons.sc.edu/etd/3218>

This Open Access Dissertation is brought to you for free and open access by Scholar Commons. It has been accepted for inclusion in Theses and Dissertations by an authorized administrator of Scholar Commons. For more information, please contact SCHOLARC@mailbox.sc.edu.

VULNERABLE SPECIES IN A CHANGING CLIMATE: THE GENOMIC RESPONSE
OF ANTARCTIC NOTOTHENIOID FISHES TO PREDICTED OCEANIC
CONDITIONS AS A MODEL OF PHYSIOLOGICAL PLASTICITY AND ADAPTIVE
CAPABILITY.

by

Troy James Huth

Bachelor of Science
University of South Carolina, 2006

Master of Science
University of South Carolina, 2008

Submitted in Partial Fulfillment of the Requirements

For the Degree of Doctor of Philosophy in

Biological Sciences

College of Arts and Sciences

University of South Carolina

2015

Accepted by:

Jeffrey L. Dudycha, Major Professor

Roger H. Sawyer, Committee Member

Sean P. Place, Committee Member

W. Joe Jones, Committee Member

Joseph M. Quattro, Committee Member

Lacy Ford, Senior Vice Provost and Dean of Graduate Studies

© Copyright by Troy James Huth, 2015

All Rights Reserved.

DEDICATION

For Emily, Aiden and Quinn: for all the times my focus was pulled away; if I had a thousand lives to repay you, I still could not; and if we had a million lives together, it would never be enough.

ACKNOWLEDGEMENTS

To the members of my committee: I would like to thank: my advisor Dr. Jeff Dudycha for inviting me into his lab when I was without a home and providing me guidance on all things, even those not concerning *Daphnia*; Dr. Sean Place, for giving me the chance to continue my graduate education and continuing to work with me from across the country; Dr. Roger Sawyer, for providing me a start to my graduate studies so many years ago; and Dr. Joe Quattro and Dr. Joe Jones, for their time, effort and counsel throughout my program.

To my colleagues: I would like to thank all my fellow graduate students and researchers whom are too numerous to name here, whose efforts were invaluable to my growth as a researcher and a person. Particularly all those that ventured to the bottom of the earth to collect, experiment, and bring back the notothenioid samples that were critical to my research. Without this extraordinary effort none of this would have been possible.

Lastly to my family: To my sisters and parents, thanks for entertaining my nerdy ways through my younger years and providing a fertile environment in which to thrive. To my wife, who endured the summers of Columbia and a seemingly eternal graduate student life, thank you for seeing this through to the end, and it did end! And to my children, for their much welcomed distraction from the persistent demands of my dissertation, know that so long as you give your all nothing is ever out of reach.

ABSTRACT

In its fifth report in 2014 the IPCC reinforced the contribution of anthropogenic CO₂ to global climate change predicting widespread and significant changes to the global climate over a relatively short time scale. The polar regions, including the Southern Ocean surrounding Antarctica, were identified as ecosystems that may experience the most rapid and severe changes. As the Southern Ocean is one of the coldest and most oceanographically stable regions on earth, the endemic fauna likely have no alternative habitats available for migration. Further compounding the challenge these species will face is the substantial degree of adaptation to the extreme cold and oxygen rich waters that may render these species particularly vulnerable to increasing temperatures and *p*CO₂.

The Perciform fishes of the suborder Notothenioidei dominate the fauna of the Southern Ocean. These fish have been relatively well studied under heat stress conditions, but only recently have research efforts begun to discern the potentially compounding effects of the multiple stressors, notably increased temperature and *p*CO₂. This effort set out to analyze the genomic response of these fish to increased water temperature (4°C) and increased *p*CO₂ levels (1000 µatm), and in doing so create a wealth of sequence data to serve as the foundation for future research efforts for three notothenioid species *Trematomus bernacchii*, *Pagothenia borchgrevinki* and *Trematomus newnesi*.

By analyzing changes in gene expression under the multi-stressor condition on the transcriptomic, pathway and gene level, I was able to draw insight into the physiological

plasticity and potential adaptability of these fish to changing climate conditions in the Southern Ocean. While all three species demonstrated a widespread and substantial response to the multi-stressor condition, these responses varied in timing, duration, intensity of response, and the biological pathways driving the response. *T. bernacchii* demonstrated a rapid and robust response that quickly returned to basal levels, *P. borchgrevinki* exhibited a more moderated response that persisted throughout all time periods, whereas *T. newnesi* exhibited the least dramatic response of the three. By further dissecting the details of each response I was able to suggest potential strengths and weakness within each species and discuss the potential impact on each species' long term survivability.

TABLE OF CONTENTS

DEDICATION	iii
ACKNOWLEDGEMENTS.....	iv
ABSTRACT	v
LIST OF TABLES	viii
LIST OF FIGURES	ix
INTRODUCTION	1
CHAPTER 1. <i>DE NOVO</i> ASSEMBLY AND CHARACTERIZATION OF TISSUE SPECIFIC TRANSCRIPTOMES IN THE EMERALD NOTOTHEN, <i>TREMATOMUS BERNACCHII</i>	5
CHAPTER 2. TRANSCRIPTOME WIDE ANALYSES REVEAL A SUSTAINED CELLULAR STRESS RESPONSE IN THE GILL TISSUE OF <i>TREMATOMUS BERNACCHII</i> AFTER LONG TERM ACCLIMATION TO MULTIPLE STRESSORS.....	40
CHAPTER 3. RNA-SEQ REVEALS A DIMINISHED ACCLIMATION RESPONSE TO THE COMBINED EFFECTS OF OCEAN ACIDIFICATION AND ELEVATED SEAWATER TEMPERATURE IN <i>PAGO THENIA BORCHGREVINKI</i>	79
CHAPTER 4. GENOME WIDE EXPRESSION ANALYSIS OF THE DUSKY ROCKCOD <i>TREMATOMUS NEWNESI</i> , DEMONSTRATES A PARADOXICAL RESPONSE TO OCEAN ACIDIFICATION AND INCREASING SEA SURFACE TEMPERATURES	110
CHAPTER 5. A BRIEF COMPARATIVE ANALYSIS OF THE DIFFERENTIAL GENE EXPRESSION OF <i>T. BERNACCHII</i> , <i>P. BORCHGREVINKI</i> AND <i>T. NEWNESI</i> UNDER THE MULTI-STRESSOR CONDITION	140
REFERENCES	151
APPENDIX A: PERMISSION TO REPRINT CHAPTER 1	168

LIST OF TABLES

Table 1.1 Read Sequencing and <i>de novo</i> Assembly Statistics.....	32
Table 1.2 <i>T. bernacchii</i> Unigene BLAST Comparison against 9 Teleost Fish.....	32
Table 2.1: A summary of major gene ontology groups demonstrating differential gene expression at the 7d, 28d, and 56d time-points of the multi-stressor condition	69
Table 3.1: <i>Pagothenia borchgrevinki</i> transcriptome assembly statistics.....	103
Table 3.2: <i>Pagothenia borchgrevinki</i> transcriptome annotation statistics.....	103
Table 3.1 Selection differentials (s) and selection gradients (β) for the correlated phenotypic traits, natural logarithm transformed body length and eye diameter.	52
Table 4.1 <i>Trematomus newnesi</i> transcriptome assembly statistics: Statistics for the filtered <i>de novo</i> assembly were computed on the transcript and gene level. The # of sequences of the transcript level represent all surviving contiguous sequences, the # of sequences on the gene level represent the number of putative genes surviving based upon groupings of homologous transcripts.....	135
Table 4.2: <i>Trematomus newnesi</i> transcriptome annotation statistics: Statistics for the filtered <i>de novo</i> assembly were computed on the transcript and gene level. The # of sequences of the transcript level represent all surviving contiguous sequences, the # of sequences on the gene level represent the number of putative genes surviving based upon groupings of homologous transcripts.....	135
Table 4.3 Pathway up- and down-regulation at each time-point: The total number of genes expressed in the up- and down-regulated sub-groups for each multi-stressor time point ($FDR \leq 0.05$) including genes associated with the gene ontology terms carbohydrate metabolic process (GO:0005975), lipid metabolic process (GO:0006629), cell death (GO:0008219), cell proliferation (GO:0008283), response to stress (GO:0006950), immune system process (GO:0002376), homeostatic process (GO:0042592), transcription (GO:0006351), translation (GO:0006412), and genes with BLAST results including heat shock related proteins. Total indicates the total number of genes of that particular category found in the reference transcriptome library as a whole.	136

LIST OF FIGURES

Figure 1.1 *De novo* assembly unigene length distribution. Length distribution of unigene sequence obtained from the de novo assembly. The unigenes are grouped from shortest to longest with each column representing the number of unigenes of that specific length. ...33

Figure 1.2 BLAST results: *T. bernacchii* protein sequences vs. unigene sequences. The percent identity of each known *T. bernacchii* full or partial protein sequence versus a unigene from the assembled transcriptome. 299 of 303 query sequences of known *T. bernacchii* protein sequences matched a unigene with an *e*-value cutoff of 10^{-10} , and of those 184 matched a unigene at greater than 95% identity.....34

Figure 1.3 Tissue specific GO comparison. Unigenes expressed in at least one treatment were included in the gene ontology analysis. GO terms were determined using BLAST2GO with an *e*-value cut off of 10^{-5} , a minimum sequence filter of 25, and sorted based on level 2 GO classifications. Any GO term that met the filter for the minimum number of sequences to include as a node ($n = 25$) was included in the comparison.35

Figure 1.4 Tissue specific enzyme code distribution of *T. bernacchii*. The stacked columns represent the number of annotated transcripts obtained from each tissue whose function could be classified by a specific enzyme code. As a comparison, the total number of enzyme codes identified in the fully assembled transcriptome is provided on the left column. The main enzyme classes included in this analysis were oxidoreductases (black bar), transferases (grey), hydrolases (blue), lysases (orange), isomerases (green) and ligases (red). Enzyme codes were determined using BLAST2GO with an *e*-value cut off of 10^{-5}36

Figure 1.5 Categorization of *T. bernacchii* unigenes to KEGG biochemical pathways. A KEGG biochemical pathway analysis was performed on the full transcriptome and individual tissue transcriptomes using every unigenes expressed in at least one treatment. The stacked columns represent the top 15 KEGG pathways found in the full transcriptome and their distribution in each tissue, using an *e*-value cut off of 10^{-5} and minimum pathway assignment cutoff of 30.37

Figure 1.6 Heatmap of the relative changes in unigene abundance across treatments. Unigenes expressed in at least one treatment and featuring GO annotation were included in the feature clustering via Pearson correlation using average linkage. A deep blue color represents baseline (control) expression across the full transcriptome. Bright yellow color represents a minimum of 3-fold up-regulation of expression in one of the treatments in comparison to the baseline. Tissue specific expression profiles were generated by pooling RNA from all individuals within a thermal acclimation treatment ($n=5$ fish) prior to creation of the double-stranded cDNA libraries.38

Figure 1.7 Differential expression of heat shock protein families in *T. bernacchii*. Relative fold-change in expression of annotated HSPs in +4 °C acclimated fish compared to control fish were obtained from the RNAseq analysis and directly compared across liver (grey), gill (blue) and brain (red). HSPs were grouped by gene family and the relative fold-change computed by averaging the change in expression of gene family constituents.39

Figure 1.8 Differential expression of redox regulator proteins in *T. bernacchii*. Relative fold-change in expression of annotated redox regulator proteins in +4 °C acclimated fish compared to control fish were obtained from the RNAseq analysis and directly compared across liver (grey), gill (blue) and brain (red). Redox proteins were grouped by gene family and the relative fold-change computed by averaging the change in expression of gene family constituents.40

Figure 2.1 Transcriptome wide sample similarity matrix and cluster dendrogram: the sample similarity matrix represents the cumulative similarity of each individual at each time-point as a reflection of transcriptome wide gene expression. Transcriptome wide expression is represented by all gene products that demonstrated an FDR ≤ 0.05 during the differential gene expression analysis. Portions of the matrix shown in yellow demonstrate a high degree of similarity in the transcriptomic expression profiles between the two samples, with a value of 1 indicating the samples are identical; whereas those shown in grey demonstrate a lower degree of similarity, with a value of 0.65 demonstrating the most dissimilar expression profiles between two samples. As the samples are extracted from the same tissue and species, the degree of similarity in this case is a minimum of 0.65. The cluster dendrogram also groups samples based upon similar expression profiles, with those samples grouped most closely demonstrating more analogous transcriptomic expression responses.....70

Figure 2.2 Over-representation analysis of gene ontology level 2 category molecular function: shown are gene ontology terms within the broad molecular function category (GO:0003674) that were significantly over-represented in the stressor treatments compared to the reference transcriptome as determined by a Fisher's exact test (p < 0.01, categories containing only one gene are not included for readability). Subgroups of up- and down-regulated gene cohorts were created for each stressor time-point (7d, 28d and 56d) and compared to the GO term distribution of the reference transcriptome. The number in each category represents the total number of genes within that over-expressed GO term category (blank = 0).....71

Figure 2.3 Over-representation analysis of the gene ontology level 2 category biological process: gene ontology terms within the broad biological process category (GO:0008150) that were significantly over-represented in the stressor treatments compared to the reference transcriptome as determined by a Fisher's exact test (p<0.01, categories containing only one gene are not included for readability). Subgroups of up- and down-regulated gene cohorts were created for each stressor time-point (7d, 28d and 56d) and

compared to the GO term distribution of the reference transcriptome. The number in each category represents the total number of genes within that over-expressed GO term category (blank = 0)72

Figure 2.4 Volcano plot - carbohydrate metabolic processes: this plot demonstrates differential gene expression for the 7d (diamonds/blue), 28d (circles/red), and 56 (triangles/purple) multi-stressor treatments (n = 4) as compared to the ambient control treatments (n = 4). All genes within the reference transcriptome associated with the gene ontology term carbohydrate metabolic process (GO:0005975) are included. Fold change is log₂ adjusted whereas FDR is loge adjusted. Points demonstrating both an abs(fold change) ≥ 2 and a FDR ≤ 0.05 are considered significant and colored according to treatment; whereas all other points are deemed not significant and are colored black.....73

Figure 2.5 Volcano plot – lipid metabolic process: this plot demonstrates differential gene expression for the 7d (diamonds/blue), 28d (circles/red), and 56 (triangles/purple) multi-stressor treatments (n = 4) as compared to the ambient control treatments (n = 4). All genes within the reference transcriptome associated with the gene ontology term lipid metabolic process (GO:0006629) are included. Fold change is log₂ adjusted whereas FDR is loge adjusted. Points demonstrating both an abs(fold change) ≥ 2 and a FDR ≤ 0.05 are considered significant and colored according to treatment; whereas all other points are deemed not significant and are colored black74

Figure 2.6 Volcano plot – cell death: this plot demonstrates differential gene expression for the 7d (diamonds/blue), 28d (circles/red), and 56 (triangles/purple) multi-stressor treatments (n = 4) as compared to the ambient control treatments (n = 4). All genes within the reference transcriptome associated with the gene ontology term cell death (GO:0008219) are included. Fold change is log₂ adjusted whereas FDR is loge adjusted. Points demonstrating both an abs(fold change) ≥ 2 and a FDR ≤ 0.05 are considered significant and colored according to treatment; whereas all other points are deemed not significant and are colored black75

Figure 2.7 Volcano plot – cell proliferation: this plot demonstrates differential gene expression for the 7d (diamonds/blue), 28d (circles/red), and 56 (triangles/purple) multi-stressor treatments (n = 4) as compared to the ambient control treatments (n = 4). All genes within the reference transcriptome associated with the gene ontology term cell proliferation (GO:0008283) are included. Fold change is log₂ adjusted whereas FDR is loge adjusted. Points demonstrating both an abs(fold change) ≥ 2 and a FDR ≤ 0.05 are considered significant and colored according to treatment; whereas all other points are deemed not significant and are colored black.....76

Figure 2.8 Volcano plot – response to stress: this plot demonstrates differential gene expression for the 7d (diamonds/blue), 28d (circles/red), and 56 (triangles/purple) multi-stressor treatments (n = 4) as compared to the ambient control treatments (n = 4). All genes within the reference transcriptome associated with the gene ontology term response to stress (GO:0006950) are included. Fold change is log₂ adjusted whereas FDR is loge adjusted. Points demonstrating both an abs(fold change) ≥ 2 and a FDR ≤ 0.05 are

considered significant and colored according to treatment; whereas all other points are deemed not significant and are colored black.....77

Figure 2.9 Volcano plot – immune system processes: this plot demonstrates differential gene expression for the 7d (diamonds/blue), 28d (circles/red), and 56 (triangles/purple) multi-stressor treatments (n = 4) as compared to the ambient control treatments (n = 4). All genes within the reference transcriptome associated with the gene ontology immune system process (GO:0002376) are included. Fold change is log₂ adjusted whereas FDR is loge adjusted. Points demonstrating both an abs(fold change) ≥ 2 and a FDR ≤ 0.05 are considered significant and colored according to treatment; whereas all other points are deemed not significant and are colored black.....78

Figure 2.10 Volcano plot – homeostatic process: this plot demonstrates differential gene expression for the 7d (diamonds/blue), 28d (circles/red), and 56 (triangles/purple) multi-stressor treatments (n = 4) as compared to the ambient control treatments (n = 4). All genes within the reference transcriptome associated with the gene ontology term homeostatic process (GO:0042592) are included. Fold change is log₂ adjusted whereas FDR is loge adjusted. Points demonstrating both an abs(fold change) ≥ 2 and a FDR ≤ 0.05 are considered significant and colored according to treatment; whereas all other points are deemed not significant and are colored black79

Figure 3.1 Transcriptome transcript size distribution: The length distribution (loge adjusted) of transcripts with a minimum length of 200bp resulting from de novo assembly (grey), following CD-HIT-EST transcript clustering with a percent identity requirement of 95% (blue) and transcript filtering after RSEM requiring an expression level of at least 1.0 FPKM (yellow).104

Figure 3.2 Top BLAST result species: Following BLASTx searches of the transcripts of the reference transcriptome against the NCBI nr database, up to 10 BLAST hits were obtained for each transcript. The BLAST hit for each sequence with the lowest e-value was designated as the top hit and the species which the result match originated was recorded. The graph represents the total number of BLAST hits out of all top BLAST hits mapped to each particular species.....105

Figure 3.3 *P. borchgrevinki* transcriptome level GO comparison: A comparison of the GO term distribution for the broad category of molecular function is provided for the previous *P. borchgrevinki* transcriptome assembly and annotation conducted by Bilyk and Cheng (2014) and the current transcriptome assembly and annotation. To provide a more direct comparison, the data bars represent the proportion of terms assigned to the specific GO term listed along the x-axis out of all GO terms within that broad category.106

Figure 3.4 Sample level gene expression correlation matrix: The correlation matrix demonstrates the level of transcriptome wide gene expression correlation from 0-1, with 0 indicating no correlation and 1 indicating an identical expression profile. The current correlation matrix is indexed between 0.5 and 0.9 with black representing a correlation of

0.5 and yellow representing a correlation of 0.9. Cluster dendrograms are provided to demonstrate the relationships between the expression profiles of each individual sample.107

Figure 3.5 GO molecular function expression: Molecular function gene ontology terms with more than 5 differentially expressed genes per category ($FDR \leq 0.05$) across all time-points are shown for each time-point. Yellow bars indicate the number of up-regulated genes associated with that GO term and blue bars indicate the number of down-regulated genes associated with that GO term.....108

Figure 3.6 GO biological process expression: Biological process gene ontology terms with more than 5 differentially expressed genes per category ($FDR \leq 0.05$) across all time-points are shown for each time-point. Yellow bars indicate the number of up-regulated genes associated with that GO term and blue bars indicate the number of down-regulated genes associated with that GO term.....109

Figure 3.7 Pathway expression summary: The number of differentially expressed genes ($FDR \leq 0.05$) for the biological process gene ontology categories: response to stress (GO:0006950), immune system process (GO:0002376), homeostatic process (GO:0042592), carbohydrate metabolic process (GO:0005975), lipid metabolic process (GO:0006629), cell proliferation (GO:0008283) and cell death (GO:0008219) are shown for each multi-stressor treatment as compared to the control for the 7d, 28d and 56d time-points. A bar above the black line indicates the number of up-regulated genes within that GO category, whereas the bar below the black lines indicates the number of down-regulated gene within that GO category110

Figure 4.1 Sample level gene-expression correlation matrix: The correlation matrix demonstrates the level of transcriptome wide gene expression correlation from 0-1, with 0 indicating no correlation and 1 indicating an identical expression profile. The current correlation matrix is indexed between 0.5 and 0.9 with black representing a correlation of 0.5 and yellow representing a correlation of 0.9. Cluster dendrograms are provided to demonstrate the relationships between the expression profiles of each individual sample.137

Figure 4.2 The stress response heatmap: The heatmap displays all differentially regulated genes ($FDR \leq 0.05$) within the GO categories response to stress (GO:0006950), immune system process (GO:0002376), and homeostatic process (GO:0042592) for each multi-stressor time-point as compared to the control (7 days, 28 days, and 42 days). The fold change is \log_2 scaled with blue representing down-regulation, black indicating no significant regulation, and yellow representing up-regulation. Any changes with an absolute fold change greater than $\log_2(2)$ (abs 4X) are represented as the maximum. The gene symbol is included for each gene with a number within parentheses indicating an isoform of that gene. Each gene symbol also includes an additional symbol associating that gene with a GO category in the following manner: response to stress = “X”, immune system process = “+”, and homeostatic process = “~”138

Figure 4.3 Transcription and translation heatmap: The heatmap displays all differentially regulated genes ($FDR \leq 0.05$) within the GO categories transcription (GO:0006351) and

translation (GO:0006412) for each multi-stressor time-point as compared to the control (7 days, 28 days, and 42 days). The fold change is \log_2 scaled with blue representing down-regulation, black indicating no significant regulation, and yellow representing up-regulation. Any changes with an absolute fold change greater than $\log_2(2)$ (abs 4X) are represented as the maximum. The gene symbol is included for each gene with a number within parentheses indicating an isoform of that gene. Each gene symbol also includes an additional symbol associating that gene with a GO category in the following manner: transcription = “-” and translation = “+” 139

Figure 4.4 – Metabolism, proliferation and death heatmap: The heatmap displays all differentially regulated genes ($FDR \leq 0.05$) within the GO categories carbohydrate metabolic process (GO:0005975), lipid metabolic process (GO:0006629), cell proliferation (GO:0008283) cell death (GO:0008219), for each multi-stressor time-point as compared to the control (7 days, 28 days, and 42 days). The fold change is \log_2 scaled with blue representing down-regulation, black indicating no significant regulation, and yellow representing up-regulation. Any changes with an absolute fold change greater than $\log_2(2)$ (abs 4X) are represented as the maximum. The gene symbol is included for each gene with a number within parentheses indicating an isoform of that gene. Each gene symbol also includes an additional symbol associating that gene with a GO category in the following manner: carbohydrate metabolic process = “#”, lipid metabolic process = “=”, cell proliferation = “+”, and cell death = “X” 140

Figure 5.1 The total number of differentially expressed genes ($FDR \leq 0.05$, fold change ≥ 2) for *T. bernacchii* (black), *P. borchgrevinki* (dark grey), and *T. newnesi* (light grey) in the multi-stressor treatment as compared to the control at each time-point 7 days, 28 days and 42/56 days for *T. newnesi* and *T. bernacchii/P. borchgrevinki*, respectively. Bars above the x-axis indicate up-regulated genes; bars below the x-axis indicate down-regulated genes..... 148

Figure 5.2 The total number of differentially expressed genes ($FDR \leq 0.05$, fold change ≥ 2) for *T. bernacchii*, *P. borchgrevinki*, and *T. newnesi* in the multi-stressor treatment as compared to the control at 7 days for the biological processes: carbohydrate metabolism (blue), lipid metabolism (light blue), cell death (dark green), cell proliferation (light green), response to stress (red), and immune system process (light red). Bars above the x-axis indicate up-regulated genes; bars below the x-axis indicate down-regulated genes. 149

Figure 5.3 The total number of differentially expressed genes ($FDR \leq 0.05$, fold change ≥ 2) for *T. bernacchii*, *P. borchgrevinki*, and *T. newnesi* in the multi-stressor treatment as compared to the control at 28 days for the biological processes: carbohydrate metabolism (blue), lipid metabolism (light blue), cell death (dark green), cell proliferation (light green), response to stress (red), and immune system process (light red). Bars above the x-axis indicate up-regulated genes; bars below the x-axis indicate down-regulated genes. 150

Figure 5.4 The total number of differentially expressed genes ($FDR \leq 0.05$, fold change ≥ 2) for *T. bernacchii*, *P. borchgrevinki*, and *T. newnesi* in the multi-stressor treatment as compared to the control at 42 (*T. newnesi*) or 56 (*T. bernacchii* and *P. borchgrevinki*) days for the biological processes: carbohydrate metabolism (blue), lipid metabolism (light blue), cell death (dark green), cell proliferation (light green), response to stress (red), and immune system process (light red). Bars above the x-axis indicate up-regulated genes; bars below the x-axis indicate down-regulated genes151

INTRODUCTION

As the consensus on global climate change becomes more resolute within the scientific community, the focus has begun to shift from whether global climate change is occurring, to how these changes will impact the biosphere. While no region is likely to escape the effects of global climate change, certain ecosystems may be particularly vulnerable (Pachauri et al., 2014). The polar regions are among those identified as most vulnerable to climate change (Pachauri et al., 2014). In fact the Southern Ocean surrounding Antarctica has already experienced a warming of approximately 0.8 °C (Gille, 2002).

When the Drake passage opened some 14-25 million years ago the circumpolar current formed around Antarctica, leading to the formation of one of the coldest more oceanographically stable environments on Earth (Livermore, Nankivell, Eagles, & Morris, 2005). As the water cooled perciform fishes of the suborder Notothenioidei began to radiate into these waters and would eventually comprise a significant portion of the fauna of the Southern Ocean (J. Eastman, 1993; Gon & Heemstra, 1990). The unique environmental pressures of the Southern Ocean necessitated a number of highly specific adaptations to vital protein families including chaperonins (Pucciarelli, Parker, Detrich, & Melki, 2006), heat shock proteins (G E Hofmann, Buckley, Airaksinen, Keen, & Somero, 2000; Place, Zippay, & Hofmann, 2004), heme proteins (O'Brien & Sidell, 2000; Sidell, Crockett, & Driedzic, 1995), tubulin kinetics (Detrich, Parker, Williams,

Nogales, & Downing, 2000), and anti-freeze proteins (Cheng, Cziko, & Evans, 2006; A. L. DeVries & Cheng, 2005). Other adaptations to the extreme cold include increased mitochondrial densities, reduction in hematocrit, and reductions in cardiovascular output (D'Amico et al., 2002; Johnston, Calvo, Guderley, & D, 1998; Lucassen, Schmidt, Eckerle, & Pörtner, 2003).

A unique aspect of Notothenioids is the apparent loss of an inducible heat shock response, and thus these fish have been relatively well studied by polar researchers with a particular focus upon the impact of heat stress on the physiology of these fish (Bilyk & DeVries, 2011; Bilyk, Evans, & DeVries, 2012; Davison, Franklin, & Carey, 1990; Forester, Franklin, H, & Daviso, 1987; H. O. Pörtner, Lucassen, & Storch, 2005; Esme Robinson & Davison, 2008; Sleadd et al., 2014; Somero & DeVries, 1967). However, addressing multiple simultaneous stressors that are likely more indicative of future oceanic conditions is essential. Prior results from non-polar marine organisms have indicated that multiple simultaneous stressors may have a greater effect than the sum of the individual stressors (O'Donnell, Hammond, & Hofmann, 2009; Rosa & Seibel, 2008; Schulte, 2007). This synergistic effect has recently been confirmed with these same three species in multiple physiological pathways where synergistically increased temperature and $p\text{CO}_2$ was found to have a greater effect than the sum of the two stressors (Enzor, Zippay, & Place, 2013; Enzor & Place, 2014, 2015).

At the commencement of this research only a handful of large scale sequencing studies had been conducted (Chen et al., 2008; Shin et al., 2012) with most sequencing data largely limited to studies of the evolutionary history and phylogenetic relationships of these fish that focused only upon a few genes of interest. Furthermore, there had been

no genomic analyses assessing the synergistic effects of multiple simultaneous stressors across multiple interacting pathways, no less studying the entire transcriptome.

Recognizing that the analysis of a limited range of molecular or cellular responses would no longer be sufficient (Gretchen E Hofmann & Todgham, 2010; Place, O'Donnell, & Hofmann, 2008) I set out to fill this gap and provide analyses of the notothenioid stress response to synergistic stressor from the transcriptomic to the gene level.

However, in order to conduct the analysis of the multi-stressor condition it was necessary to create the genomic resources by which gene expression would be determined. Utilizing newly developed methods to accurately assemble billions of short read raw sequence data (Grabherr et al., 2011; Haas et al., 2013), I was able to create raw transcriptomic libraries that were then annotated utilizing sequencing homology to known sequences (Altschul, Gish, Miller, Myers, & Lipman, 1990; Conesa et al., 2005). These transcriptomic libraries not only made it possible to determine differential expression under the multi-stressor condition, they established valuable transcriptomic databases for these notothenioid species. Once the initial genomic resources were in place I was able to proceed with the main thrust of the study, to analyze physiological pathways separately and in conjunction across the entire transcriptome. Thereby enhancing our understanding of the physiological plasticity of notothenioids to forecasted conditions of the Southern Ocean, and to impute these findings upon the survivability of these same species on a changing planet.

Differential gene expression analyses were initially conducted on the transcriptomic level permitting an overview of the total gene expression profile at each treatment time-point. Once this data was collected it was possible to identify particular

biological pathways that exhibited significant differential expression between the control and multi-stressor treatments; to this end I focused primarily upon pathways associated with metabolism, response to stress, immune system processes, cell proliferation and cell death. Then within these pathways I was able to identify specific genes that drove the observed changes in expression, some expected, others not, and draw conclusions as to the ramifications of these changes. Ultimately the analysis was framed to reflect the two often conserved responses to environmental stress; the rapid, transient response known as the cellular stress response (CSR) and the more permanent response termed the cellular homeostasis response (CHR) (Kültz, 2005). I believed that different species would demonstrate differences in their responses, and these differences would influence the relative success of each species in adapting to a changing Southern Ocean.

CHAPTER 1

DE NOVO ASSEMBLY AND CHARACTERIZATION OF TISSUE SPECIFIC TRANSCRIPTOMES IN THE EMERALD NOTOTHEN, *TREMATOMUS* *BERNACCHII*.¹

¹ Huth, T. J., & Place, S. P. (2013). *De novo* assembly and characterization of tissue specific transcriptomes in the emerald notothen, *Trematomus bernacchii*. *BMC Genomics*, 14, 805. doi:10.1186/1471-2164-14-805. Reprinted here in accordance with the BioMed Central Open Access Charter.

1.1 ABSTRACT

Background

The notothenioids comprise a diverse group of fishes that rapidly radiated after isolation by the Antarctic Circumpolar Current approximately 14-25 million years ago. During this period, unique adaptations evolved in several members of this fish clade, such as the tolerance of sub-freezing temperatures. Although able to thrive under temperatures below the thermal limits for most organisms, the astounding stability of their environment has resulted in an extremely narrow window of physiological tolerances. Given that evolutionary adaptation has led to finely tuned traits with narrow physiological limits in these organisms, this system provides a unique opportunity to examine physiological trade-offs and limits of adaptive responses to environmental perturbation. As such, notothenioids have a rich history with respect to studies attempting to understand the vulnerability of polar ecosystems to the negative impacts associated with global climate change. Unfortunately, despite being a model system for understanding physiological adaptations to extreme environments, we still lack fundamental molecular tools for much of the Nototheniidae family.

Results

Specimens of the emerald notothen, *Trematomus bernacchii*, were acclimated for 28 days in flow-through seawater tanks maintained near ambient seawater temperatures (-1.5 °C) or at +4 °C. Following acclimation, tissue specific cDNA libraries for liver, gill and brain were created by pooling RNA from n=5 individuals per temperature treatment. The tissue specific libraries were bar-coded and used for 454 pyrosequencing, which yielded over 700 thousand sequencing reads. A *de novo* assembly and annotation of these

reads produced a functional transcriptome library of *T. bernacchii* containing 30,107 unigenes, 13,003 of which possessed significant homology to a known protein product. Digital gene expression analysis of these extremely cold adapted fish reinforced the loss of an inducible heat shock response and allowed the preliminary exploration into other elements of the cellular stress response.

Conclusions

Preliminary exploration of the transcriptome of *T. bernacchii* under elevated temperatures enabled a semi-quantitative comparison to prior studies aimed at characterizing the thermal response of this endemic fish whose size, abundance and distribution has established it as a pivotal species in polar research spanning several decades.

The comparison of these findings to previous studies demonstrates the efficacy of transcriptomics and digital gene expression analysis as tools in future studies of polar organisms and has greatly increased the available genomic resources for the suborder Notothenioidei, particularly in the Trematominae subfamily.

1.2 INTRODUCTION

Perciform fishes of the suborder Notothenioidei comprise a major portion of the Southern Ocean fauna (J. Eastman, 1993; Gon & Heemstra, 1990). They began to radiate into Antarctic waters in the early Tertiary, gradually adapting to the progressive cooling, which set in after the opening of the Drake passage and the formation of the circumpolar current some 14-25 million years ago (Arntz, Brey, & Gallardo, 1994; J. Eastman, 1993). Isolation of the Antarctic continental shelf by the Polar Front has produced arguably the

coldest, most oceanographically stable environment on the planet. However, in direct opposition to this highly stenothermic environment are the profound environmental extremes produced by the transition from 24 hours of sunlight to complete darkness over the winter months, resulting in significant variation in primary productivity. As a result, Antarctic marine organisms inhabiting these ice-laden waters have faced unique metabolic and physiological challenges for survival and persistence. The impacts of low temperatures and seasonally limited food availability have long been recognized as primary selective forces driving the evolution of the many endemic species found in Antarctica today (Arntz et al., 1994; A Clarke, Johnston, Murphy, & Rogers, 2007; Andrew Clarke, 2011; Peck, Clark, Morley, Massey, & Rossetti, 2009; Peck, Webb, & Bailey, 2004; H. Pörtner, Peck, & Somero, 2006). In addition to the high degree of endemism produced by these evolutionary processes, a wide-array of functional adaptations have been fixed among protein families of several Antarctic fish, including chaperonins (Pucciarelli et al., 2006), heat shock proteins (G E Hofmann et al., 2000; Place et al., 2004), heme proteins (O'Brien & Sidell, 2000; Sidell et al., 1995), tubulin kinetics (Detrich et al., 2000), and anti-freeze proteins (Cheng et al., 2006; A. L. DeVries & Cheng, 2005). This rigid oceanographic stability however, may have resulted in an ecosystem filled with endemic fauna that are poorly poised to deal with rapid climate variation (A Clarke et al., 2007; Peck, Barnes, & Willmott, 2005). For instance, cold specialization has resulted in increased mitochondrial densities at uncompensated capacities in some notothenioids (D'Amico et al., 2002; Johnston et al., 1998; Lucassen et al., 2003). These increased densities have also been combined with reductions in hematocrit and cardiovascular output (S. Egginton, 1997; Stuart Egginton, 1998).

Specialization has thus forced some of these species to lead a less active, rather sluggish lifestyle.

Although a significant amount of sequencing work has been done to elucidate the evolutionary history and phylogenetic relationships among these unique fishes, much of the available sequence information is constrained to a few highly conserved genes such as ribosomal and mitochondrial genes, or highly specified genes such as the antifreeze glycoprotein genes. Recent advances in DNA sequencing technology have led to a significant increase in the availability of molecular tools to ecologists and physiologists. A particular research niche that is poised to benefit greatly from this rapid increase in sequence data is the field of polar biology. The availability of well-annotated transcriptomes from a variety of polar species will provide the groundwork for future functional genomics studies aimed at elucidating the impact of global climate change on polar ecosystems. With the application of next generation sequencing tools in an ecological setting, we can begin to investigate organismal responses at a level of complexity that was not approachable in years past. To date, only two large-scale sequencing studies of transcribed genes have been published for any Antarctic notothen, including an EST library for *Dissosticus mawsoni* in the subfamily Pleuragramminae (Chen et al., 2008) and a comparative study of the transcriptomes from a member of the Nototheniinae and Pleuragramminae sub-families (Shin et al., 2012). To date, relatively little sequence information is available for any member of the Trematominae subfamily despite the ecological importance of these fish in coastal Antarctic environments. Due to its circumpolar distribution, abundance and relative ease of collection, *Trematomus bernacchii* has long been a target species for physiological and biochemical studies

assessing the plasticity of this highly stenothermic family of fishes and the cost of adaptation to such a cold stable environment (Bilyk & DeVries, 2011; Davison, Axelsson, Forster, & Nilsson, 1995; Davison, Franklin, & McKenzie, 1994; a L. DeVries & Wohlschlag, 1969; Enzor et al., 2013; G E Hofmann et al., 2000; Place et al., 2004; Somero & DeVries, 1967). While earlier attempts at using heterologous hybridizations to a cDNA array of a temperate goby provided insight into the transcriptional response of highly conserved genes in this species (Buckley & Somero, 2009), we still lack a robust approach to functional genomics in these unique fish. Here we describe the *de novo* assembly and annotation of the transcriptome of the emerald notothen, *T. bernacchii*. In addition, we provide a glimpse into the tissue specific response to thermal stress at the level of the transcript that highlights the sensitivity and utility of these applications in polar fish.

1.3 RESULTS AND DISCUSSION

Sequence data and de novo assembly

Roche 454 sequencing generated a total of 738,379 unpaired reads across six samples with an average length of 335.80 bp. The raw data were deposited at the NCBI Sequence Read Archive under the study accession number [SRP026018]. After sequence trimming for adapter removal, and screening of sequences based on quality and ambiguity scores, 735,507 reads remained with an average length of 320.98 bp. *De novo* assembly of these reads using the CLC Genomics *de novo* assembly tool matched 468,721 reads leaving 266,786 unmatched singletons. The final transcriptome contained 30,107 unigenes with an average length of 605bp, an average coverage of 6.45X, and a

N75, N50, and N25 of 466bp, 671bp, and 1,085bp respectively (Table 1.1). The unigene length distribution can be seen in Figure 1.1.

Overall, the resulting number of unigenes produced in our assembly is in line with results reported in previous studies utilizing Roche 454 data for *de novo* full transcriptome assemblies of other fish species, including 1,150,339 reads yielding 36,811 unigenes with an average length of 888 bp in Common Carp (*Cyprinus carpio*) (Ji et al., 2012); and 1,004,081 reads yielding 33,191 unigenes with an average length of 991 in Asian Seabass (*Lates calcariefer*) (Xia et al., 2013). Furthermore, our average coverage (6.45X) is comparable to 454 *de novo* transcriptome assemblies conducted with similar number of sequencing reads (Logacheva et al., 2011); and possesses a similar percentage of reads mapping back to the unigenes (63.7%) as well (Ferreira de Carvalho et al., 2013; Logacheva et al., 2011).

To further validate our transcriptome, we compared the alignment and similarity of our unigenes to the 303 known full and partial *T. bernacchii* sequences currently available on NCBI at the time of our study using BLASTx. This comparison yielded 236 matches with an *e*-value $< 10^{-10}$, of which 180 sequences possessed a percent identity $> 95\%$ (Fig. 1.2). Despite the limited sequence data available for *T. bernacchii*, these alignment metrics indicate a relatively accurate transcriptome assembly.

Of the 303 *T. bernacchii* sequences available, only 4 failed to align to a unigene sequence. Two of these known sequences form interphotoreceptor retinoid-binding protein (IRBP), a protein that accumulates in the subretinal space and facilitates exchanges during the “visual cycle” (Stenkamp, Cunningham, Raymond, & Gonzalez-Fernandez, 1998). Due to the high degree of specificity to the visual process, it is unlikely

that this product would be found in the liver, gill or brain tissues that were sequenced in this effort. Another unmatched query represented a partial of E3 ubiquitin protein ligase 2; however, six different unigenes (1260, 4958, 15902, 18843, 22152, and 27842) matched E3 ubiquitin ligase-like proteins during annotation, thus it is likely that this partial query sequence did not overlap with the available assembled sequence of the unigenes, which themselves are not complete representations of the entire coding region of E3 ubiquitin. The last query that failed to align was that of a putative voltage-activated sodium channel alpha subunit (SCNA) which are functionally conserved and with lengths ranging between 3300-3500bp in teleost fish (Novak et al., 2006). As the partial sequence available for *T. bernacchii* SCNA is only 276bp, it is very likely our sequencing efforts simply failed to provide areas of overlap with the partial cDNA sufficient to align it to a unigene.

In an effort to further validate our transcriptome assembly, we compared our assembly to the transcriptomes of nine other prior sequenced teleost fish including: *Notothenia coriiceps*, *Chaenocephalus aceratus*, *Pleuragramma antarcticum*, *Gasterosteus aculeatus*, *Takifugu rubripes*, *Oryzias latipes*, *Tetraodon nigroviridis*, *Oreochromis niloticus* and *Danio rerio* (Table 1.2). BLAST searches were conducted using the our assembled unigenes as query sequences against the available transcriptome of each fish using either BLASTx or BLASTn, depending on the form of the sequence database available. The BLASTn results demonstrated a high degree of similarity between the transcriptome generated for *T. bernacchii* and that of *N. coriiceps*, a related notothenioid species (19,253 hits e-value < 10⁻³, 15,861 hits e-value < 10⁻¹⁰), as well as strong similarity to the two other more distantly related Antarctic fish, *P. antarcticum*

(16,822 hits $e\text{-value} < 10^{-3}$, 10,033 hits $e\text{-value} < 10^{-10}$) and *C. aculeatus* (14,533 hits $e\text{-value} < 10^{-3}$, 10,138 hits $e\text{-value} < 10^{-10}$). BLASTx searches against the non-polar fish in our analysis yielded results similar to previous comparisons between the transcriptomes of notothenioid fishes and those of non-polar fish species (Table 1.2) (Coppe et al., 2013).

Annotation, classification, and analysis

BLASTx results using the unigene sequences as queries against the non-redundant protein sequences (nr) database at NCBI yielded 9,243 significant alignments ($e\text{-value} 10^{-3}$), and when combined with an additional 3,760 BLASTn results from our searches against the nucleotide collection (nr/nt) database, yielded a total of 13,003 unigene sequences with a significant BLAST result. Of these results, 7,677 unigene sequences mapped to GO terms using the B2GO software package. Ultimately InterProScan results merged with B2GO annotations yielded a total of 6,528 fully annotated unigene sequences. The final distribution of annotated unigenes included 5,351 unigenes sequences with a significant BLAST result only, 1,149 unigene sequences mapped in B2GO, and 6,528 unigene sequences fully annotated with GO terms. Overall, approximately 43% of our unigenes had a significant hit in the nr protein or nucleotide database and we were able to assign GO annotation to 21.6% of unigenes in the dataset, which was highly comparable to recent assembly and annotation efforts for other non-model fish species (Coppe et al., 2013; Shin et al., 2012; Heidrun Sigrid Windisch, Lucassen, & Frickenhaus, 2012).

Tissue specific gene expression

The transcriptome wide gene ontology in WEGO format yielded 14,181 (~35%) GO annotation results for cellular component, 17,515 (~44%) GO annotation results for biological process, and 8,447 (~21%) GO annotation results for molecular function in *T. bernacchii*. For the most part, expression levels associated with individual GO classifications were found to be very similar across the entire transcriptome and individual tissues (Fig. 1.3). However, some gene expression trends can be detected that are likely associated with differences in functional roles of the tissues. For example, when comparing the biological processes between tissues, the role of the liver in protein metabolism is evident with 24.7% of its total biological processes dedicated to metabolic processes as compared to 22.9% in the gill and 21.1% in the brain. Also, the gill tissue demonstrated elevated representation for the GO classification ‘response to stimuli’, perhaps due to their more immediate exposure to the external environment, with approximately 8.2% of biological processes dedicated to this function as opposed to 5.1% in the brain.

The molecular function of expressed transcripts also displayed variation that mirror physiological differences between the tissues. For instance, despite being a primary site for cellular detoxification, liver did not exhibit sufficient antioxidant activity to meet the applied threshold ($n \geq 25$ transcripts) for this GO term, whereas the GO term antioxidant activity was highly represented in the gill, perhaps due to this tissue’s direct contact with the extremely cold, highly oxygenated water of the Southern Ocean (Fig. 1.3). These results parallel previous expression patterns of antioxidant proteins in the gill and liver tissue of *T. bernacchii*; and Place (Enzor & Place, 2014) report protein

concentrations of two isoforms of the antioxidant enzyme family superoxide dismutase (SOD1 and SOD2) are relatively higher in gill tissue compared to liver tissue and total SOD activity is also elevated in gill tissue. As for cellular components, each tissue largely mirrored one another and the transcriptome as a whole (Fig. 1.3).

Enzyme code distributions for each tissue calculated by the main enzyme classes: oxidoreductases, transferases, hydrolases, lysases, isomerases, yielded the following: liver (359, 542, 559, 74, 71, 127), gill (252, 269, 308, 39, 44, 72) and brain (245, 355, 377, 52, 59, 93) respectively (Fig. 1.4). The liver displayed the greatest variety of enzymes, commiserate with its involvement in protein and lipid metabolism.

A comparison of the unigenes against the KEGG database, a resource for understanding high-level functions and utilities of biological systems (Kanehisa & Goto, 2000), yielded 1,948 sequences with a significant match (BLASTx e -value $< 10^{-5}$) to 119 KEGG pathways and 784 enzymes. Of the 119 pathways there were 62 pathways with over 10 sequences assigned. The pathway for purine metabolism was the most commonly assigned (153, 7.85%), followed by oxidative phosphorylation (73, 3.75%), nitrogen metabolism (71, 3.64%), glycolysis/gluconeogenesis (59, 3.03%), pyrimidine metabolism (51, 2.62%), glutathione metabolism (45, 2.31%), methane metabolism (45, 2.31%), drug metabolism- other enzymes (43, 2.2%), T-cell receptor signaling pathway (38, 1.95%), and pentose phosphate pathway (36, 1.85%), with the remaining 119 pathways listed in the supplemental information. When analyzing dominant KEGG pathways assigned to the unigenes expressed in each tissue, the most commonly assigned KEGG pathways generally followed the most commonly assigned pathways for *T. bernacchii* as a whole, with a few exceptions (Fig. 1.5). Overall, liver tissue matched 1,196 unique sequences to

114 KEGG pathways and 592 enzymes; gill tissue matched 1,397 unique sequences to 114 KEGG pathways and 674 enzymes; brain tissue matched 1,272 unique sequences to 111 KEG pathways and 620 enzymes.

Digital gene expression analysis

The cellular response to temperature stress in fish is highly conserved, and the unique evolutionary history and resulting physiological response to elevated temperature previously reported in *T. bernacchii* provides a useful backdrop to discuss the findings from our study. It should be noted, that this study was not designed to explicitly test the effects of temperature on gene expression, since RNA from individuals within a thermal acclimation treatment was pooled prior to library construction. However, an initial qualitative comparison can be performed, and the results compared to previous studies that have performed more quantitative gene expression analyses. To simplify the expression analysis for comparison of tissue specific changes in gene expression across treatments, we limited our consideration to only those unigenes annotated with either a BLAST result, functional mapping, or full GO annotation. We then characterized the relative changes in tissue specific expression patterns in -1.5 °C (control) and +4 °C acclimated fish. Heatmaps of all annotated unigenes from each tissue highlight the high degree of tissue specific changes observed in the transcriptome of these fish when acclimated to elevated temperature (Fig. 1.6). After screening to remove data pairs that did not exhibit expression in either treatment, we achieved our final expression datasets for each tissue. In all, the expression levels of 6,656 unigene pairs were compared in the liver in which we found 1,685 unigenes were down-regulated 2-fold or greater while 3,862 were found to be up-regulated 2-fold or greater. For gill tissue, comparison of the

expression levels of 10,084 unigene pairs showed 4,369 unigenes were down-regulated and 3,065 unigenes were up-regulated at least 2-fold or greater. For expression analysis of the brain tissue we compared the expression levels of 9,044 unigene pairs, of which 3,347 were down-regulated and 3,965 were up-regulated at least 2-fold.

Below we discuss the general gene expression trends that emerged from our preliminary RNAseq analyses with respect to the most highly expressed gene families under ambient conditions. In addition, in order to more fully interpret the effects of long-term acclimation to elevated temperatures on *T. bernacchii*, we extended our analysis beyond that of the most highly represented gene families, and in doing so, focus on three particular areas that encompass the cellular response to elevated temperature observed in *T. bernacchii*.

Tissue specific gene expression profiles under ambient conditions

Prior studies characterizing the gene expression profiles of nothothenioid fishes held under ambient conditions found tissue specific transcriptomes that were dominated by a few highly expressed transcripts (Chen et al., 2008). We found a similar pattern among our tissues sampled from *T. bernacchii*, albeit to a lesser degree with the 10 most highly expressed annotated unigenes in the liver, gill and brain tissues representing ~8.2%, ~3.2% and ~2.67% of total transcripts respectively. Similar to results reported for the liver transcriptome of *D. mawsoni*, we found apolipoproteins and fibrogen chains were among the most highly expressed genes in the liver of *T. bernacchii* under ambient conditions (14 kda apolipoprotein = 1.19%, apolipoprotein A-I = 0.66%, apolipoprotein b-like protein = 0.57%, and fibrogen α chain-like = 1.70% of total transcripts) (Chen et al., 2008). This over-representation appears to be further exaggerated by long-term

acclimation to elevated temperatures. Analysis of the liver transcriptome of fish acclimated to +4 °C for 28 days showed apolipoproteins were considerably up-regulated with the 14 kda apolipoprotein undergoing a 7.1-fold increase to represent 5.10% of all transcripts and apolipoprotein A-I undergoing a 11.5-fold increase to represent 4.65% of all transcripts. Given their role in lipid mobilization and transport, it seems plausible this significant increase in apolipoproteins is playing an important role in offsetting the rapid increase in metabolic demands previously associated with the acclimatory response of *T. bernacchii* to elevated temperature (& Place, 2014).

In addition to the liver, we found similar patterns of gene expression in the brain tissue of *T. bernacchii* and compared to those of *D. mawsoni*. Chen and colleagues report a number of transcripts that are involved in the protection, maintenance, and repair of neural tissue, including S100 β and ependymin-1, which are highly represented in the transcriptome of *D. mawsoni* brain tissue (Chen et al., 2008). Under ambient temperature conditions, S100 β and ependymin-1 comprise 0.30% and 0.18% respectively of the expressed genes in *T. bernacchii* brain tissue, and when exposed to a thermal stress, the expression of these two transcripts increased significantly. In fish acclimated to +4 °C, S100 β increase over 13-fold, representing 2.21% of all expressed transcripts and ependymin-1 increased by greater than 7-fold to represent ~2% of all expressed transcripts in the brain. Although only semi-quantitative at this point, these data suggest *T. bernacchii* maintain a strong capacity to respond to environmental conditions perturbing to neural function.

The gill tissue displayed a somewhat different trend with respect to the highly expressed transcripts found in the ambient and +4 °C acclimated fish. In the gill tissue

from fish acclimated to +4 °C, we saw an overall down-regulation of many of the most highly expressed transcripts found in ambient fish including, 60s ribosomal proteins (8.8-fold), zinc finger proteins (14.3-fold), MAPKs (4.7-fold) and translation initiation factor eif2b (3.4-fold). Interestingly, many of these genes were reported to show a moderate up-regulation (<1.5-fold) after an acute heat shock event (4h at +4 °C) in a previous study employing a transcriptome wide analysis of *T. bernacchii* (Buckley & Somero, 2009). The differences in gene expression profiles between these two studies likely capture the transition that occurs between immediate response to stress and the long-term physiological adjustments that follow. The general down-regulation of gene families involved in transcription and translation in our long-term treatment may indicate a diminished capacity for protein turnover at elevated temperatures. However, despite a general down-regulation of one of the cells major energy consuming pathways in the gill tissue, we see a 2.5-fold up-regulation of cytochrome c oxidase I and a 1.5-fold up-regulation of cytochrome b which mirrors the increased capacity for aerobic metabolism found under conditions of acute thermal stress in *T. bernacchii* (Buckley & Somero, 2009). These findings, along with the strong up-regulation of apolipoproteins in the liver suggest that mobilization of energy stores and ATP production continue to play a central role in the capacity of *T. bernacchii* to mitigate the effects of elevated temperatures long-after cellular restructuring has likely occurred.

Protein homeostasis and the Heat Shock Response (HSR): Heat shock proteins (HSPs) have long been known to play a significant role in folding of nascent polypeptides as well as the rescue and refolding of proteins under conditions of cellular stress (Feder & Hofmann, 1999; Saunders & Barber, 2003). Despite the functional roles for these protein

families being highly conserved across all taxa, Antarctic notothenioids display divergent expression patterns that might be related to environmental constraints. Previous studies have observed that inducible HSP isoforms and protein-specific chaperones are continuously up-regulated in several notothenioid species, potentially indicating a persistent system-wide requirement for mitigating the denaturing effect of the constant cold of the Southern Ocean (Chen et al., 2008; Place & Hofmann, 2005; Place et al., 2004). As a result of this persistent elevation of the heat shock response (HSR), it is believed that the extremely cold adapted notothenioids, including *T. bernacchii*, are no longer capable of further up-regulating inducible isoforms of HSPs when exposed to thermal stress (G E Hofmann et al., 2000; Place et al., 2004). To see if similar trends were identified in our long-term acclimations of *T. bernacchii*, we compared the level of expression for several molecular chaperones involved in the HSR. Two particular HSPs previously found to be up-regulated in fish exposed to chronic high temperature are Hsp70 and Hsp90 (Podrabsky & Somero, 2004). Consistent with previous findings for acute thermal stresses, we found that Hsp70 expression was generally insensitive to long-term acclimation at elevated temperature with only moderate changes detected (≤ 1.5 -fold in all tissues, Fig. 1.7). Similarly, the inducible isoform of Hsp90 (Hsp90 α) also showed only small variations in expression in all three tissues (liver 1-fold, gill 1.7-fold, brain 1.4-fold) (Fig. 1.7). Also seen with the Hsp70 molecular chaperone, gill tissue appeared to be the most responsive, which may be attributable to the direct contact of these cells to the water and thus environmental variations. Overall our findings for the expression patterns of HSPs in *T. bernacchii* reflect previous findings and further substantiate the belief that much of its ability to mount a HSR has been lost (Buckley & Somero, 2009;

Place & Hofmann, 2005; Place et al., 2004). Intriguingly, although no significant changes were seen in the inducible HSP isoforms, we did observe a significant decrease in expression levels of the constitutive isoform, Hsc71, in liver and gill (2.7 & 3.7-fold respectively). This down-regulation of Hsc71 was also accompanied by moderate decreases in the constitutively expressed Hsp90 β (Fig. 1.7).

In addition to the major molecular chaperone families represented in the transcriptome, we also identified a number of contigs with homology to several members of the α -crystallin-type super family, collectively referred to as small heat shock proteins (sHSPs). Although sHSPs are known have similar cytoprotective effects as those found with larger size class molecular chaperones, they are often found expressed in lower abundances and in some instances their function may be non-essential for cell survival (Bartelt-Kirbach & Golenhofen, 2014; MacRae, 2000; Narberhaus, 2002). In our study, we found the sHSPs showed tissue specific responses with sHSPs in the liver displaying the greatest magnitude change. After acclimation to +4 °C, transcript levels for Hsp27/B1, Hsp30/B11 and α -crystallin all showed a 2-fold or greater up-regulation in liver tissue. However, in gill and brain tissue, expression of these sHSPs were either not detected or down-regulated, except in the case of α -crystallin in the brain tissue which displayed a 3-fold increase.

As this is only a preliminary characterization of the transcriptome of *T. bernacchii* under chronic thermal stress, we are unable to elucidate the importance of the trends identified with respect to the expression of HSPs. However, in combination with the expression patterns of the transcriptional machinery mentioned above, we speculate this could be related to an overall decrease in transcription with long-term acclimation to

elevated temperatures, potentially as a means to conserve energy. We have previously shown metabolic rates in *T. bernacchii* are initially elevated when acclimated to +4 °C but gradually return to baseline levels (Enzor et al., 2013). A general reduction in transcription rates could represent physiological trade-offs associated with long-term physiological adjustments necessary to reduce the cellular demand for oxygen. Alternatively, these reductions in capacity for protein synthesis and chaperoning may represent hallmarks of temperature compensation at the cellular level in these fish. These results represent potentially novel insight into the thermal acclimation of these fish and highlight the sensitivity and utility of these approaches for understanding physiological responses in this system.

Cellular Stress Response (CSR)

The cellular stress response (CSR) is a conserved defense reaction activated at the cellular level when exterior forces cause strain on an organism (Kültz, 2005). The heat shock proteins that serve as molecular chaperones and the HSR described above are probably the most well-known constituents of the CSR, but there are a number of additional cellular pathways involved in the cell's response to stress that are likely co-regulated, including: redox regulation proteins, DNA damage sensing/repair proteins, protein degradation proteins, fatty acid/lipid metabolism proteins and energy metabolism proteins (Kültz, 2005). Notothenioid fishes are known to significantly elevate their resting metabolic rates at these temperatures, which could in turn lead to a significant increase in the potential for oxidative damage to macro molecules (Enzor et al., 2013). Thus, in organisms adapted to extreme environments such as the notothenioids where the

HSR has largely been lost, these additional CSR mechanisms could play a more significant role in maintaining cellular homeostasis.

The alteration of cellular redox potential due to stress is a major trigger of the CSR and the expression of certain reductases, redoxins and dehydrogenases signify a robust CSR to changing conditions (Adler, Yin, Tew, & Ronai, 1999; Kültz, 2005). We analyzed these redox regulators using our dataset to provide preliminary insight into the broader CSR of *T. bernacchii*. Each tissue demonstrated a general trend of up-regulation of redox regulators with all but three of the annotated redox regulators being up-regulated in at least two tissues (aldehyde reductase, aldehyde dehydrogenase, isocitrate dehydrogenase), and 4 of 8 up-regulated in all three tissues (thioredoxin, peroxiredoxin, superoxide dismutase, succinate dehydrogenase) (Fig. 1.8). The brain tissue displayed the greatest magnitude of response for redox regulators, with 7 of 8 redox regulators up-regulated 2-fold or greater compared to the liver in which only 5 were found up-regulated and only 1 redox regulator up-regulated 2-fold or more (Fig. 1.8). While *T. bernacchii* does appear to up-regulate redox regulators as part of its CSR, much like the HSPs, the ability to increase the expression of redox regulators may be moderated to some extent and is highly tissue specific.

High Mobility Group B1 protein and its role as a global temperature sensor

Previous studies have indicated that the high mobility group b1 (HMGB1) protein, which has a key function in the assembly of transcription initiation and enhanceosome complexes, may serve as a gene expression temperature sensor in fish (Podrabsky & Somero, 2004). When subjecting the killifish *Austrofundulus limneaus* to heat shock conditions, the killifish responded by reducing its expression of HMGB1

(Podrabsky & Somero, 2004). The expression levels of HMGB1 in *T. bernacchii* support the idea that HMGB1 is highly responsive to temperature and may serve as a gene expression temperature sensor in fish. However, HMGB1 expression patterns in *T. bernacchii* dramatically differ with those reported for *A. limneaus*. We found HMGB1 undergoes substantial up-regulation when exposed to chronic thermal stress, not down-regulation as seen in the killifish. In all three tissues characterized in this study, HMGB1 showed a 2-fold or greater increase in expressed transcripts when acclimated to elevated temperatures. If we consider the functional role of HMGB1 we might be able to draft some potential insight into these contradictory results.

HMGB1 has two functional roles, an intra-nuclear function where it positively regulates transcription by affecting chromatin structure (Skoko, Wong, Johnson, & Marko, 2004), and an intracellular role (demonstrated in human models) where it can stimulate the inflammatory process by stimulating cytokines from endothelial cells, monocytes and macrophages (Andersson et al., 2000; Bae & Rezaie, 2011; Fiuza et al., 2003). *T. bernacchii* may be increasing intracellular levels of HMGB1 during exposure to elevated temperatures to increase transcription rates, restructure membrane components and increase aerobic capacity to in an effort to meet an elevated demand for oxygen associated with acclimation to these temperatures (Enzor et al., 2013). Alternatively, it is possible that the increased expression of HMGB1 is a result of inflammation due to cellular damage sustained from the +4 °C acclimation temperature. While it is unclear if the differences in HMGB1 regulation in *T. bernacchii* and *A. limneaus* are representative of the adaptive differences between the species, or potentially related to the difference in

acclimation times used within the two studies, these data further supports the case for HMGB1 as an important regulator of thermal stress response in fish.

1.4 CONCLUSION

To our knowledge this is the first large-scale effort aimed at sequencing and assembling the transcriptome of a species from the ecologically important subfamily Trematominae. With this dataset, we now have an annotated transcriptome from at least one member of all three major subfamilies in Notheniidae. Our sequencing, assembly, and annotation efforts yielded an annotated transcriptome library for *T. bernacchii* containing 30,107 unigenes of which 13,003 possess strong homology to known proteins. The subsequent application of this library to characterize tissue specific changes in relative abundance using raw sequencing reads allowed us to observe the transcriptomic composition of a polar organism in much greater detail than previously available. Our preliminary RNAseq analysis of a portion of the CSR demonstrates the potential of digital gene expression analysis to greatly increase our understanding of notothenioids, and polar organisms in general, on a genomic level.

Continued efforts to refine these resources for *T. bernacchii* may well serve to establish these unique fish as a ‘model’ organism for research in polar adapted species and as an important part of a greater effort to increase the genomic resources for polar organisms that inhabit the extreme, yet static polar environments like the Southern Ocean. As global climate change accelerates, and its effects are experienced most rapidly and dramatically at high latitudes (Walther et al., 2002), continued generation of these

resources will prove vital to our understanding of the adaptive potential of endemic polar organisms.

1.5 METHODS

Tissue collection and RNA extraction

All procedures were conducted in accordance with the Animal Welfare Act and were approved by the University of South Carolina Institutional Animal Care and Use Committee (ACUP protocol # 100377). To obtain a broad representation of genes expressed in various tissues under normal and stressed conditions, we used gill, liver and brain tissue that had been collected from a total of ten different fish acclimated to either -1.5 °C or +4 °C (n=5 fish per treatment) for 28 d in flow-through seawater tanks located in the Crary Science and Engineering Center at McMurdo Station Antarctica.

Immediately after euthanizing the fish, tissues were excised in a -2 °C environmental chamber and flash frozen in liquid nitrogen and shipped back to our home institution on dry ice where they were stored at -80 °C until used. Total RNA from approximately 100 mg of frozen tissue was extracted using TRIzol (Invitrogen) following the manufacturer's recommendations. The RNA was further cleaned by re-suspending in 0.1 ml of RNase/DNase-free water and adding 0.3 ml of 6 M guanidine HCl and 0.2 ml of 100% ethylalcohol (EtOH). The entire volume was loaded onto a spin column (Ambion) and centrifuged for 1 min at $12,000 \times g$ at 4 °C. Flow-through was discarded, and filters were washed twice with 0.2 ml 80% EtOH. RNA was eluted off of the filters twice with 0.1 ml of DEPC-treated water. RNA was precipitated by the addition of 0.1 vol of 3 M sodium acetate (pH 5.0) and 2.5 vol of 100% EtOH, mixed by inversion of tubes and placed at -

80 °C for 1 h. After this period, tubes were centrifuged at $12,000 \times g$ for 20 min at 4° C. Pellets were washed twice with 80% EtOH and re-suspended in 30 µl of RNase/ DNase-free water. Lastly, RNA was DNase treated at 30 °C for 10 min. After quality assessment and determination of specific concentration using an Agilent 2100 BioAnalyzer and picogreen assay respectively.

cDNA library preparation and 454 sequencing

For each tissue, 10 µg of total RNA from all individuals within a thermal acclimation treatment (n=5 fish) was pooled and tissue specific, double-stranded cDNA libraries were synthesized using the SMART cDNA synthesis and amplification method (Shagin et al., 2002). To increase the representation of lowly expressed transcripts, SMART-prepared cDNA was then normalized using duplex-specific nuclease (DSN) method (Shagin et al., 2002; Zhulidov et al., 2004) that was modified for downstream compatibility with Roche FLX titanium chemistry and 454 pyrosequencing. Briefly, first strand cDNA synthesis was carried out using a SMART cDNA Library Construction kit (Clontech) according to the manufacturer's recommended protocol except for the use of a modified CDS-3M adapter (5' – AAG CAG TGG TAT CAA CGC AGA GTG GCC GAG GCG GCC TTT GTT TTT TTT TCT TTT TTT TTT VN – 3'). Second strand synthesis and amplification was carried out using an Advantage 2 PCR kit (Clontech), purified using a QiaQuick PCR purification kit (Qiagen) and quantified with picogreen Quant-iT (Invitrogen). The amplified library was then DSN normalized with a Trimmer-Direct cDNA Normalization kit (Evrogen) followed by amplification of the normalized cDNA. The normalized cDNA was then proteinase K treated, *sfiI* digested and size fractionated using chromaspin 400 columns (Clontech) according to the published

SMART cDNA protocol. Lastly, the tissue specific libraries from each thermal acclimation treatment were barcoded with MID-tags and pyrosequencing was carried out using Titanium FLX chemistry on a Roche GS-FLX sequencer by the engencore facility at the University of South Carolina.

Sequence filtering, de novo assembly, and assembly validation: To maximize the relatively high accuracy of Roche GS-FLX 454 sequencing and to ensure a more accurate *de novo* transcriptome assembly we accepted sequences for assembly only after a stringent quality control and trimming process. The 454 sequence primers for the plus strand (CGTATCGCCTCCCTCGCGCCATCAG) and for the minus strand (CTATGCGCCTTGCCAGCCCGCTCAG) were removed. Sequences were then screened for ambiguity and quality; all sequences of low quality (limit = 0.05) or with more than three consecutive ambiguous nucleotides were trimmed or removed if no untrimmed sequence remained.

De novo assembly was conducted using the CLC Genomics Workbench *de novo* assembly tool (CLC Bio, 2012a). A word size of 21 and bubble size of 320 were selected as parameters because of the relatively high accuracy of 454 sequencing, and the moderate coverage depth (roughly 8X based upon the expectation of 30,000 genes within the transcriptome (Ensembl, n.d.), an average gene length of 1,350 (L. Xu et al., 2006), and ~250,000,000 total bases sequenced) to maximize accuracy and unigene length (CLC Bio, 2012b). Reads were mapped back to the unigenes with a minimum percent identity = 0.9 and minimum length = 0.5.

To validate the accuracy of the *de novo* assembly, absent a significantly similar, fully annotated reference genome, the resulting unigenes were gathered into a BLAST

database and sequence similarity was compared to all known full and partial protein sequences available for *T. bernacchii* on NCBI unigene database using tBLASTn (*e*-value 10^{-10} , word size 3, gap penalty -9, gap extension penalty -2, mismatch penalty -2, match award 1) (Altschul et al., 1990). The distribution of the *e*-value and greatest percent identity between unigene query and protein result was gathered and greatest percent identity charted to demonstrate the quality and accuracy of the resulting *de novo* transcriptome assembly.

Transcriptome annotation and analysis

The resulting unigenes were loaded in the BLAST2GO software package (B2GO) for further analysis (Conesa et al., 2005). Using the unigenes as query sequences, BLASTx searches were conducted against the non-redundant protein sequences (nr) database and BLASTn searches were conducted against nucleotide collection (nr/nt) database at NCBI, the acceptance cutoff was an *e*-value of 10^{-3} . Unigenes with BLAST results were mapped and annotated using the mapping and annotation functions of B2GO. InterProScan searches were conducted for each unigene (Jones et al., 2014) and all annotation information was merged into the B2GO interface generating our final gene ontology (GO) annotations. GO annotations were exported from B2GO in Web Gene Ontology (WEGO) format and input into the BGI WEGO Annotation Plotting tool to provide the gene ontology distribution of the *T. bernacchii* transcriptome at GO level 2 (Ye et al., 2006). Pathway assignments were determined using the Kyoto Encyclopedia of Genes and Genomes pathway database (KEGG) (Kanehisa & Goto, 2000) using a BLASTx threshold cutoff of 10^{-5} .

Tissue Specific Gene Expression

Reads from each tissue (liver, gill and brain) and treatment (-1.5 °C control and +4 °C acclimated fish) were individually analyzed to characterize the functional representation of expressed genes. The CLC Genomics Workbench RNAseq analysis tool was employed to calculate read expression for each sample using the unigene library as the reference transcriptome. The sequencing reads from each tissue were mapped back to the reference unigenes based upon a minimum similarity of 0.9 and length fraction of 0.5 (Mortazavi, Williams, McCue, Schaeffer, & Wold, 2008). Any unigene with at least one successfully mapped sequencing read from either treatment was deemed expressed in that tissue sample. Expressed unigene subsets were created for each tissue type in B2GO to provide tissue specific gene ontology and used to generate a graphical comparison of the transcriptome and tissue specific gene ontology. Furthermore, the enzyme code distribution for each tissue was generated using B2GO and compared between tissues. Lastly, the pathway assignments of the expressed unigenes in each tissue were determined using the KEGG database with a BLASTx *e*-value cutoff of 10^{-5} and compared between the full transcriptome and specific tissues.

Digital Gene Expression Analysis

The results obtained from the RNAseq analysis of the control and heat shock groups of each tissue were input into the Transcriptomics Experimental Design Tool within the CLC genomics workbench to generate a paired samples expression analysis for each tissue. The experimental results were refined by removing any paired sample that did not exhibit expression in at least one treatment. Experimental pairs were annotated using the annotated unigene transcriptome library. Lastly, a Pearson correlation

hierarchical clustering using average linkage was performed on each tissue sample in the CLC Genomics Workbench to visualize differential gene expression between treatments in similarly expressed groups.

Table 1.1. Read Sequencing and *de novo* Assembly Statistics

Sequencing and Assembly Statistics	
Reads sequenced	738,379
Reads after screening	735,507
Assembled reads	468,721
Singletons reads	266,786
Unigene count	30,107
Average unigene length (bp)	605
Coverage (X)	6.45
N75	466
N50	671
N25	1,085

Table 1.2. *T. bernacchii* Unigene BLAST Comparison Against 9 Teleost Fish

Species	Sequences available for subject species	<i>T. bernacchii</i> hit e-Value < 10⁻³	<i>T. bernacchii</i> hit e-Value < 10⁻¹⁰
<i>Notothenia coriiceps</i>	34,371	19,235	15,861
<i>Chaenocephalus aceratus</i>	17,233	14,533	10,138
<i>Pleuragramma antarcticum</i>	19,945	16,822	10,033
<i>Gasterosteus aculeatus</i>	27,576	9,056	8,010
<i>Takifugu rubripes</i>	47,841	8,539	7,541
<i>Oryzias latipes</i>	24,674	8,686	7,630
<i>Tetraodon nigroviridis</i>	23,118	8,382	7,393
<i>Oreochromis niloticus</i>	26,763	9,116	8,066
<i>Danio rerio</i>	43,309	8,972	7,800

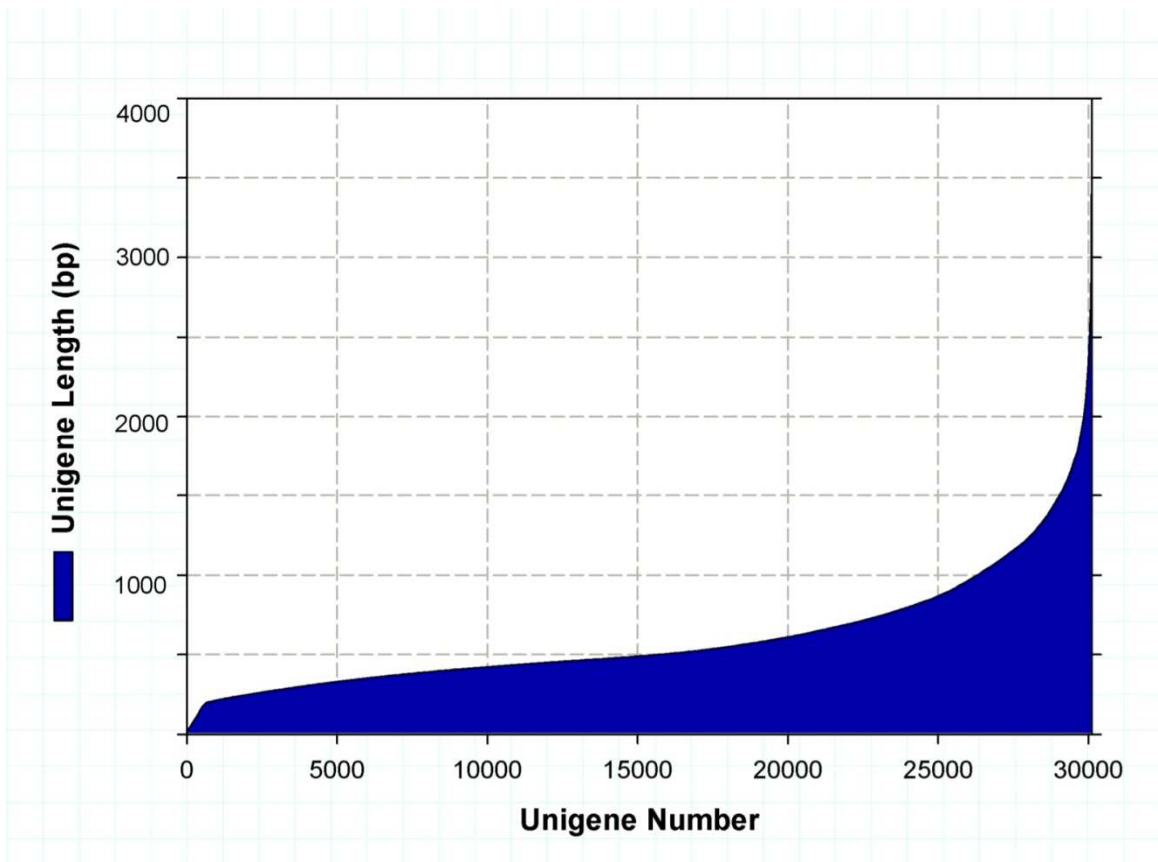


Figure 1.1: *De novo* assembly unigene length distribution. Length distribution of unigene sequence obtained from the *de novo* assembly. The unigenes are grouped from shortest to longest with each column representing the number of unigenes of that specific length.

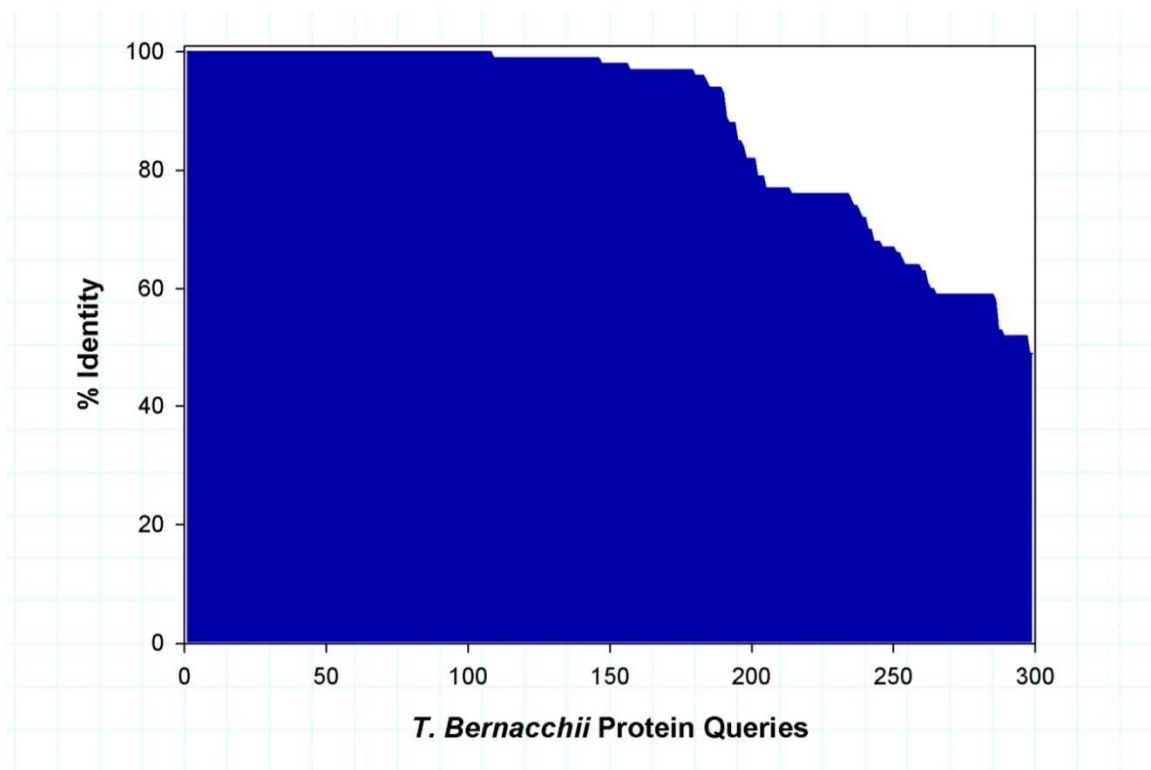


Figure 1.2: BLAST results: *T. bernacchii* protein sequences vs. unigene sequences. The percent identity of each known *T. bernacchii* full or partial protein sequence versus a unigene from the assembled transcriptome. 299 of 303 query sequences of known *T. bernacchii* protein sequences matched a unigene with an e -value cutoff of 10^{-10} , and of those 184 matched a unigene at greater than 95% identity.

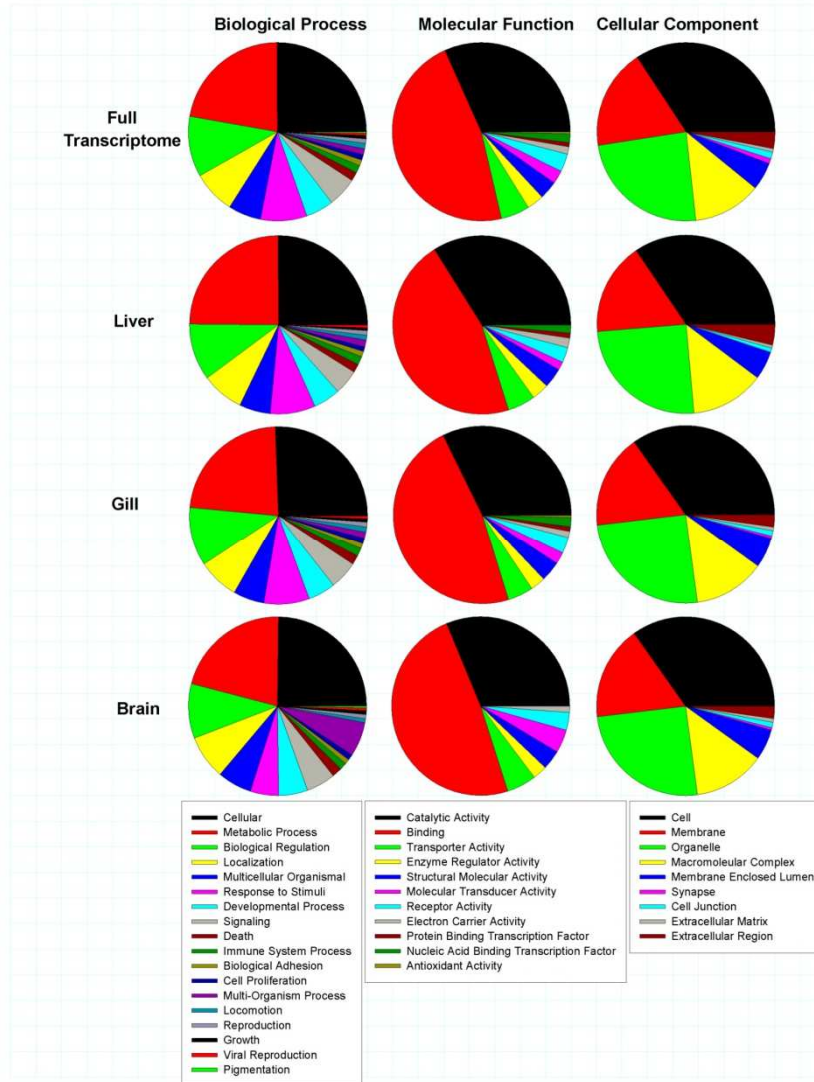


Figure 1.3: Tissue specific GO comparison. Unigenes expressed in at least one treatment were included in the gene ontology analysis. GO terms were determined using BLAST2GO (Enzor & Place, 2014) with an e -value cut off of 10^{-5} , a minimum sequence filter of 25, and sorted based on level 2 GO classifications. Any GO term that met the filter for the minimum number of sequences to include as a node ($n = 25$) was included in the comparison.

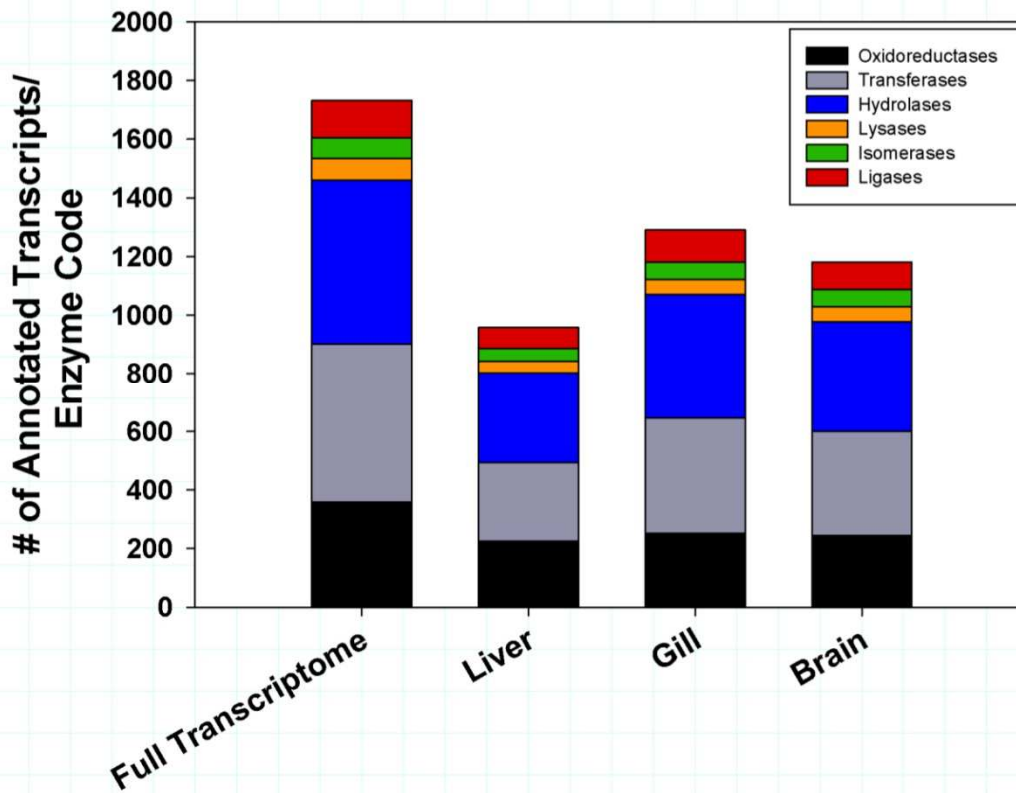


Figure 1.4: Tissue specific enzyme code distribution of *T. bernacchii*. The stacked columns represent the number of annotated transcripts obtained from each tissue whose function could be classified by a specific enzyme code. As a comparison, the total number of enzyme codes identified in the fully assembled transcriptome is provided on the left column. The main enzyme classes included in this analysis were oxidoreductases (black bar), transferases (grey), hydrolases (blue), lysases (orange), isomerases (green) and ligases (red). Enzyme codes were determined using BLAST2GO with an *e*-value cut off of 10^{-5} .

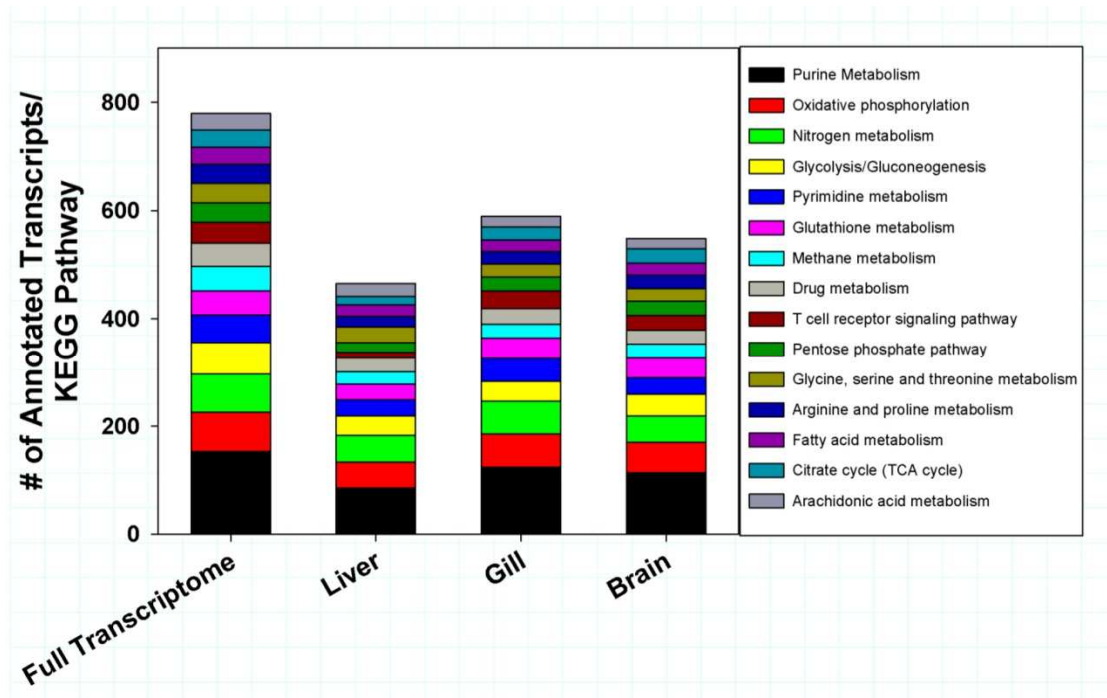


Figure 1.5: Categorization of *T. bernacchii* unigenes to KEGG biochemical pathways. A KEGG biochemical pathway analysis was performed on the full transcriptome and individual tissue transcriptomes using every unigenes expressed in at least one treatment. The stacked columns represent the top 15 KEGG pathways found in the full transcriptome and their distribution in each tissue, using an e -value cut off of 10^{-5} and minimum pathway assignment cutoff of 30.

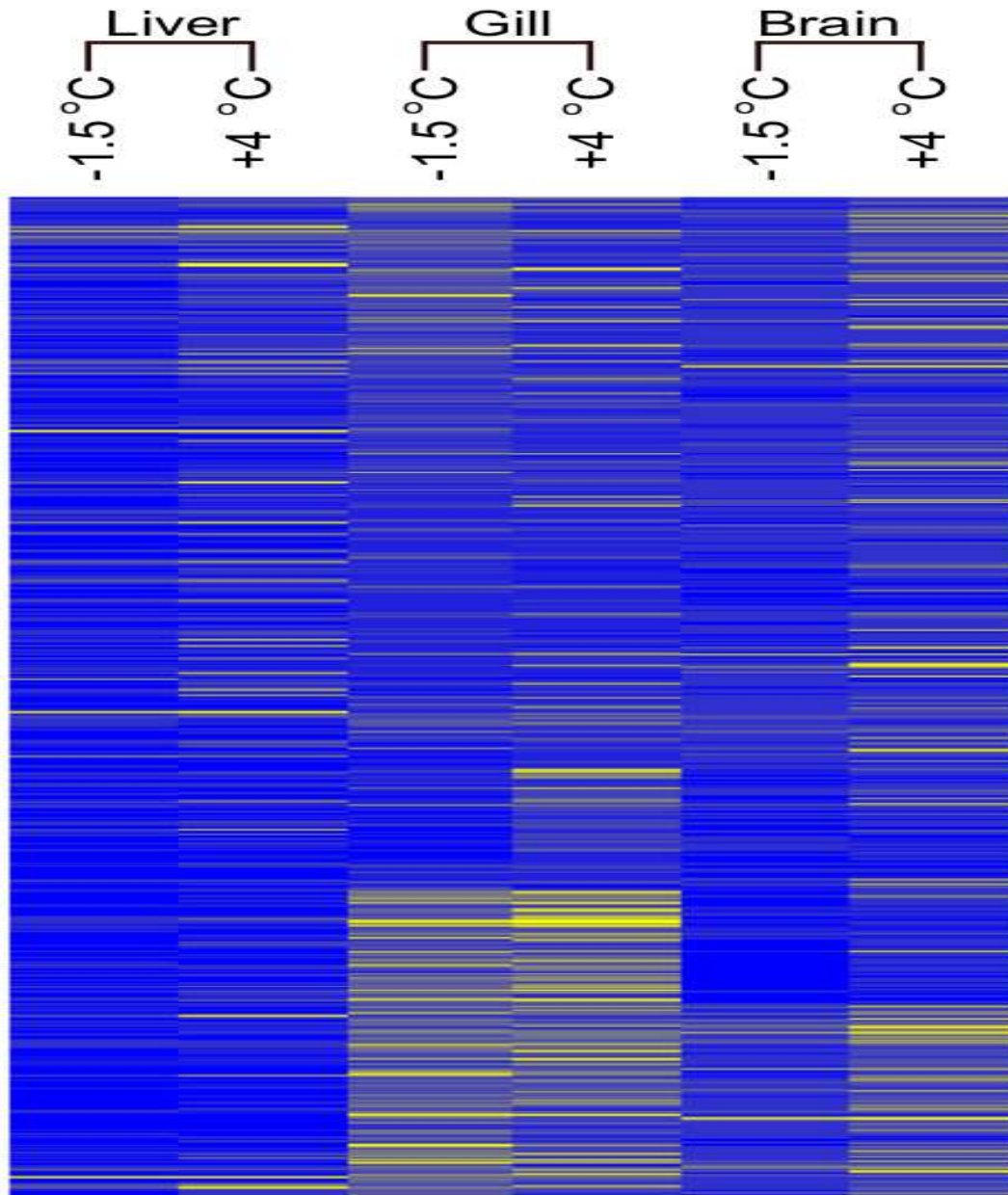


Figure 1.6: Heatmap of the relative changes in unigene abundance across treatments. Unigenes expressed in at least one treatment and featuring GO annotation were included in the feature clustering via Pearson correlation using average linkage. A deep blue color represents baseline (control) expression across the full transcriptome. Bright yellow color represents a minimum of 3-fold up-regulation of expression in one of the treatments in comparison to the baseline. Tissue specific expression profiles were generated by pooling RNA from all individuals within a thermal acclimation treatment (n=5 fish) prior to creation of the double-stranded cDNA libraries.

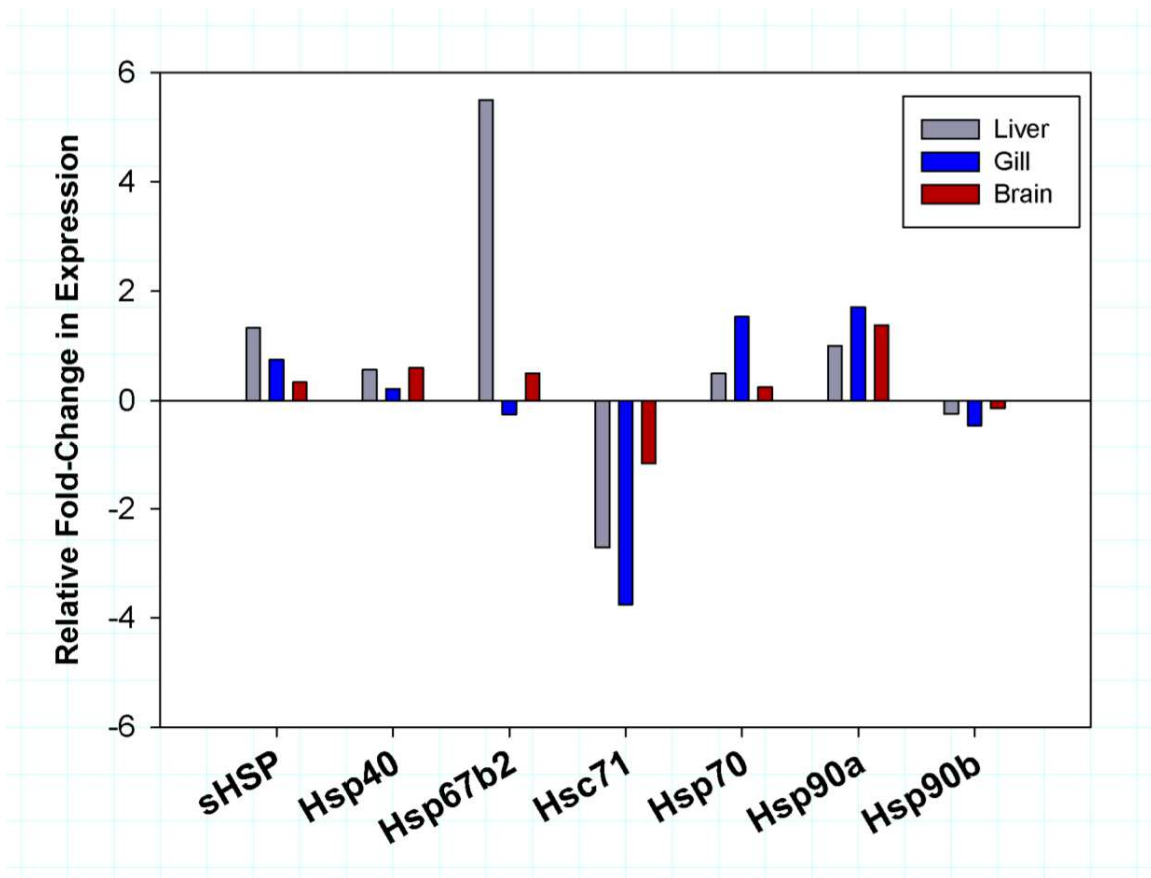


Figure 1.7: Differential expression of heat shock protein families in *T. bernacchii*. Relative fold-change in expression of annotated HSPs in +4 °C acclimated fish compared to control fish were obtained from the RNAseq analysis and directly compared across liver (grey), gill (blue) and brain (red). HSPs were grouped by gene family and the relative fold-change computed by averaging the change in expression of gene family constituents.

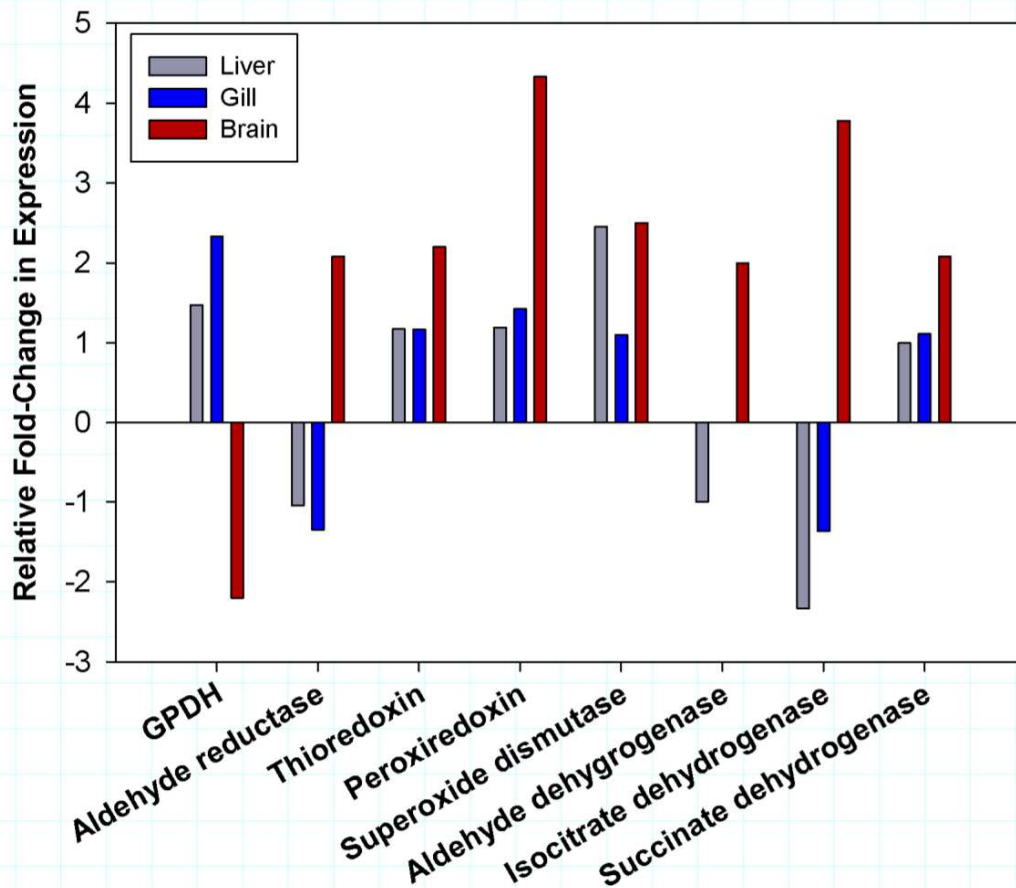


Figure 1.8: Differential expression of redox regulator proteins in *T. bernacchii*. Relative fold-change in expression of annotated redox regulator proteins in +4 °C acclimated fish compared to control fish were obtained from the RNAseq analysis and directly compared across liver (grey), gill (blue) and brain (red). Redox proteins were grouped by gene family and the relative fold-change computed by averaging the change in expression of gene family constituents.

CHAPTER 2

TRANSCRIPTOME WIDE ANALYSES REVEAL A SUSTAINED CELLULAR
STRESS RESPONSE IN THE GILL TISSUE OF *TREMATOMUS BERNACCHII*
AFTER LONG-TERM ACCLIMATION TO MULTIPLE STRESSORS.²

² Huth, T. J., & Place, S. P. Submitted to *BMC Genomics*.

2.1 ABSTRACT

Background

As global climate change progresses, the Southern Ocean surrounding Antarctica is poised to undergo potentially rapid and substantial changes in temperature and $p\text{CO}_2$. To survive in this challenging environment, the highly cold adapted endemic fauna of these waters must demonstrate sufficient plasticity to accommodate these changing conditions or face inexorable decline. Previous studies of notothenioids have focused upon the short term response to heat stress; and more recently the longer term physiological response to the combined stress of increasing temperatures and $p\text{CO}_2$. This inquiry explores the transcriptomic response of *Trematomus bernacchii* to increased temperatures and $p\text{CO}_2$ at 7, 28 and 56 days, in an attempt to discern the innate plasticity of *T. bernacchii* available to cope with a changing Southern Ocean

Results

Differential gene expression analysis supported previous research in that *T. bernacchii* exhibits no inducible heat shock response to stress conditions. However, *T. bernacchii* did demonstrate a strong stress response to the multi-stressor condition in the form of metabolic shifts, DNA damage repair, immune system processes, and activation of apoptotic pathways combined with negative regulation of cell proliferation. This response declined in magnitude over time, but aspects of this response remained detectable throughout the acclimation period.

Conclusions

When exposed to the multi-stressor condition, *T. bernacchii* demonstrates a cellular stress response that persists for a minimum of 7 days before returning to near

basal levels of expression at longer acclimation times. However, subtle changes in expression persist in fish acclimated for 56 days that may significantly affect the fitness *T. bernacchii* over time.

2.2 BACKGROUND

Isolation of the Antarctic continental shelf by the Polar Front has arguably produced the coldest, most oceanographically stable environment on the planet. However, this long-term oceanographic stability may have resulted in the evolution of an ecosystem filled with endemic fauna that are poorly poised to deal with rapid climate variation (Peck et al., 2005; Rogers, Murphy, Johnston, & Clarke, 2007). In the face of global climate change, marine organisms are perceived to have but three options: they can migrate to more favorable environments, alter their biology through physiological plasticity, or evolve in response to the altered environment (Hoegh-guldberg & Bruno, 2010; Portner & Knust, 2007; Solomon et al., 2007; Somero, 2010; Tillmann, 2011). Given the unique environment afforded by the Southern Ocean, it is highly unlikely that population migration is a viable option for its endemic biota. While evolutionary responses may benefit the species in some longer time frame, they may be outpaced by environmental change. Thus, for extant communities in the Antarctic, use of physiologically plastic responses may be the only available method of persisting under near-term future environmental variations.

The Southern Ocean is dominated by an endemic suborder of perciform fishes, the Notothenioidei (Gon & Heemstra, 1990). The effects of increased temperature on the plasticity of Antarctic fish have been well documented providing some important insight

into the physiological plasticity of a number of Antarctic fish species to a single stress (Bilyk & Cheng, 2013; Bilyk & DeVries, 2011; Bilyk et al., 2012; Davison et al., 1990; Forester et al., 1987; H. O. Pörtner et al., 2005; Esmé Robinson & Davison, 2008; Somero & DeVries, 1967). However, we have very little information regarding what impact interacting and synergistic stressors will have on the physiological tolerances of these unique fish. This is problematic for identifying physiological tipping-points for polar species, as previous measurements of their capacity to respond may be overly conservative since they do not account for non-additive effects of the joint action of multiple stressors. This point has been highlighted by recent studies that assessed the physiological response of temperate and eurythermal organisms to the combined stress of ocean acidification and elevated temperature. Results reported from these studies suggest significant trade-offs in performance and stress tolerance may exist when two or more environmental conditions are varied (O'Donnell et al., 2009; Rosa & Seibel, 2008; Schulte, 2007). An important outcome of these studies is an increased understanding among physiological ecologists that relevant assessment of species vulnerabilities will require consideration of multiple environmental variables (Gutt et al., 2014; Gretchen E Hofmann & Todgham, 2010). Equally important is the realization that it is no longer sufficient to focus on a single cellular or molecular response, but rather the consideration of multiple co-regulated processes is critical (Gretchen E Hofmann & Todgham, 2010; Place et al., 2008).

Genomics-based approaches hold the promise of greatly facilitating our understanding of physiological plasticity in these endemic fishes, especially when considering the impact dynamic environments have on multiple physiological pathways

(Bilyk & Cheng, 2014; Buckley, Gracey, & Somero, 2006; Huth & Place, 2013; Jia, Jurkowska, Zhang, Jeltsch, & Cheng, 2007). With modern genomic techniques, we can now ask: to what extent are conserved patterns of gene expression absent in the Antarctic fishes and how does this affect their ability to adjust to major changes in their environment? To this end, we have used RNA-seq analyses to profile the genomic response of an endemic Antarctic fish to predicted levels of ocean acidification and global increases in mean sea surface temperature (SST). In this investigation of multiple stressors related to climate change, our goal was to assess the molecular response of *Trematomus bernacchii* to conditions consistent with scenarios laid out by the IPCC with respect to anthropogenic increases in atmospheric CO₂ (Solomon et al., 2007) while providing direct comparison to previous studies looking at thermal stress in this organism.

2.3 RESULTS AND DISCUSSION

Reference Transcriptome

Following assembly, the transcriptomic library initially consisted of 421,044 unigenes (unique gene products including all isoforms) and 537,064 transcripts with a median transcript length of 444bp, mean transcript length of 1,011bp and N50 of 2,160bp. After removing transcripts with expression levels below 0.001 FPKM (fragments per kilobase million) and clustering at 100% identity; 314,638 transcripts and 246,333 unigenes remained. Transcript level annotation yielded 98,451 BLAST hits (1×10^{-6} cutoff value) and 34,096 GO (gene ontology) annotations.

Sequencing Read Quality Control and Mapping

Sequencing yielded an average of 27,141,939 reads (s.d. = $\pm 2,544,475$; min = 22,080,886; max = 30,834,415) per sample. Trimmomatic (Bolger, Lohse, & Usadel, 2014) quality processing retained an average of 94.28% (s.d. = $\pm 0.14\%$; min = 93.99%; max = 94.58%) of the input reads; resulting in samples containing an average of 25,591,193 reads (s.d. = $\pm 2,413,885$; min = 20,760,581; max = 29,083,777). Bowtie2 (Langmead & Salzberg, 2012) mapping achieved an average of 90.90% (s.d. = $\pm 5.76\%$; min = 89.52%; max = 91.72%) of the trimmed sequencing reads mapped to the reference transcriptome, which corresponded to an average number of mapped reads per sample of 23,261,884 (s.d. = $\pm 2,206,537$; min = 18,817,366; max = 26,562,213).

Transcriptome-wide Differential Gene Expression Analysis

Differential gene expression analysis using edgeR (M. D. Robinson, McCarthy, & Smyth, 2010) yielded a total of 4,880 differentially expressed genes across all three time points ($FDR \leq 0.05$). A sample similarity comparison demonstrated that the 7d multi-stressor treatment resulted in considerable differential gene expression when compared to the 7d control treatment (Fig. 2.1). Furthermore, the 7d multi-stressor individuals clustered as an outgroup in the cluster dendrogram of all treatments and time-points, demonstrating the consistent and distinct effect of this treatment-time combination on overall gene expression as compared to all others (Fig. 2.1). The 28d and 56d multi-stressor treatments also segregated from their respective control treatments indicating differential expression compared to the control, although to a lesser extent than the 7d multi-stressor treatment (Fig. 2.1).

Direct comparisons of the control and multi-stressor treatment at each time-point demonstrates 2,528 differentially expressed genes within the 7d multi-stressor treatment; 209 differentially expressed genes within the 28d multi-stressor treatment; and 419 differentially expressed genes within the 56d multi-stressor treatment. Of the 2,528 differentially expressed genes of the 7d multi-stressor treatment, 1,642 were up-regulated and 886 were down-regulated. Of the 209 differentially expressed genes in the 28d multi-stressor treatment 123 were up-regulated with 86 down-regulated. Lastly, the 56d multi-stressor treatment demonstrated 187 up-regulated genes and 232 down-regulated genes out of the 419 total differentially expressed. These metrics indicate a robust initial response to the 7d multi-stressor treatment, which tapers off considerably in fish acclimated to the multi-stressor treatment for 28d and 56d. A slight increase in the number of differentially expressed genes was observed between the 28d and 56d time-points which may provide insight into the long-term acclimation tactics in these fish.

Gene ontology over-representation analysis

Fisher's Exact Tests for gene ontology term over-representation further supported a robust initial transcriptome-wide response in gill tissues that diminishes over time, with the 7d stressor treatment exhibiting the most differentially expressed and over-represented gene ontology terms.

For fish within the 7d multi-stress acclimation group, GO terms within the molecular function subclasses associated with differentially up-regulated genes indicate these fish experienced large-scale cellular remodeling (Fig. 2.2). Among the up-regulated genes in the 7d multi-stressor treatment we found that GO terms associated with nucleic acid binding, transcription factor activity, helicase activity, and double-stranded RNA

binding activity were over-represented; indicating a significant change in transcription activation and RNA processing. Furthermore, the increased expression of GTPase activity, GTP binding, and tRNA ligase activity suggests a significant up-regulation of a diverse number of cellular functions such as trafficking across the nuclear membrane and protein biosynthesis in the 7d multi-stressor-acclimated group. Lastly, there also appears to be a considerable amount of protein recycling occurring in fish acclimated to the multi-stress treatment for 7 days as evidence by the significant increase in the expression of 23 genes associated with peptidase activity. This spike in protein degradation coincides with a marked increase in oxidative damaged in the same fish tissue (Enzor & Place, 2014). It has been previously demonstrated that transcriptional regulation, RNA processing, protein biosynthesis and proteolysis are highly active gene ontology groups when exposing *T. bernacchii* to short term heat stress (4°C for 4 h) (Buckley & Somero, 2009); our findings indicate that this initial cellular stress response continues well into the first 7 days. It was further observed that peptidase activity remained up-regulated in fish acclimated to the multi-stressor treatment for 28d, before being down-regulated in the 56d stressor treatment specimens.

Over-representation analysis of GO terms in the biological processes category identified a significant number of genes associated with a sustained response to cellular damage in the gill cells of fish acclimated to the 7d multi-stressor treatment (Fig. 2.3). The top 4 over-represented categories included immune system response (23 genes), response to stress (19), cell death (11), and protein ubiquitination (5). Whereas the biological processes highly over-represented in the down-regulated genes in the gill tissues of the same fish include signal transduction (54 genes), embryo or morphological

development (11), and cell proliferation (6). The over-representation of any biological processes is largely absent in fish acclimated to the multi-stressor treatment for 28d, while we observed an slight increase in the positive regulation of the cell cycle (8) and DNA metabolic processes (5) in the 56d multi-stressor treatment. Taken together, the analysis of molecular and biological functions suggest *T. bernacchii* maintains a sustained response to cellular stress in its gills for at least 7 days and returns to a homeostatic state by 28 days of acclimation. Specimens acclimated to the multi-stressor treatment may experience a second adjustment in transcriptional activity that may indicate a potentially long-term acclimation response at the 56d time-point.

Organisms experiencing environmental stress can often display two conserved responses, a rapid, transient response known as the cellular stress response (CSR) and a more permanent response termed the cellular homeostasis response (CHR) (Kültz, 2005). It is likely expression profiles observed in the 7d and then the 28d or 56d acclimated fish highlights the transition from the CSR to the CHR, and are representative of both the immediate and long-term adjustments necessary to cope with these environmental conditions. Therefore, a more detailed analysis of the biological processes found to be over-represented was conducted for cell death and immune system process; in addition to a number of more specific GO terms for biological processes potentially involved in the acclimation to multiple stressors including: carbohydrate metabolic processes, lipid metabolic processes, cell proliferation, cell death, response to stress, and homeostatic processes. These sub-categories are further investigated below in an attempt to identify specific gene products involved in the initial 7d time-point response, and those that may indicate a capacity for long term acclimation at the 28d and 56d time-points (Table 2.1).

2.4 PATHWAY SPECIFIC RESPONSES

Carbohydrate and Lipid Metabolism

Analysis of significant changes in mRNA expression levels for genes associated with the GO category for carbohydrate metabolism (Fig. 2.4) demonstrated a nearly equal number of genes that were up- and down-regulated at 7d in fish acclimated to the multi-stressor treatment relative to the control treatment (30 up-regulated, 31 down-regulated). Of the up-regulated genes in this category, nearly half (12) were associated with hydrolysis of carbohydrates while 13 genes displaying significant down-regulation were associated with carbohydrate synthesis. While fish in the 28d treatment groups displayed little difference between control and multi-stressor treatments, a closer examination of the up-regulated genes in fish acclimated to the 56d multi-stressor treatment indicated a particular up-regulation of pathways involved in the catabolism of simple sugars (triosephosphate isomerase, 2.1-fold; phosphoglycerate, 2.4-fold; fructose-bisphosphate aldolase, 108.4-fold; phosphomannomutase, 1.8-fold) and the glycolytic enzyme 2-phospho-d-glycerate hydro-lyase (aka enolase, 98.6-fold).

The same general trend was observed in lipid metabolism, with 20 genes up-regulated and 22 genes down-regulated in fish acclimated to the multi-stressor treatment for 7d, which then fell to 4 up-regulated/ 0 down-regulated in the 28d fish and 6 up-regulated/ 2 down-regulated in fish acclimated for 56d (Fig. 2.5). Of the genes found to be up-regulated at the 7d time-point, a large number of genes were associated with small molecule metabolic processes (11), most notably genes involved in phospholipid biosynthesis and membrane maintenance such as SERINC5, PLCXD1, PLCXD3, and EPT1. Among the down-regulated genes, 16 were associated with lipid biosynthesis or

catabolism (Fig. 2.5).

Previous heat stress studies in Notothenioids have demonstrated an up-regulation of genes associated with both carbohydrate and lipid metabolism, albeit it on a much shorter time scale of 4 hours (Buckley & Somero, 2009). An increased glycolytic capacity is paralleled by a significant increase in resting metabolic rates when specimens are acclimated to stressful conditions for 7 days (Enzor et al., 2013). The rapid increase in capacity and oxygen consumption likely fuels the massive cellular reorganization captured in the expression profiles of fish acclimated to the multi-stressor treatment for 7 days. Notothenioids are thought to rely primarily on lipids to fuel glycolytic metabolism under non-stressed conditions (Crockett & Sidell, 1990; H. O. Pörtner et al., 2005); however, the significant down-regulation of lipid mobilization and catabolism pathways observed after 7 days of acclimation to stressful conditions suggests *T. bernacchii* has shifted away from its reliance on lipids as a primary energy source for ATP generation. This is further reinforced by the simultaneous up-regulation of carbohydrate hydrolysis and down-regulation of carbohydrate synthesis pathways in addition to a nearly 2-fold increase in lactate dehydrogenase (LDH, 1.8-fold). Similar shifts in apparent glycolytic substrate preference have been noted for a number of other Antarctic species via changes in enzyme activity for LDH, citrate synthase (CS), cytochrome-c oxidase (cyt-c) and hydroxyacyl-CoA dehydrogenase (HOAD). In specimens of a closely related notothenioid, *Pagothenia borchgrevinki*, acclimated to elevated temperature, both LDH and cyt-c activity were found to be elevated (Seebacher, Davison, Lowe, & Franklin, 2005). A distantly related species, the eelpout *Pachycara brachycephalum*, exhibited increased cyt-c activity coupled with decreased CS activity at elevated temperatures (H.

S. Windisch, Kathover, Portner, Frickenhaus, & Lucassen, 2011). Lastly, Jayasundara et al. (2013) reported a similar increase in LDH activity coupled with decreased CS activities in *T. bernacchii* specimens acclimated to +4.5 °C (Jayasundara et al., 2013).

Following the initial cellular stress at the 7d time-point, expression of genes associated with metabolic pathways largely appeared to return to basal levels as there were very few differentially expressed genes in fish acclimated to the 28d and 56d multi-stressor treatments. However, the few genes that remain differentially expressed in the longer time periods of 28d and 56d may be evidence of the more persistent metabolic changes that are required for long-term acclimation to elevated seawater temperatures and $p\text{CO}_2$ levels. For example, the 56d multi-stressor treatment experiences a strong up-regulation of multiple diacylglycerol kinase isoforms (2.4-fold, 3.1-fold), a potential indicator of a persistently elevated challenge in maintaining the integrity of cellular membranes. Furthermore, the heavier reliance on carbohydrate utilization and anaerobic glycolysis for ATP generation may also persist beyond the initial cellular stress response observed in the first 7 days. Indeed, this apparent change in energy usage has been shown to persist for at least 14 days in *T. bernacchii* when thermally stressed (Jayasundara et al., 2013). Furthermore, we have recently collected LDH activity data in these same fish that when combined with the changes in carbohydrate catabolism pathways noted above, suggests these fish may not have fully compensated for the increased energetic demands of acclimating to this multi-stressor treatment even after nearly 2 months (Enzor & Place, 2015).

Cellular Death and Proliferation

In addition to the metabolic changes that were seen in the gill tissue of 7d multi-stressor acclimated fish, we also observed a significant change in the regulation of cell survival with the activation of several genes associated with apoptosis (Fig. 2.6). Gill tissue isolated from these fish demonstrated a significant up-regulation of a number of caspases (1.7 to 3.0-fold); and multiple suppressors of cytokine signaling (4.5 to 7.4-fold). Interestingly, a down regulation of angiopoietin-related proteins (2.3 to 4.2-fold,) and endothelial pas domain-containing proteins (2.2 to 2.3-fold), which can activate the cell's hypoxia response, are also observed at 7d.

As seen with lipid and carbohydrate metabolism, the changes in genes associated with cellular death are also heavily diminished in the 28d and 56d acclimated fish (Fig. 2.6). At 28d few genes are differentially regulated with the notable exceptions of the down-regulation of caspase-8 related genes (2.0 to 2.7-fold) which continued through the 56d treatment (2.2 to 2.5-fold decrease). Fish in both the 28d and 56d multi-stressor groups appeared to exhibit dramatic changes in expression of caspase-3 precursor (+621.7-fold and -3396.9-fold, respectively). However, a closer analysis at the individual level of the expression of this particular gene indicates that these dramatic changes in expression are driven by a single individual within each treatment group, and thus are likely an aberration.

As to cell proliferation, fish in the 7d multi-stressor treatment demonstrated a strong trend of down-regulation overall (4 up-regulated, 20 down-regulated) (Fig. 2.7) that suggests long-term cell cycle arrest may occur in the gill tissue. Specifically we observed a strong down-regulation in a number of growth factors including insulin

growth factors (7.7 to 13.0-fold); fibroblast growth factors (3.6 to 12.1-fold); myostatin (4.6-fold); bone morphogenic protein (3.4 to 3.6-fold), and platelet-derived growth factor (3.0-fold), among others. This strong negative regulation of the cell proliferation appears to be limited to the initial cellular stress response as no genes in this GO category were differentially regulated in the fish acclimated for 28d and only one was observed in fish acclimated for 56d in the multi-stressor treatment (Fig. 2.7).

Our data indicate the positive regulation of cell-cycle arrest and apoptosis observed under acute thermal challenges continue for at least 7 days into a chronic cellular stress event. Taken together with the remodeling of metabolic pathways discussed above and the physiological and biochemical analyses previously performed on these same specimens (Enzor et al., 2013; Enzor & Place, 2014), it appears *T. bernacchii* requires somewhere between 14-28 days to transition from a bio-energetically costly cellular stress response to a state of relative cellular homeostasis. However, even after 56 days of continual exposure to a multi-stressor scenario, *T. bernacchii* may not be capable of fully compensating for elevated temperatures and $p\text{CO}_2$ levels.

Response to Stress

Our results support previous studies, which found a lack of inducible heat shock response in *T. bernacchii* (Buckley, Place, & Hofmann, 2004; G E Hofmann et al., 2000; Huth & Place, 2013). Despite the considerable transcriptome-wide changes in expression demonstrated above; of the 64 heat shock and heat shock-related genes expressed in the reference transcriptome, only 7 were found to be differentially regulated ($\text{FDR} \leq 0.05$) in fish exposed to the 7d multi-stressor treatment, with none in the 28d multi-stressor treatment and only 3 in the 56d multi-stressor treatment.

Overall, of the three HSP families typically induced in a teleost heat shock response (Basu et al., 2002), there is almost no response for the HSP90, HSP70 and small HSP families. Among those heat shock proteins that did show significant changes in regulation, HSP40 demonstrated the clearest up-regulation with both HSP40 genes found to be up-regulated (2.0 and 1.9-fold) in the 7d multi-stressor treatment group. A similar trend was observed in *P. borchgrevinki* acclimated to +4 °C for 4 days. In this study, Bilyk & Cheng report HSP47 as the only HSP transcript displaying significant up-regulation in this closely related species (Bilyk & Cheng, 2014). In our previous description of the *de novo* transcriptome assembly of *T. bernacchii* we noted a down-regulation of constitutively expressed chaperones in a number of tissues after long-term (28d) acclimation to +4 °C alone (Huth & Place, 2013). Bilyk & Cheng confirmed a similar trend in liver tissues of *P. borchgrevinki* after a short-term acclimation to elevated temperatures (Bilyk & Cheng, 2014). We also noted a conspicuous 4.5-fold decrease in transcript levels for the constitutively expressed chaperone, HSC71 after 56d of acclimation to +4 °C and 1000 μ ATM $p\text{CO}_2$.

While none of the inducible HSP isoforms were differentially regulated, there did appear to be a number of endoplasmic reticulum (ER) specialized molecular chaperones that did show moderate increases in the 7d multi-stressor treatment. For instance, of the over twenty HSP70-related genes annotated in our reference library, only 2 transcripts (*hsp70-12b*, 2.3-fold and *hsp70-14*, 1.9-fold) demonstrated significant up-regulation (2.3-fold and 1.9-fold, respectively). Similarly, GRP94, a member of the Hsp90 family that plays a role in assembly of secreted proteins and is localized in the ER, was up-regulated ~ 2.5-fold in the 7d fish.

In opposition to the lack of a robust HSR, *T. bernacchii* does display a strong response to DNA damage. The gill tissue from fish acclimated to the multi-stressor treatment for 7d displayed up-regulation of a number of genes associated with activation of DNA damage response pathways (Fig. 2.8). Among the genes up-regulated are several members of the GADD45 family of proteins which mediate the activation of the p38/JNK pathway, resulting in cell cycle arrest, DNA repair, cell senescence, and apoptosis (Liebermann & Hoffman, 2008). Furthermore, two key genes directly involved in DNA repair also displayed significant increases. Proliferating cell nuclear antigen (PCNA), which has a stimulatory effect on the 3'-5' exonuclease activity of DNA polymerase and RAD2, which is a structure-specific 5'-flap endonuclease, were both up-regulated over 2-fold in 7d fish.

In one of the few studies that has looked at cell proliferation and DNA damage in Antarctic fish under conditions of cellular stress, Sleadd et al. (2014) found a significant increase in PCNA protein concentrations in *T. bernacchii* after being held at +4 °C for 72 hours (Sleadd et al., 2014). Unlike our findings at the transcript level, Sleadd et al. (2014) found that PCNA protein levels had returned to control values by 168 hours (7d). In our multi-stressor study, we found PCNA transcript levels were still significantly elevated in the gill tissue of *T. bernacchii* after a 7d acclimation that included a +4 °C thermal stress. It is possible the additional stressor (elevated $p\text{CO}_2$) extended the response of PCNA in our study; however, given the differences in tissues observed between the two studies (gill vs liver) and the molecule considered (mRNA vs protein) it is difficult to draw more concrete conclusions.

Immune System Processes

An aggressive immune response is a common characteristic of teleosts when stressed from any number of cellular perturbations (Wendelaar Bonga, 1997) and this appeared to hold true for *T. bernacchii*. Genes associated with immune system processes demonstrated a general trend of up-regulation in the 7d multi-stressor treatment (39 up-regulated, 14 down-regulated) (Fig. 2.9). Unlike many of the other GO sub-categories assessed in this study, a more sustained differential gene expression response was observed within immune system processes (7 up-regulated at 28d; 5 up-regulated, 4-down regulated at 56d) (Fig. 2.9).

This response is highlighted by the up-regulation of a number of chemokines (CXCL6, 11.3-fold; CXCL, 3.7-fold; CXCL11, 14.4-fold) that recruit elements of the immune system including macrophages, t-cells and neutrophils (Cole et al., 1998; Wuyts et al., 1997). The notable exception is the down-regulation of CXCL-14 (2.8-fold), which is thought to inhibit the signaling action of CXCL-12 and immune cell migration (Hara & Tanegashima, 2014). In addition to members of the CXC-type chemokine family, the strong up-regulation of SOCS1, which is thought to serve a vital role in both innate and adaptive immune responses (Alexander & Hilton, 2004; Ben-Zvi, Yayon, Gertler, & Monsonogo-Ornan, 2006), further supports the occurrence of a robust immune response to the multi-stressor treatment at the 7d time-point.

While it may be possible that the immune system is responding to a latent infection that is able to manifest due to the effects of the multi-stressor treatment on *T. bernacchii*, the more likely scenario is that the observed response is to wide spread cellular damage and remodeling directly resulting from the multi-stress treatment.

This argument is supported by indicators of cellular damage, such as PSMB9, which is also up-regulated at the 7d (2.5-fold) and 28d (2.3-fold) time-points. PSMB9, also known as 20S proteasome subunit β -1i, is an essential subunit of the proteasome and may be associated with a more specialized form of the proteasome known as the immune proteasome (Basler, Kirk, & Groettrup, 2013). PSMB9 is required for the production of MHC class-1 restricted T-cell epitopes, and thus plays an important role in antigen processing. Furthermore, a previous study measuring stress at the cellular level found that several notothenioids exhibit considerable increases in oxidative damage after 7 days of heat and $p\text{CO}_2$ stress, which diminishes, but does not cease at 28 and 56 days (Enzor & Place, 2014); indicating a sufficient level of protein damage likely exists to result in the activation of the immune proteasome seen here.

Homeostatic Processes

In teleost fish, the maintenance of ionic and acid-base homeostasis are invariably linked; however, unlike terrestrial organisms, which can alter plasma pH by increasing or decreasing ventilation rates, acid-base balance in fish requires direct exchange of ions with the external environment via specialized chloride cells within the gill epithelium (Karnaky, 1986). As such, when experiencing hypercapnic conditions, fish cannot “off-gas” CO_2 by increasing ventilation rates. The compensation for imbalance requires the direct transfer of an acid (H^+) and base (HCO_3^-) for Na^+ and Cl^- respectively, across the gills, kidneys and/or intestine (Claiborne, Edwards, & Morrison-Shetlar, 2002; Evans, Piermarini, & Choe, 2005; Gilmour & Perry, 2009; Heisler, 1989).

We found fish acclimated to the 7d multi-stressor treatment demonstrated a robust gene response associated with maintaining acid-base homeostasis. In all, 18 genes in this

GO category were significantly up-regulated while only 2 were significantly down-regulated (Fig. 2.10). As seen with previous categories, this response tapered off rapidly at 28d (2 up-regulated), and transitioned into a potentially more permanent physiological state at 56d with 5 genes up-regulated and 4 down-regulated (Fig. 2.10). Sodium-hydrogen exchangers are known to be a primary mechanism for acid-base regulation in the gill tissue of fish, with fish excreting protons in order to achieve acid-base homeostasis when subjected to increased CO₂ concentrations (Perry & Gilmour, 2006). The acidification resulting from the increased *p*CO₂ is likely responsible for the observed up-regulation of SLC9A5 (3.2-fold), which is a member of the sodium-hydrogen exchanger family (Bobulescu & Moe, 2006). We do observe a concurrent down-regulation of SLC9A6 (1.8-fold), however this variant is thought to localize to the mitochondria (Miyazaki, Sakaguchi, Wakabayashi, Shigekawa, & Mihara, 2001) and not the cellular plasma membrane where SLC9A5 is found, and thus is likely not involved in maintaining cellular pH counter to the external environment.

In addition to perturbations to acid-base balance, increases in temperature and decreases in pH can also impact redox potential within the cell, leading to increased oxidative stress (Lushchak, 2011). A common biomarker of oxidative stress, protein carbonyl concentrations, have previously been shown to significantly elevate in *T. bernacchii* exposed to the same multi-stressor conditions (Enzor & Place, 2014). Similarly, in the expression profiles of fish in the 7d multi-stressor treatment, we find the up-regulation of redox related proteins including TXN (thioredoxin, 2.9-fold) and SH3BGRL3 (SH3 Domain Binding Glutamate-Rich Protein Like 3, 1.9-fold). The up-

regulation of SH3BGRL3 is again seen in the 56d multi-stressor treatment (1.76 fold) suggesting a continued effort to compensate for changes in cellular redox-potential.

Interestingly, a number of genes encoding for disulfide-isomerases are also up-regulated (8 gene variants up-regulated at least 1.5 fold) in the 7d multi-stressor treatment. Protein disulfide-isomerases (“PDIs”) are known to assist in proper protein folding or corrective protein folding in the ER and play key roles in the unfolded protein response (UPR) in the lumen of the ER (Kriegenburg, 2012; Lee et al., 2010). PDIs are essential in disulfide bond formation and are likely involved in the biogenesis of a large number of membrane bound proteins necessary during cellular remodeling (Hatahet & Ruddock, 2009). Their up-regulation is a further indication of the large-scale changes involving membrane bound processes such as ion regulation, acid-base balance and potentially even the redox potential of mitochondria.

The concurrent up-regulation of pH regulators, redox regulators and disulfide isomerases at the 7 day time-point in the multi-stressor condition is indicative of the challenges *T. bernacchii* faces in maintaining homeostasis under these conditions. After the short term acclimation response, *T. bernacchii* no longer experiences dramatic changes in expression of proteins related to the maintenance of cellular homeostasis, suggesting these fish are capable of at least partially compensating for the changes in extracellular pH and osmolarity likely caused by the multi-stressor condition. A notable exception is the continued up-regulation of SH3BGRL3, which may indicate the continued need for assisted folding of membrane associated proteins under the multi-stressor condition and may be representative of a long-term cost to cellular maintenance.

2.5 CONCLUSION

Our efforts have uncovered several key findings concerning the molecular response of *T. bernacchii* under the multi-stressor condition brought on by increased sea surface temperature and ocean acidification. First, although previous studies using acute thermal stress suggest a portion of the conserved cellular stress response is retained in these fish, we have now shown that *T. bernacchii* is capable of mounting a robust and coordinated response to stress and that this response persists for at least 7 days and perhaps as long as 2 weeks. Among the conserved responses observed were DNA repair pathways accompanied by cell-cycle arrest and apoptosis; maintenance of acid-base balance and redox-potential; and cytokine signaling and cellular inflammation. As found in previous studies under heat stress alone, *T. bernacchii* does not possess an inducible heat shock response when exposed to synergistic heat and $p\text{CO}_2$ stress. However, the up-regulation of chaperones and PDIs localized in the ER may indicate the unfolded-protein response of the ER remains intact in these fish.

Second, the multi-stressor treatment results in significant cellular damage that continues for at least 7 days after the initial exposure. In addition to the increase in oxidatively damaged proteins previously noted in these fish, there also appears to be a significant amount of DNA damage accrued as indicated by the up-regulation of pathways associated with cellular death, DNA damage responses, and immune system responses. And third, the multi-stressor treatment induces a strong initial response that likely comes at a significant energetic cost to the organism. In addition to the activation of stress responsive pathways, we also observed changes in gene expression patterns that

suggest a shift in substrate preference for glycolysis and the possible reliance on anaerobic pathways to supplement ATP generation.

Our findings demonstrate that the multi-stressor condition induces a strong short term response that may temporarily reduce *T. bernacchii*'s overall fitness. However, *T. bernacchii* returns to near basal levels of expression within most of the studied pathways, indicating some degree of compensation to the environmental changes has set in. This would seem to indicate that *T. bernacchii* possesses the physiological plasticity to cope with an environment similar to the multi-stressor condition and thus also with the changing climate of the Southern Ocean.

However, we must approach such a conclusion with caution. Although our study demonstrates that after 56 days of exposure to the multi-stressor condition, expression levels across the transcriptome and largely returned to near basal levels, we did identify subtle changes in expression that persist through the 56d time-point (such as shifts towards carbohydrate metabolism) that may significantly affect *T. bernacchii*'s fitness over a longer period of time. Furthermore, as this study focused upon the gills of adult fish only, and did not investigate juveniles, other tissues, or the overall reproductive cycle; it is difficult to surmise the overall effect that these synergistic stressors may have on the fitness of *T. bernacchii* at the population level and over the course of many generations. Further inquiry is necessary to address these concerns, and to further elucidate *T. bernacchii*'s potential to adapt to changing environmental conditions.

2.6 METHODS

Collection of fish

Specimens of *T. bernacchii* were collected in McMurdo Sound, Antarctica from September through December, 2012. Fish were caught using hook and line through 10-inch holes drilled through the sea ice and transported back to McMurdo Station in aerated coolers where they were housed in a flow-through aquaria maintained at ambient seawater temperature (-1.5°C). Fish were then tank-acclimated under ambient conditions for one week prior to being placed in experimental tanks. All procedures were conducted in accordance with the Animal Welfare Act and were approved by the University of South Carolina Institutional Animal Care and Use Committee (ACUP protocol # 100377).

Experimental Design

We used four, 1240 L experimental tanks to assess the combined effects of elevated temperature and $p\text{CO}_2$ on *T. bernacchii*. Our two experimental treatments consisted of a control tank which was held near ambient conditions (-1°C and 430 μatm) and a high temperature + high $p\text{CO}_2$ treatment (+4°C/ 1000 μatm). Fish were placed in experimental tanks and acclimated for a total of 56 days. Five fish per treatment were removed at 7d, 28d, and 56d time-points, after which fish were sacrificed and gill tissues were collected and immediately flash-frozen in liquid nitrogen. Although we recognize a fully replicated experimental design is ideal to exclude tank effects as a possible confounding factor, the constraints of working in Antarctica prevented us from using this approach. However, our previous analyses show no tank effect when treatments were

alternated between tanks across multiple seasons (Enzor et al., 2013; Enzor & Place, 2014).

Manipulation of seawater conditions

Temperature and $p\text{CO}_2$ levels were manipulated within the experimental treatment tanks using a $p\text{CO}_2$ generation system first described by Fangué et al. (2010) (Fangué et al., 2010) and adapted for use with large-scale applications and combined with thermostated titanium heaters (Process Technology, Brookfield CT, USA; Enzor et al. (2013) (Enzor et al., 2013)). Atmospheric air was pumped through drying columns (filled with drierite) to remove moisture, and air was scrubbed of CO_2 using columns filled with Sodasorb. Pure CO_2 and CO_2 -free air were then blended using digital mass flow controllers and bubbled into header tanks that were continuously replenished with ambient seawater using venturri injectors, which in turn fed into experimental treatment tanks.

Temperature, pH (total scale), salinity, total alkalinity (T_A) and oxygen saturation were measured daily from both incoming seawater as well as experimental treatment tanks. For $p\text{CO}_2$ analysis, we followed the SOP as described in the Best Practices Guide (Gattuso, Bijma, Gehlen, Riebesell, & Turley, 2011) for the spectrophotometric determination of pH using m-cresol purple and measurement of total alkalinity via acid titration using a computer-controlled T50 Titrator (Mettler Toledo, Columbus, OH, USA). Temperature was measured with a calibrated digital thermocouple (Omega Engineering Inc., Stamford, CT, USA) and salinity was measured using a YSI 3100 Conductivity meter (Yellow Springs, OH, USA). CO_2 *calc* (Robbins, Hansen, Kleypas, & Meylan, 2010), using the constants of Mehrbach et al. (1973) (Mehrbach et al., 1973) as

refit by Dickson & Millero (1987) (Dickson & Millero, 1987), was used to calculate all other carbonate parameters. Oxygen saturation was recorded using a galvanic oxygen probe (Loligo Systems, Denmark). Mean values (\pm s.d.) of temperature ($^{\circ}\text{C}$) and $p\text{CO}_2$ (μatm) over the course of the experiment were first reported in Enzor and Place (2014) (Enzor & Place, 2014). Additionally, treatment tanks were sampled daily for the presence of ammonia, nitrite and nitrates, with no significant increase in waste products noted over the course of the experiment (data not shown).

Tissue collection and RNA extraction

To obtain individual gill-specific expression profiles, we separately indexed and sequenced RNA samples from gill tissue that had been collected from fish acclimated to the two experimental treatments described above ($n=5$ fish per treatment) for 7 days, 28 days and 56 days. Immediately after euthanizing the fish, tissues were excised in a -2°C environmental chamber, flash frozen in liquid nitrogen, and shipped back to our home institution on dry ice where they were stored at -80°C until used. Total RNA from approximately 100 mg of frozen tissue was extracted using TRIzol (Invitrogen) following the manufacturer's recommendations. The RNA was further cleaned by re-suspending in 0.1 ml of RNase/ DNase-free water and adding 0.3 ml of 6 M guanidine HCl and 0.2 ml of 100% ethylalcohol (EtOH). The entire volume was loaded onto a spin column (Ambion) and centrifuged for 1 min at $12,000 \times g$ at 4°C . Flow-through was discarded, and filters were washed twice with 0.2 ml 80% EtOH. RNA was eluted off of the filters twice with 0.1 ml of DEPC-treated water. RNA was precipitated by the addition of 0.1 vol of 3 M sodium acetate (pH 5.0) and 2.5 vol of 100% EtOH, mixed by inversion of tubes and placed at -80°C for 1 h. After this period, tubes were centrifuged at $12,000 \times g$

for 20 min at 4° C. Pellets were washed twice with 80% EtOH and re-suspended in 30 µl of RNase/ DNase-free water. Lastly, RNA was DNase treated at 30 °C for 10 min. Total RNA from n=5 fish within an acclimation treatment was submitted to the Vaccine and Gene Therapy Institute (VGTI) Florida for quality assessment and determination of specific concentration using an Agilent 2100 BioAnalyzer. From the original samples, the 4 highest quality replicates from each treatment and time point were selected for cluster generation using the Illumina® TruSeq RNA Sample Prep v2 Hs Protocol and sequencing via an Illumina® HiSeq 2500 Rapid Run initialized for single-end 100bp reads.

Sequencing Read Quality Control and Mapping

Raw reads from each of the twenty-four samples were processed using Trimmomatic (Bolger et al., 2014). Illumina® TruSeq RNA Sample Prep v2 HS adapters were removed as well as any bases on the end of the reads with a PHRED33 score of <20 or any portion of the read that did not average at least a PHRED33 score >20 across a minimum span of 4bp (Trimmomatic parameter input: ILLUMINACLIP:Trimmomatic-0.32/adapters/TruSeq2-SEMultiplex.fa:2:30:10 LEADING:20 TRAILING:20 SLIDINGWINDOW:4:20 MINLEN:75). Following trimming, only sequencing reads ≥ 75 bp in length were retained. The remaining sequencing reads were individually mapped to an existing transcriptome using Bowtie2-2.2.3 with standard parameters (Langmead & Salzberg, 2012). The transcriptome employed as a reference was an enhancement of the previously published *T. bernacchii* transcriptome (Huth & Place, 2013) using 150bp paired-end Illumina reads as additional input into the Trinity Assembly program (Grabherr et al., 2011) under default parameters. Assembly was

conducted on the XSEDE Blacklight Supercomputing Resource utilizing the native Trinity module (Pittsburgh Supercomputing Center - Blacklight Supercomputer, 2014). The additional Illumina reads were obtained from pooled RNA isolated from the gill, liver and brain tissue of *T. bernacchii*. After assembly the transcriptome was pruned using RSEM (Li & Dewey, 2011) with any transcripts with expression values less than 0.001 FPKM removed, and then further compacted using CD-HIT-EST (Fu, Niu, Zhu, Wu, & Li, 2012) at a percent identity of 100%. Annotation was facilitated by the XSEDE Stampede Supercomputer (Texas Advanced Computing Center - Stampede Super Computer, 2014) utilizing the native ncbi-Blast module in a massively parallel structure (Camacho et al., 2009) and then completed on local resources with the BLAST2GO command line utility (BLAST2GO Command Line, 2014).

Differential Gene Expression Analysis

Using raw mapping counts from Bowtie2 (Langmead & Salzberg, 2012), RNA-Seq by Expectation-Maximization (“RSEM” version 1.2.18) (Li & Dewey, 2011) analyses were conducted to generate estimated read-count (count) and fragments per kilobase million (FPKM) counts for each sample at the transcript and gene level. The Trinity pipeline (Trinity version trinityrnaseq_r20140717) (Haas et al., 2013) was used to aggregate these counts into master matrices for import into the *R* statistical package (R Core Team, 2013). Before import, the samples were grouped by time-point and treatment similarity to conduct pairwise analyses of the effect of the multi-stressor treatment over time as compared to the control. Empirical analysis of digital gene expression data in *R* (“edgeR” version 3.4.2) was implemented to conduct differential gene expression analyses (M. D. Robinson et al., 2010); dispersion values were calculated using the

replicate groups; and exact tests utilizing a negative binomial distribution with a cutoff false discovery rate of 0.05 were used to identify differentially expressed transcripts and genes.

A sample-level differential expression heat map was generated from the differential gene expression analyses resulting from edgeR using the Trinity pipeline. Within the BLAST2GO graphical interface package (Conesa et al., 2005) Fisher's Exact tests ($FDR \leq 0.05$) were conducted for differentially expressed transcripts of the multi-stressor treatment to identify over-represented gene ontology terms within the up- and down- regulated transcripts within each treatment group in general. Using custom Python scripts annotation and expression data files were combined, and GO categories and genes of interest were extracted for further analysis.

Table 2.1: A summary of major gene ontology groups demonstrating differential gene expression at the 7d, 28d, and 56d time-points of the multi-stressor condition.

Gene Ontology Category	Total Genes Found in the Transcriptome	7d Differentially Expressed			28d Differentially Expressed			56d Differentially Expressed		
		Total	U P	DOW N	Total	U P	DOW N	Total	U P	DOW N
Carbohydrate Metabolic Process	480	61	3 0	31	2	2	0	9	8	1
Cell Death	171	32	2 0	12	3	1	2	4	1	3
Cell Proliferation	155	19	4	15	0	0	0	1	1	0
Homeostatic Process	194	20	1 8	2	2	2	0	9	5	4
Immune System Process	246	53	3 9	14	7	7	0	9	5	4
Lipid metabolic Process	409	42	2 0	22	4	4	0	8	6	2
Response to Stress	420	62	4 8	14	3	3	0	12	7	5

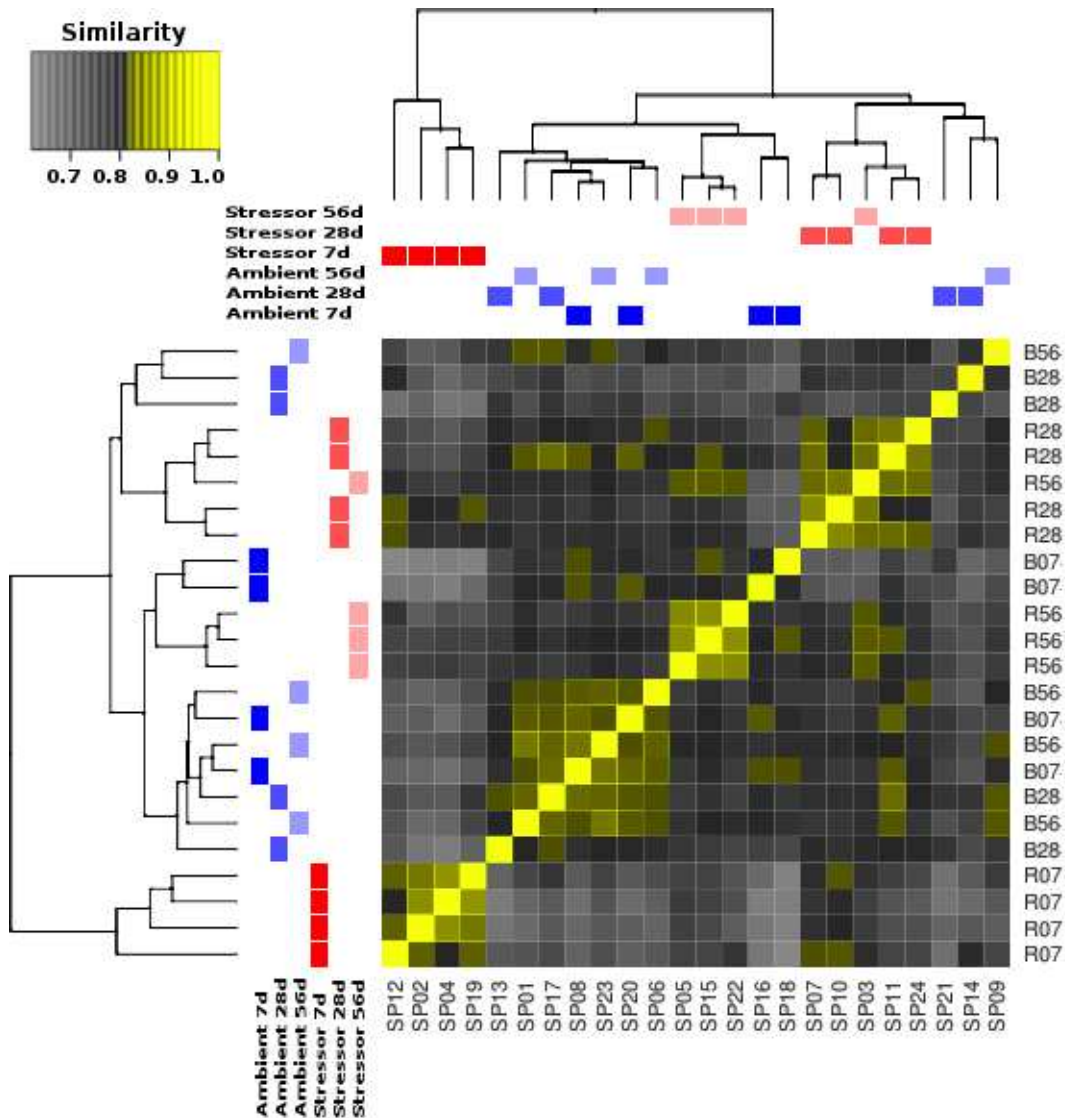


Figure 2.1: Transcriptome wide sample similarity matrix and cluster dendrogram: the sample similarity matrix represents the cumulative similarity of each individual at each time-point as a reflection of transcriptome wide gene expression. Transcriptome wide expression is represented by all gene products that demonstrated an $FDR \leq 0.05$ during the differential gene expression analysis. Portions of the matrix shown in yellow demonstrate a high degree of similarity in the transcriptomic expression profiles between the two samples, with a value of 1 indicating the samples are identical; whereas those shown in grey demonstrate a lower degree of similarity, with a value of 0.65 demonstrating the most dissimilar expression profiles between two samples. As the samples are extracted from the same tissue and species, the degree of similarity in this case is a minimum of 0.65. The cluster dendrogram also groups samples based upon similar expression profiles, with those samples grouped most closely demonstrating more analogous transcriptomic expression responses.

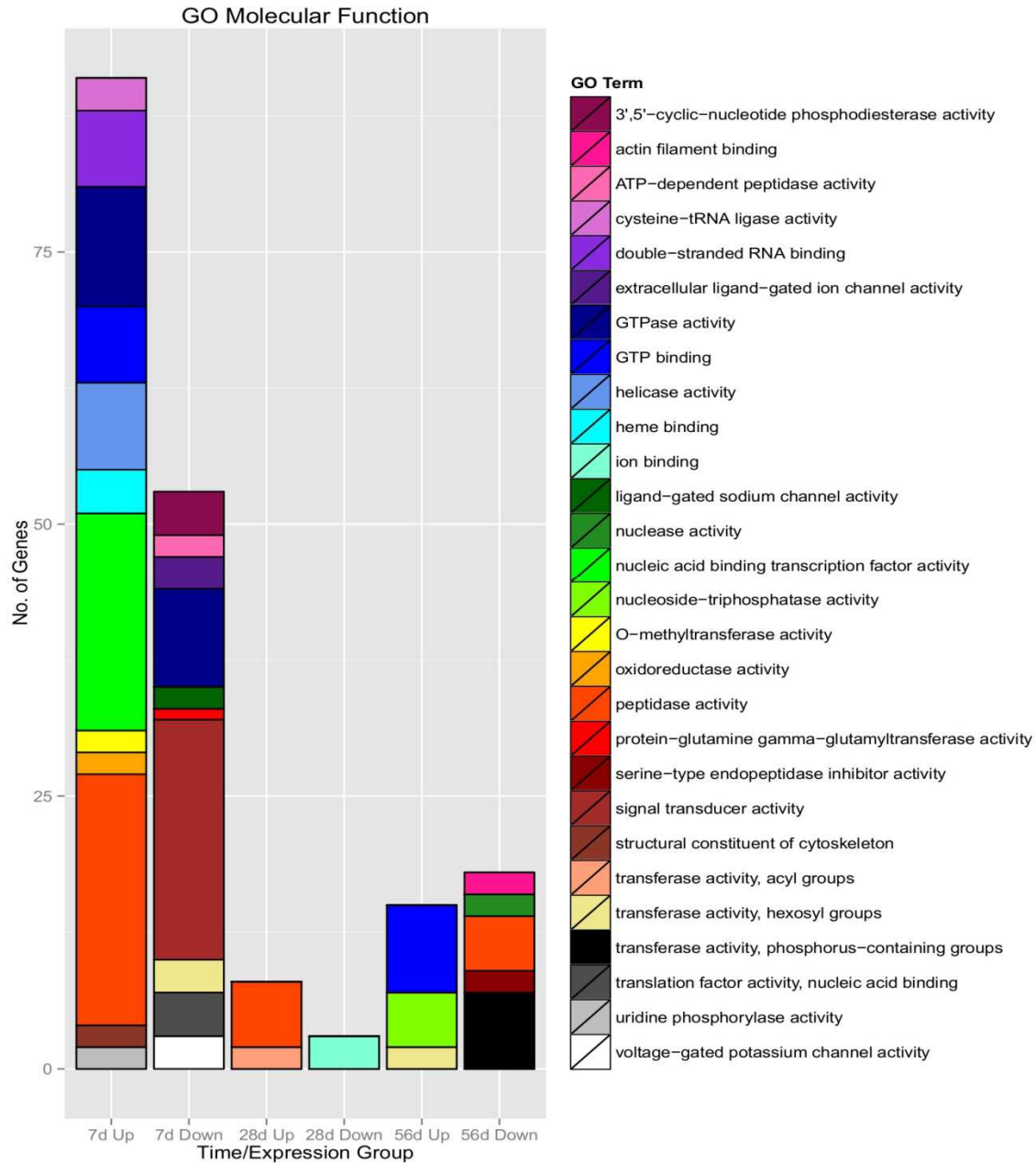


Figure 2.2: Over-representation analysis of gene ontology level 2 category molecular function: shown are gene ontology terms within the broad molecular function category (GO:0003674) that were significantly over-represented in the stressor treatments compared to the reference transcriptome as determined by a Fisher's exact test ($p < 0.01$, categories containing only one gene are not included for readability). Subgroups of up- and down-regulated gene cohorts were created for each stressor time-point (7d, 28d and 56d) and compared to the GO term distribution of the reference transcriptome. The number in each category represents the total number of genes within that over-expressed GO term category (blank = 0).

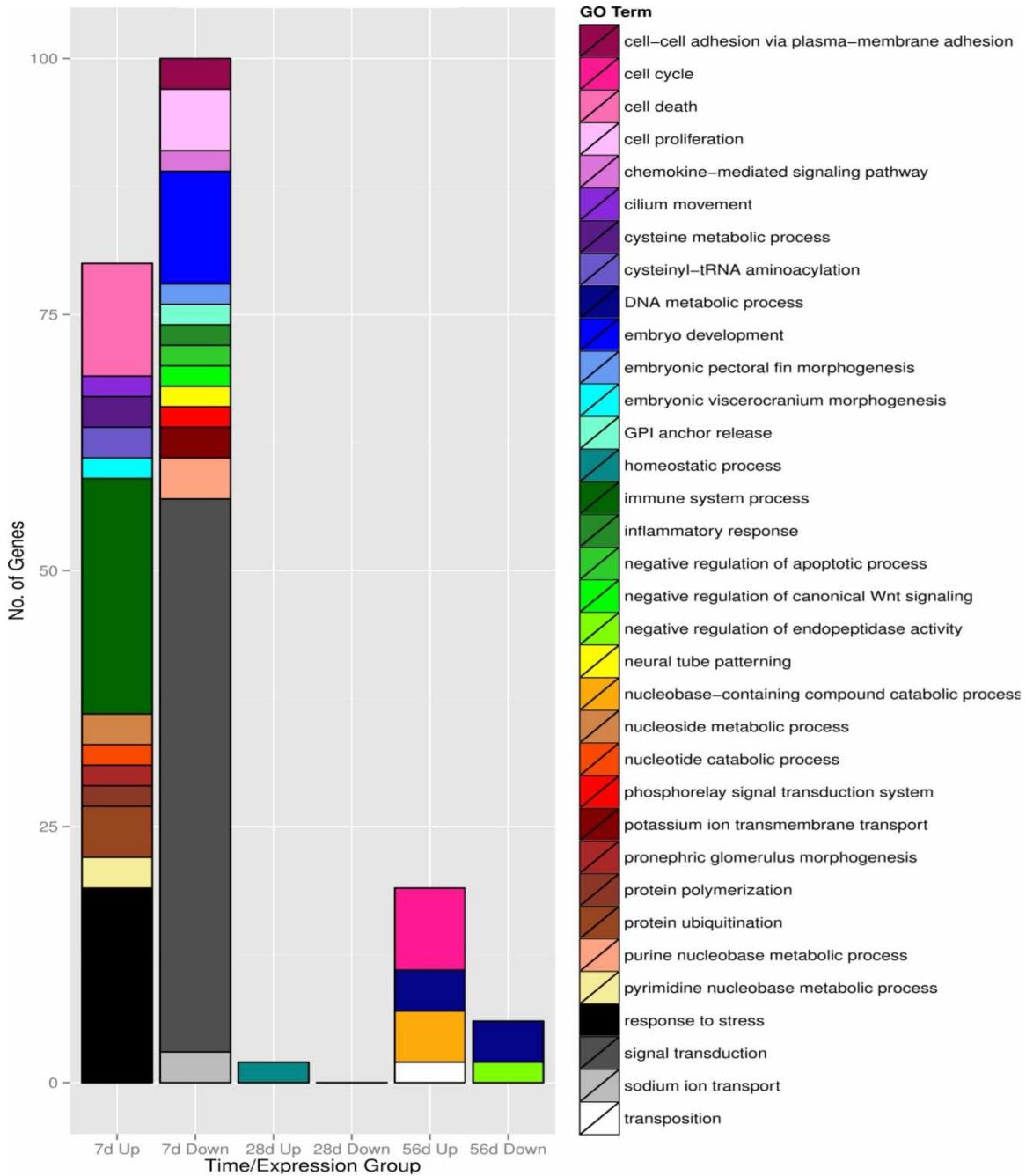


Figure 2.3: Over-representation analysis of the gene ontology level 2 category biological process: gene ontology terms within the broad biological process category (GO:0008150) that were significantly over-represented in the stressor treatments compared to the reference transcriptome as determined by a Fisher's exact test ($p < 0.01$, categories containing only one gene are not included for readability). Subgroups of up- and down-regulated gene cohorts were created for each stressor time-point (7d, 28d and 56d) and compared to the GO term distribution of the reference transcriptome. The number in each category represents the total number of genes within that over-expressed GO term category (blank = 0).

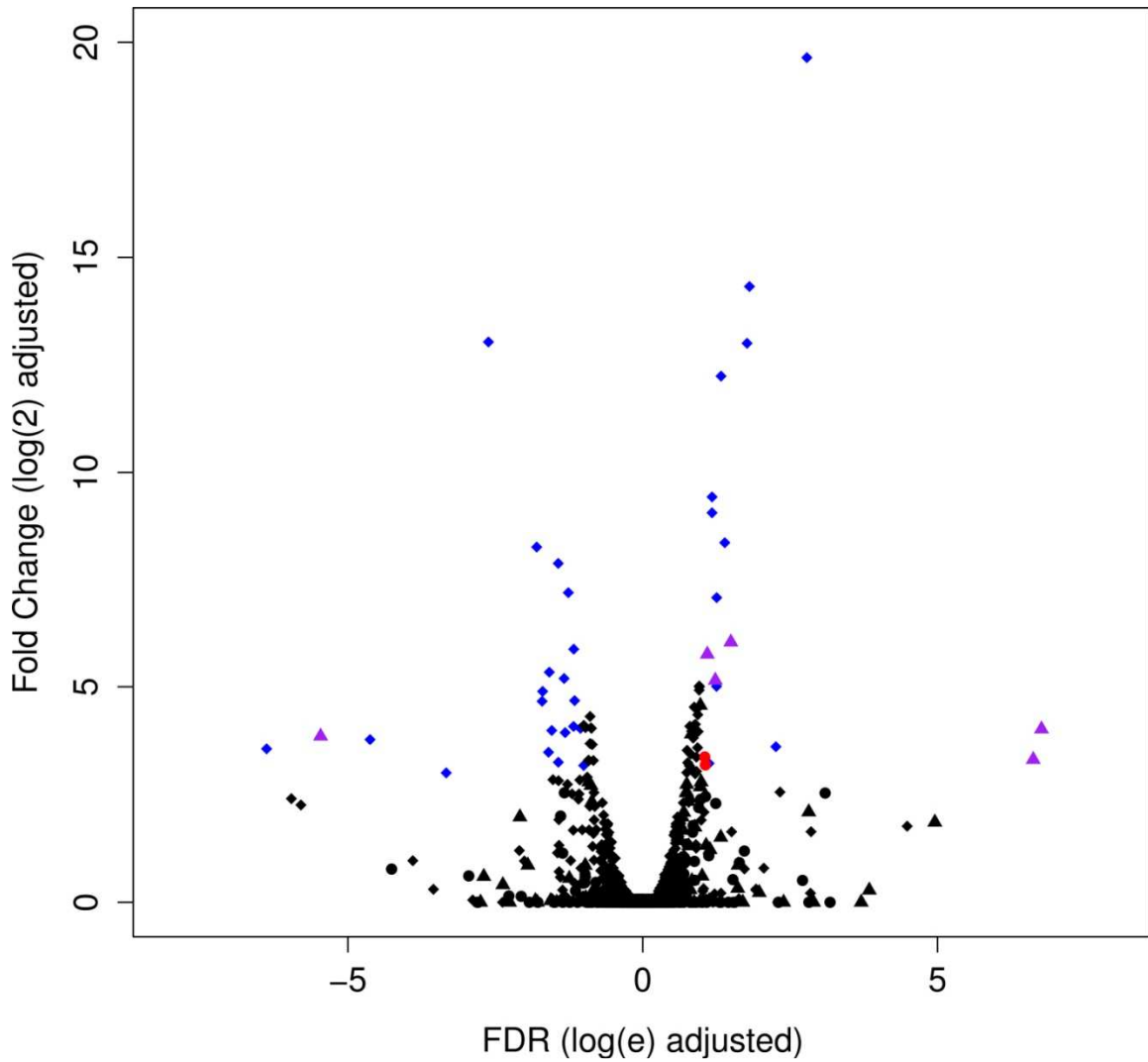


Figure 2.4: Volcano plot - carbohydrate metabolic processes: this plot demonstrates differential gene expression for the 7d (diamonds/blue), 28d (circles/red), and 56 (triangles/purple) multi-stressor treatments (n = 4) as compared to the ambient control treatments (n = 4). All genes within the reference transcriptome associated with the gene ontology term carbohydrate metabolic process (GO:0005975) are included. Fold change is \log_2 adjusted whereas FDR is \log_e adjusted. Points demonstrating both an $\text{abs}(\text{fold change}) \geq 2$ and a $\text{FDR} \leq 0.05$ are considered significant and colored according to treatment; whereas all other points are deemed not significant and are colored black.

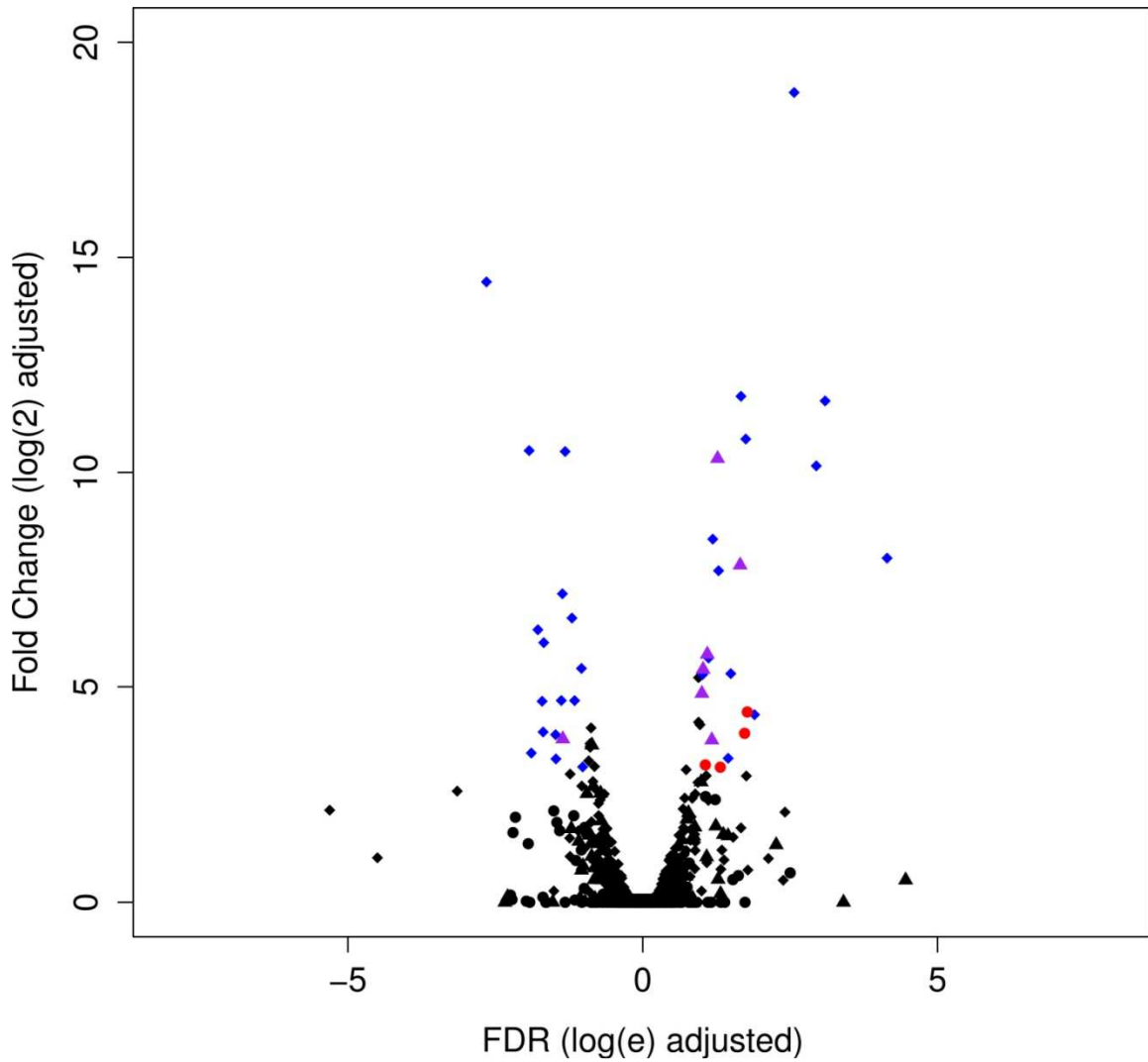


Figure 2.5: Volcano plot – lipid metabolic process: this plot demonstrates differential gene expression for the 7d (diamonds/blue), 28d (circles/red), and 56 (triangles/purple) multi-stressor treatments ($n = 4$) as compared to the ambient control treatments ($n = 4$). All genes within the reference transcriptome associated with the gene ontology term lipid metabolic process (GO:0006629) are included. Fold change is \log_2 adjusted whereas FDR is \log_e adjusted. Points demonstrating both an $\text{abs}(\text{fold change}) \geq 2$ and a $\text{FDR} \leq 0.05$ are considered significant and colored according to treatment; whereas all other points are deemed not significant and are colored black.

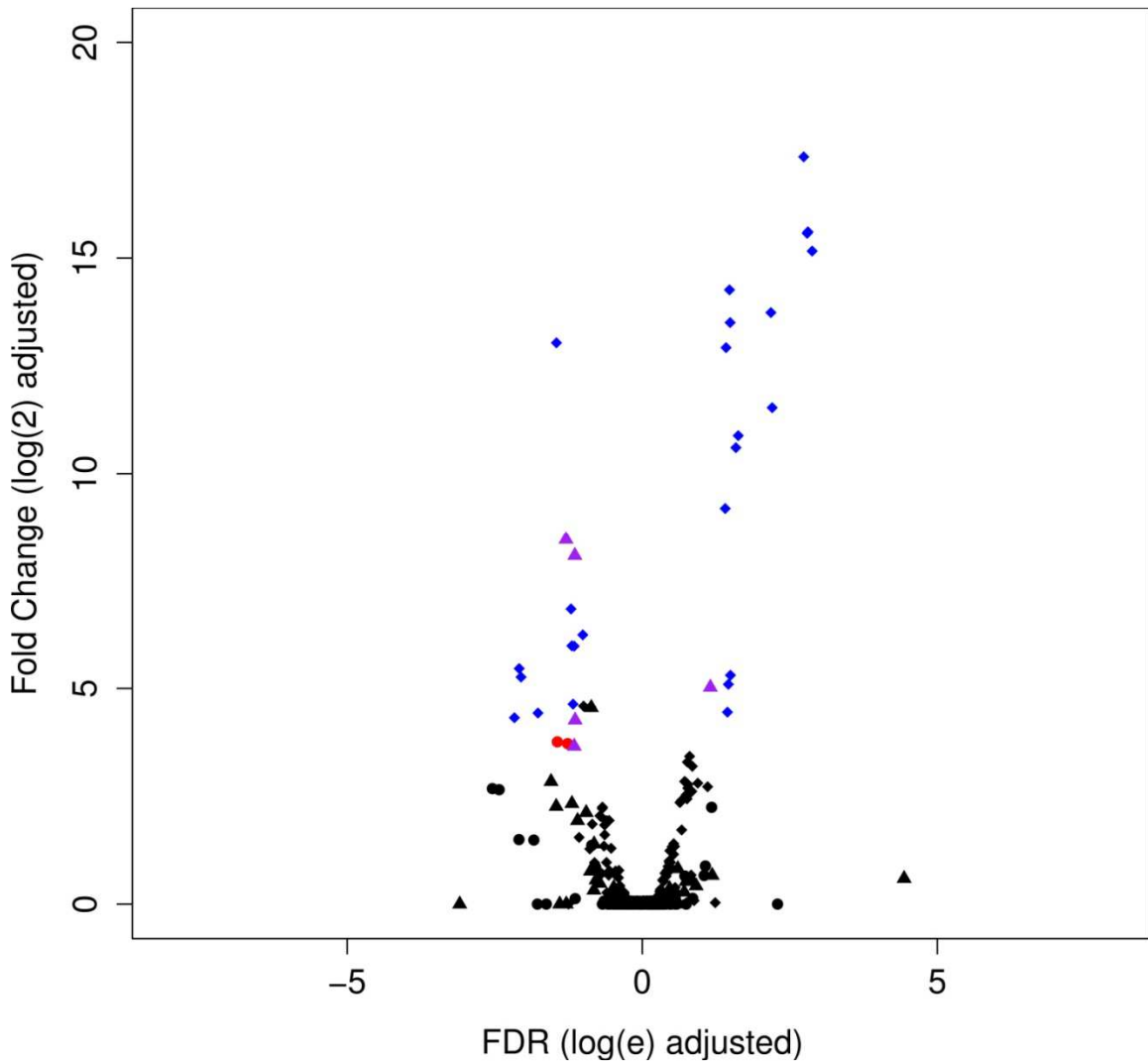


Figure 2.6: Volcano plot – cell death: this plot demonstrates differential gene expression for the 7d (diamonds/blue), 28d (circles/red), and 56 (triangles/purple) multi-stressor treatments ($n = 4$) as compared to the ambient control treatments ($n = 4$). All genes within the reference transcriptome associated with the gene ontology term cell death (GO:0008219) are included. Fold change is \log_2 adjusted whereas FDR is \log_e adjusted. Points demonstrating both an $\text{abs}(\text{fold change}) \geq 2$ and a $\text{FDR} \leq 0.05$ are considered significant and colored according to treatment; whereas all other points are deemed not significant and are colored black.

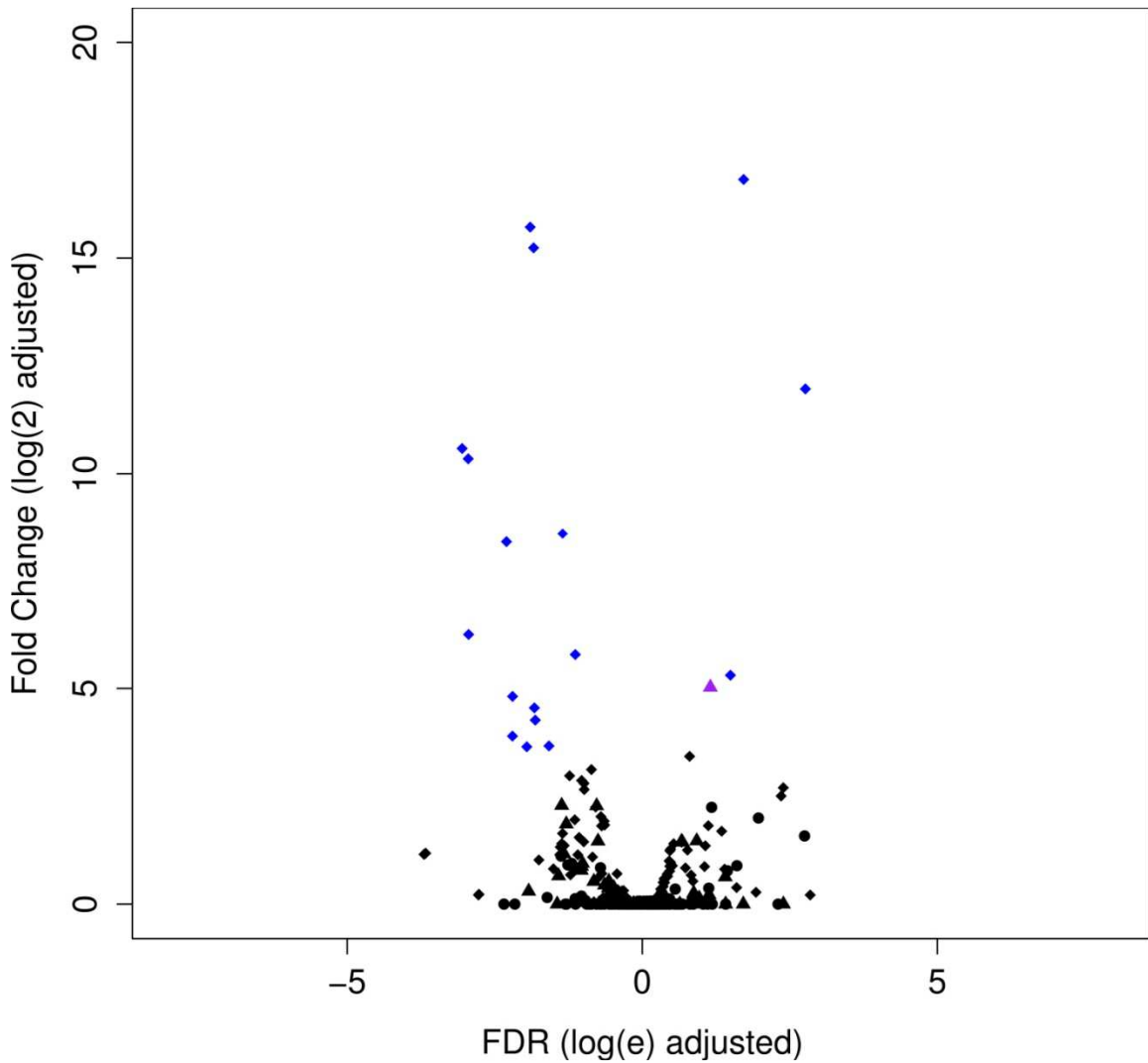


Figure 2.7: Volcano plot – cell proliferation: this plot demonstrates differential gene expression for the 7d (diamonds/blue), 28d (circles/red), and 56 (triangles/purple) multi-stressor treatments ($n = 4$) as compared to the ambient control treatments ($n = 4$). All genes within the reference transcriptome associated with the gene ontology term cell proliferation (GO:0008283) are included. Fold change is \log_2 adjusted whereas FDR is \log_e adjusted. Points demonstrating both an $\text{abs}(\text{fold change}) \geq 2$ and a $\text{FDR} \leq 0.05$ are considered significant and colored according to treatment; whereas all other points are deemed not significant and are colored black.

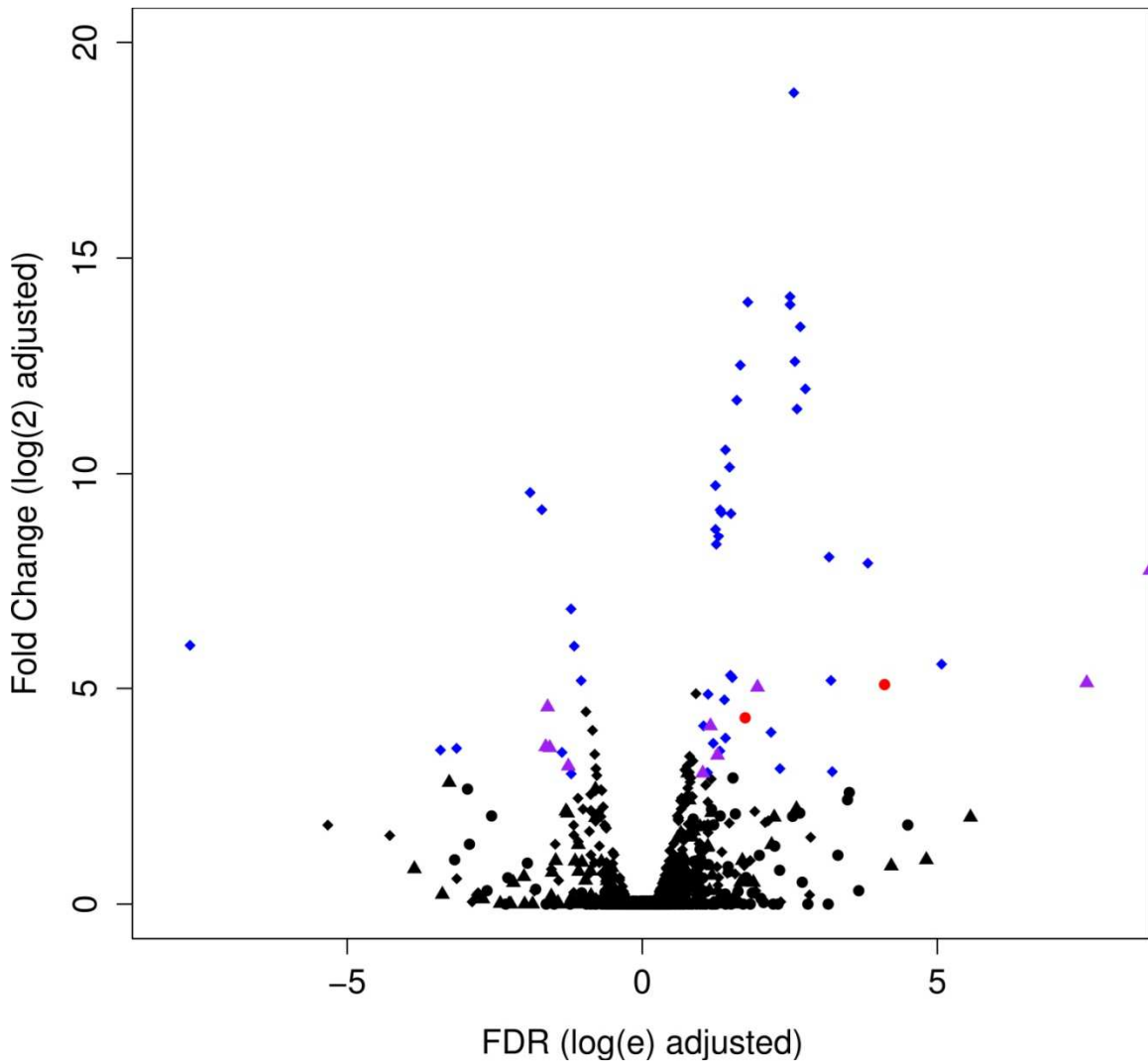


Figure 2.8: Volcano plot – response to stress: this plot demonstrates differential gene expression for the 7d (diamonds/blue), 28d (circles/red), and 56 (triangles/purple) multi-stressor treatments (n = 4) as compared to the ambient control treatments (n = 4). All genes within the reference transcriptome associated with the gene ontology term response to stress (GO:0006950) are included. Fold change is \log_2 adjusted whereas FDR is \log_e adjusted. Points demonstrating both an $\text{abs}(\text{fold change}) \geq 2$ and a $\text{FDR} \leq 0.05$ are considered significant and colored according to treatment; whereas all other points are deemed not significant and are colored black.

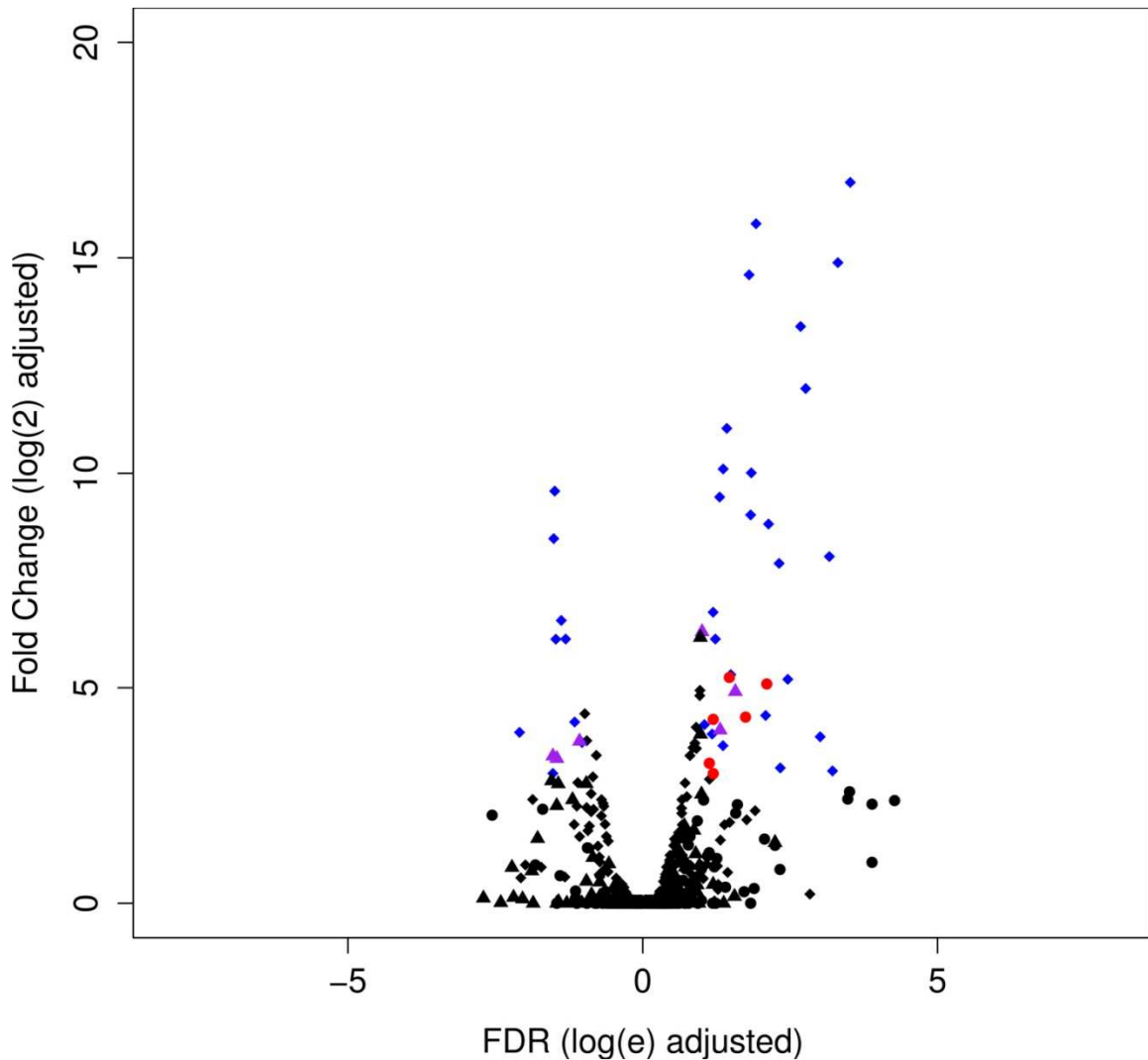


Figure 2.9: Volcano plot – immune system processes: this plot demonstrates differential gene expression for the 7d (diamonds/blue), 28d (circles/red), and 56 (triangles/purple) multi-stressor treatments (n = 4) as compared to the ambient control treatments (n = 4). All genes within the reference transcriptome associated with the gene ontology immune system process (GO:0002376) are included. Fold change is \log_2 adjusted whereas FDR is \log_e adjusted. Points demonstrating both an $\text{abs}(\text{fold change}) \geq 2$ and a $\text{FDR} \leq 0.05$ are considered significant and colored according to treatment; whereas all other points are deemed not significant and are colored black.

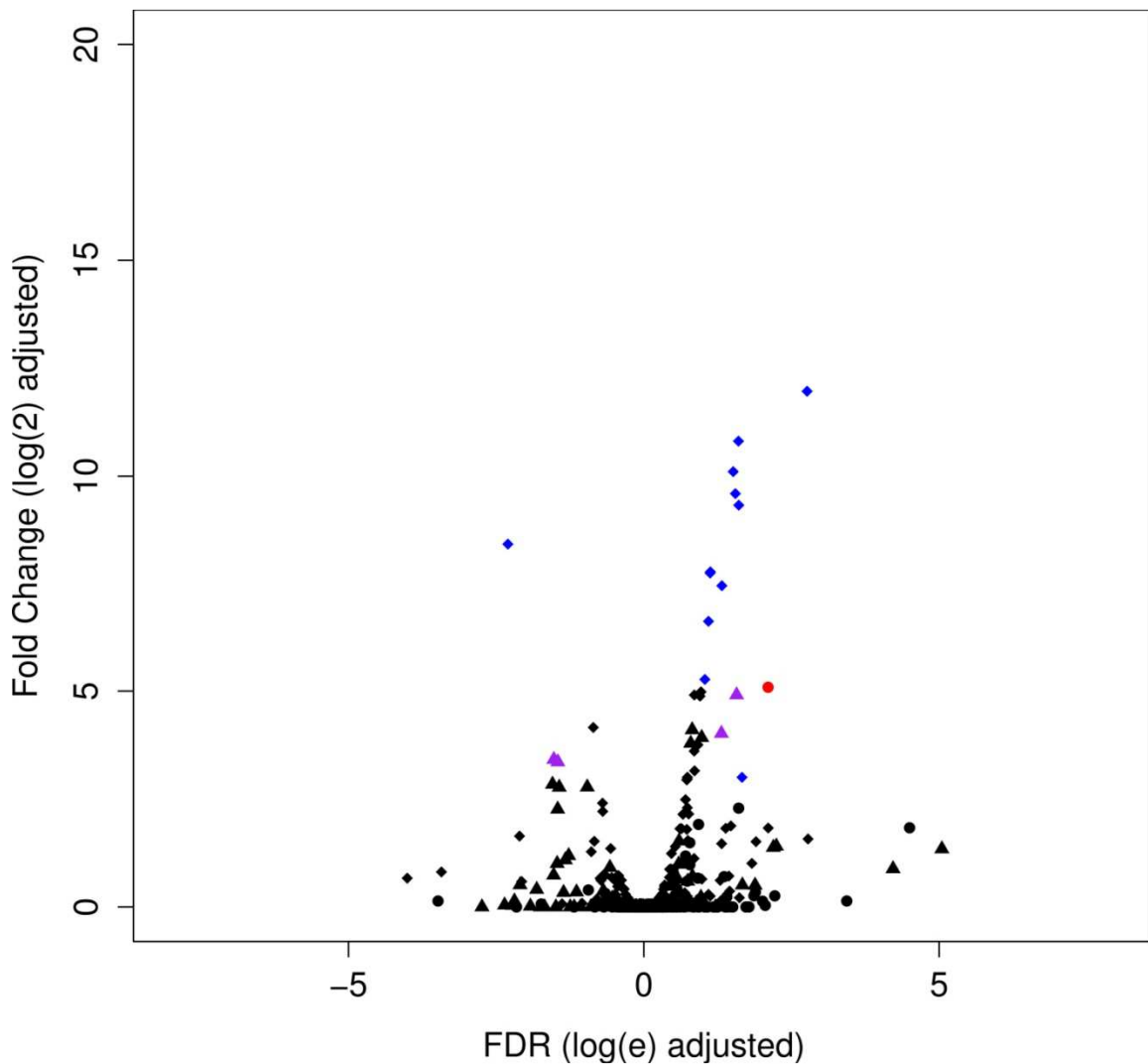


Figure 2.10: Volcano plot – homeostatic process: this plot demonstrates differential gene expression for the 7d (diamonds/blue), 28d (circles/red), and 56 (triangles/purple) multi-stressor treatments (n = 4) as compared to the ambient control treatments (n = 4). All genes within the reference transcriptome associated with the gene ontology term homeostatic process (GO:0042592) are included. Fold change is \log_2 adjusted whereas FDR is \log_e adjusted. Points demonstrating both an $\text{abs}(\text{fold change}) \geq 2$ and a $\text{FDR} \leq 0.05$ are considered significant and colored according to treatment; whereas all other points are deemed not significant and are colored black.

CHAPTER 3

RNA-SEQ REVEALS A DIMINISHED ACCLIMATION RESPONSE TO THE
COMBINED EFFECTS OF OCEAN ACIDIFICATION AND ELEVATED
SEAWATER TEMPERATURE IN *PAGOTHENIA BORCHGREVINKI*.³

³ Huth, T. J., & Place, S. P. Submitted to *Marine Genomics*.

3.1 ABSTRACT

Purpose

The IPCC has reasserted the strong influence of anthropogenic CO₂ contributions on global climate change and highlighted the polar-regions as a highly vulnerable. With these predictions the cold adapted fauna endemic to the Southern Ocean, which is dominated by fishes of the sub-order Notothenioidei, will face considerable challenges in the near future. Recent physiological studies have demonstrated that the synergistic stressors of elevated temperature and ocean acidification have a considerable, although variable, impact on notothenioid fishes. The present study explored the transcriptomic response of *Pagothenia borchgrevinki* to increased temperatures and pCO₂ after 7, 28 and 56 days of acclimation. We compared this response to short term studies assessing heat stress alone and foretell the potential impacts of these stressors on *P. borchgrevinki*'s ability to survive a changing Southern Ocean.

Results

P. borchgrevinki did demonstrate a coordinated stress response to the multi-stressor condition, and even indicated that some level of inducible heat shock response may be conserved in this notothenioid species. However, the stress response of *P. borchgrevinki* was considerably less robust than that observed previously in the closely related notothenioid, *Trematomus bernacchii*, and varied considerably when compared across different acclimation time-points. Furthermore, the molecular response of these fish under multiple stressors displayed distinct differences compared to the response to short term heat stress alone.

Conclusions

When exposed to increased sea surface temperatures, combined with ocean acidification, *P. borchgrevinki* demonstrated a coordinated stress response that has already peaked by 7 days of acclimation and quickly diminished over time. However, this response is less dramatic than other closely related notothenioids under identical conditions, supporting previous research suggesting that this notothenioid species is less sensitive to environmental variation.

3.2 BACKGROUND

In its Fifth Assessment, the Intergovernmental Panel on Climate Change (IPCC) confirmed that human influence on the global climate system is clear and growing, with average land and sea surface temperatures already exhibiting a warming of approximately 0.85 °C over the period from 1880 to 2012 (Pachauri et al., 2014). While the IPCC anticipates that these changes will have severe, pervasive, and irreversible impacts on all ecosystems; the polar environments, including the Southern Ocean surrounding Antarctica, may be affected to a greater extent by global climate change (Pachauri et al., 2014). Though the Southern Ocean has recently experienced a degree of warming (Gille, 2002), it still represents an extremely cold and oceanographically stable environment with fauna that have adapted to this unique environment (J. Eastman, 1991, 1993; Ritchie, Lavoué, & Lecointre, 1997; Rogers et al., 2007). Due to its unique and extreme nature, there is no foreseeable similar environment to which its endemic fauna can migrate if the Southern Ocean undergoes significant change at a rapid pace. Thus, this

fauna will likely have to adapt to the changing environment or face potentially precipitous declines.

The notothenioids, an endemic sub-order of perciform fishes found in the Southern Ocean, have been thoroughly studied on a physiological level with a particular focus on the impact of heat stress in these fish (Bilyk & DeVries, 2011; Bilyk et al., 2012; Davison et al., 1990; Forester et al., 1987; H. O. Pörtner et al., 2005; Esme Robinson & Davison, 2008; Sleadd et al., 2014; Somero & DeVries, 1967). Several genomic-based studies analyzing thermal stress in notothenioids have also been more recently conducted, elucidating the transcriptomic response to one of the potential stressors brought about by global climate change (Bilyk & Cheng, 2014; Huth & Place, 2013). These transcriptomic studies, along with several physiological studies performed on notothenioid fishes, suggest many of these fishes have retained at least some capacity to acclimate to warmer oceans (Bilyk & DeVries, 2011; Bilyk et al., 2012; Franklin, Davison, & Seebacher, 2007; E. Robinson & Davison, 2008; M. D. Robinson, McCarthy, & Smyth, 2010; Seebacher, Davison, Lowe, & Franklin, 2005). However, prior results from a variety of marine organisms have indicated that the variation of multiple environmental stressors simultaneously may have a greater effect than the sum of individual stressors, potentially reducing their capacity to respond (O'Donnell et al., 2009; Rosa & Seibel, 2008; Schulte, 2007). Some more recent studies on notothenioid fishes have begun to investigate the physiological effects of multiple stressors on their physiology and have identified similar synergistic effects when climate change related stressors are co-varied (Enzor et al., 2013; Enzor & Place, 2014, 2015). Furthermore, in one of the first studies to assess the genome-wide response of a notothenioid fish to

multiple stressors, we noted the effects of these synergistic stressors resulted in a prolonged cellular stress response in *Trematomus bernacchii* that may reduce the acclimation capacity of this benthic species (Huth & Place, 2015b). With the understanding that assessing a species vulnerability to environmental change requires the consideration of multiple variables (Gutt et al., 2014; Gretchen E Hofmann & Todgham, 2010) and the assessment of multiple co-regulated processes (Gretchen E Hofmann & Todgham, 2010; Place et al., 2008); it is clear that further inquiry into the effects of these synergistic stressors on notothenioids is necessary.

Application of transcriptome-wide differential gene expression analyses allows us to examine any number of physiological pathways separately and in conjunction, and thus further our understanding of the physiological plasticity of notothenioids to conditions brought about by global climate change (Bilyk & Cheng, 2014; Huth & Place, 2013, 2015b). To this end, we utilized RNA sequencing (RNA-seq) to study the molecular effects of the synergistic stressors of elevated temperature and ocean acidification (OA) on the cryopelagic notothenioid, *Pagothenia borchgrevinki*, with the goal of assessing the potential ramifications of global climate change as forecasted by the IPCC (Pachauri et al., 2014). In doing so, we were also able to compare the long-term effects of synergistic stressors against the acute effects of heat stress in *P. borchgrevinki* (Bilyk & Cheng, 2014) to assess the additional impacts of duration and multiple stressors, as well as assess the overall physiological plasticity of *P. borchgrevinki* under these conditions.

3.3 RESULTS AND DISCUSSION

Sequencing and quality control

Paired end sequencing of 150bp paired-end reads of all 23 individual samples (derived from one Illumina HiSeq 2500 Rapid Run lane) yielded an average of 28,930,437 paired-end reads (s.d. = 5,166,515) per sample. After aggressive quality control to ensure high quality input data for assembly; where reads exhibiting overall low quality and reads orphaned from their pairs were eliminated; an average of 66.4% of input reads remained (s.d. = 1.28%) Resulting quality controlled samples possessed an average of 19,238,626 paired end reads (s.d. = 3,549,213) for input into the assembly.

Single end sequencing of 100bp reads of all 23 individual samples on two Illumina HiSeq 2500 Rapid Run lanes yielded an average of 25,850,311 single reads (s.d. = 4,609,844). Quality control removed single reads that exhibited overall low quality, however, read quality was generally high with an average of 89.5% of reads surviving the quality control screening (s.d. = 0.14%). Following quality control the individual samples possessed an average of 23,203,167 single end reads (s.d. = 4,139,946).

Reference transcriptome assembly and annotation

Following *de novo* assembly the transcriptome consisted of 474,450 transcripts (contigs) and 276,892 'genes' (unique gene products including all related transcripts); with a median transcript length of 484bp, mean transcript length of 1050bp and N50 of 3356bp (Fig. 3.1). Following transcript compacting to eliminate redundant sequences; 278,744 transcripts and 205,132 genes remained (median = 410bp, mean = 743bp, N50 = 1746bp). Lastly, RSEM filtering applying a minimum expression threshold of FPKM \geq 1 to remove transcripts with very low expression produced a final reference transcriptome

containing 83,869 transcripts and 46,176 genes; with a median transcript length of 1002bp, mean transcript length of 1533bp and N50 of 2590bp (Table 3.1).

BLASTx searches yielded hits for 59,012 transcripts (70.4%), which represented 28,729 hits on the gene level (62.2%, Table 3.2). An analyses of the Top Blast hit per transcript (as determined by minimum e-value) reveals the high degree of similarity between notothenioids and their distinctiveness from non-polar fishes with 32,069 top-hits attributed to *Notothenia coriiceps*, which is over 3 times as many as the next nearest species (Fig. 3.2). Gene Ontology annotation yielded a total of 38,497 transcripts (65.2%) with assigned GO Terms, representing 19,577 GO annotated genes (68.1%, Table 3.2).

Transcriptomic comparisons

De novo assemblies of other teleost fish sequenced with similar technology, assembled with the Trinity *de novo* assembler, and pruned in a similar manner generated equivalent results to the current transcriptome with 44,990 genes in *Oncorhynchus mykiss* (Pierson, Lamers, Flik, & Mayer-Gostan, 2004); and 96,641 transcripts and 54,429 genes from the head kidney of *Trematmous bernacchii* (Gerdol, Buonocore, Scapigliati, & Pallavicini, 2015).

Additionally, comparisons to a previously assembled transcriptome of *P. borchgrevinki* from Bilyk and Cheng (2013) demonstrated a high degree of similarity between the two transcriptomes. The previous transcriptome assembly conducted by Bilyk and Cheng (2013) for *P. borchgrevinki* contained 39,758 contigs in the final pruned transcriptome, similar to the 46,176 genes found in the current transcriptome assembly. Direct comparisons of sequence homology (BLAST cutoff = 10E-3) using the current reference transcriptome as query sequences against a database composed of the contigs

from Bilyk and Cheng (2013) resulted in 70,915 transcripts with a BLAST result or a 84.6% match rate. GO Slim comparisons further confirmed the high degree of homology between these two transcriptomes, with both transcriptomes demonstrating similar distributions of the GO terms for biological process, cellular component, and molecular function categories (Fig. 3.3). The small differences found within the BLAST results and GO distribution are likely attributable to tissue specific differences in gene expression. The current reference transcriptome was assembled solely from RNA extracted from gill tissue, whereas the previously published *P. borchgrevinki* transcriptome was assembled from RNA extracted from gill, liver, brain, white muscle, spleen, head kidney, gill and lens (Bilyk & Cheng, 2013).

Transcriptome level differential gene expression analysis

Mappings of the trimmed reads to the reference transcriptome yielded an average of 21,009,072 mapped reads per sample (s.d. = 3,691,533) representing an average mapping rate of 90.5% (s.d. = 0.5%).

The overall trends observed in the gene expression patterns of *P. borchgrevinki* were similar to the trends previously observed in a closely related notothenioid, *T. bernacchii* (Huth & Place, 2015b). However, the overall magnitude of change observed in *P. borchgrevinki* was much lower than that previously observed in *T. bernacchii* (Huth & Place, 2015b). Of the roughly 46,000 gene products in our transcriptome, we identified 3,872 differentially expressed (DE) gene products demonstrating at least a two-fold change in expression ($FDR \leq 0.05$) across all treatments and time-points. The greatest number of differentially expressed genes (923) was observed in fish acclimated to the multi-stressor treatments for 7d, of which, 665 genes were up-regulated while 258 were

down-regulated in the gills of these fish. This was nearly 50% lower than the total number of DE genes identified in *P. borchgrevinki* after 4 days of acclimation to an acute thermal stress alone (Bilyk & Cheng, 2014). The number of DE genes in the 28d acclimated fish fell to 372 (221 up-regulated and 151 down-regulated) and then rose again in the 56d acclimated fish which exhibited 606 DE genes (220 up-regulated and 386 down-regulated).

Pairwise comparison of gene expression profiles across treatments and time-points indicated a high level of correlation between individuals within the same acclimation group which suggests the multi-stressor treatment had a significant impact on the physiology of the fish over both short and long time scales (Fig. 3.4). However, a high level of correlation was not observed between the multi-stressor treatments at different time-points (Fig. 3.4). This indicated that the gene level response of *P. borchgrevinki* to the effects of elevated sea surface temperature and OA changes significantly over time.

Transcriptome-wide gene ontology analysis

Comparison of GO terms within the broad molecular function category revealed increases in genes responsible for ATP binding, metal ion binding, protein binding, DNA transcription factor activity, zinc ion binding and chemokine activity for fish in the 7d multi-stressor acclimation group (Fig. 3.5). Additionally, the gill tissue of these fish demonstrated relatively high levels of gene up-regulation in the biological processes: chemotaxis, immune response, protein ubiquitination, pyrimidine metabolism, regulation of transcription, and signal transduction (Fig. 3.6). Interestingly, despite observing nearly one thousand DE genes in the gill tissue of fish in the 7d acclimation group, Fisher's

exact tests did not reveal any over-represented GO terms at any treatment time-point (FDR < 0.05). These findings differed substantially from those for *T. bernacchii* specimens acclimated to the same conditions (Huth & Place, 2015b) as well as specimens of *P. borchgrevinki* acclimated to short-term thermal stress alone (Bilyk & Cheng, 2014). On the surface, these results may be an indication that the major cellular response to the multi-stressor study has already passed, which would suggest the acclimation period is much shorter in this notothenioid species. Alternatively, the additional stress associated with OA may have resulted in a more muted transcriptional response as severe hypercapnia has been shown dampen physiological responses and result in metabolic depression (Buckley et al., 2006; Gracey, Troll, & Somero, 2001; Hennet, Richter, & Peterhans, 1993; Jeffries, Hinch, Sierocinski, Pavlidis, & Miller, 2014; Logan & Somero, 2011; Podrabsky & Somero, 2004; K Schulze-Osthoff, Beyaert, Vandevoorde, Haegeman, & Fiers, 1993; Klaus Schulze-Osthoff et al., 1992; Tomalty et al., 2015).

Organisms experiencing environmental stress can often display two conserved responses, a rapid, transient response known as the cellular stress response (CSR) and a more permanent response termed the cellular homeostasis response (CHR) (Kültz, 2005). Given the differences in gene expression patterns observed within fish acclimated to the multi-stressor treatments for varying amounts of time, it is likely the DE genes observed in the 7d compared to the 28d and 56d acclimated fish highlights the transition from the CSR to the CHR, and are representative of both the immediate and long-term adjustments necessary to cope with these environmental conditions. As such, we performed a more detailed analysis of gene pathways involved in several biological processes generally associated with cellular homeostasis and response to stress (Almroth *et al.*, 2015; Bilyk

et al., 2012; Enzor & Place, 2014; Enzor *et al.*, 2013; Gerdol *et al.*, 2015; Huth & Place, 2013; Kültz, 2005; Robinson & Davison, 2008a).

3.4 PATHWAY SPECIFIC RESPONSES

Immune system processes

Of all the gene ontology categories considered, immune responses and stress responses displayed the greatest number of DE genes, although the total number of DE expressed genes in any GO category were a fraction of that observed in other species.

For the GO Slim category immune system process (GO:0002376), 44 of the 471 genes associated with immune response in the reference transcriptome were differentially regulated ($FDR \leq 0.05$) in at least one time-point (Figure 5). Fish in the 7d multi-stressor group demonstrated the largest number of DE genes with 31 total, of which 28 are up-regulated and 3 down-regulated. This strong initial response undergoes a substantial reduction with 9 differentially expressed genes at the 28d time-point (8 up-regulated, 1 down-regulated) and only 5 at 56d (4 up-regulated, 1 down-regulated).

The initial up-regulation of immune system related genes is consistent with a broader suite of changes associated with the cellular stress response and is highlighted by the up-regulation of a diverse family of chemokines. The chemokine super family plays a central role in recruiting various elements of the immune system including monocytes, macrophages, t-cells, neutrophils, and natural killer (NK) cells (Cole *et al.*, 1998; Robertson, 2010; Weber *et al.*, 2011; Wuyts *et al.*, 1997). By the 28d time-point we no longer observed an up-regulation of any of these chemokines, but did observe a large

scale up-regulation of SAMHD1, which may play a role in mediating pro-inflammatory responses to TNF-alpha signaling.

While it is possible that the immune response observed in these fish is in response to a latent infection that is able to manifest due to the effects of the multi-stressor treatment on *P. borchgrevinki*, the inflammation response observed here is more likely associated with intracellular damage to macromolecules. *P. borchgrevinki* has been shown to exhibit a significant increase in oxidative damage after a 7d acclimation to elevated temperature and $p\text{CO}_2$ (Enzor & Place, 2014). Furthermore, the nuclear transcription factor κB (NF- κB) has been implicated in the transcriptional up-regulation of inflammatory genes in response to oxidants or changes in cellular oxidation-reduction status (Hennet *et al.*, 1993; Schulze-Osthoff *et al.*, 1992). Thus, the more likely scenario is that wide spread cellular damage and remodeling are activating these pathways. The significant increase in the inflammatory response may also serve to partially compensate for the reduced heat shock response observed in *P. borchgrevinki* (Place & Hofmann, 2005).

Response to stress

In teleost fish, environmental perturbation of cellular homeostasis is often marked by a massive transcriptional up-regulation of genes associated with a conserved cellular stress response (CSR) (Buckley *et al.*, 2006; Gracey *et al.*, 2001; Jeffries *et al.*, 2014; Podrabsky & Somero, 2004; Tomalty *et al.*, 2015). Although *P. borchgrevinki* displayed a clear stress response at the level of the transcript, this response was significantly muted in comparison to other fish species. Of the 696 total genes associated with the GO category response to stress (GO: 0006950) found in the reference transcriptome, only 30

transcripts displayed significant changes in expression ($FDR \leq 0.05$) in at least one of the multi-stressor treatments (Fig. 3.7). In contrast, a closely related species, *T. bernacchii*, showed nearly four-times as many DE genes in this GO category after a 7d acclimation to the same treatment (Huth & Place, 2015b).

Typically the teleost heat shock response involves 3 major HSP families: HSP90, HSP70 and the small HSPs (Basu et al., 2002). However, notothenioids have consistently demonstrated the lack of an inducible heat shock response (Bilyk & Cheng, 2014; Buckley *et al.*, 2004; Buckley & Somero, 2009; Huth & Place, 2013; Place & Hofmann, 2005; Place *et al.* 2004). Even more striking, significant down-regulation of HSPs has been observed in *P. borchgrevinki* when exposed to thermal stress alone for 2-4d (Bilyk & Cheng, 2014) and *T. bernacchii* after 28d (Huth & Place, 2013). Overall, the lack of significant changes in mRNA levels held true for the majority of HSP families annotated in our transcriptome, including HSP70. However, in the first known deviation from this apparent lack of an inducible HSR in an archetypal notothenioid, we observed a significant up-regulation of two contigs encoding HSP90 α (4.9 and 6.4-fold) in fish acclimated to the multi-stressor treatment for 7d. Interestingly, by 28d of acclimation, this up-regulation of HSP90 α reversed, and in fact, a single HSP90 α contig experienced a 3.4-fold down-regulation.

The initial up-regulation of HSP90 α at the 7d time-point contrasts with HSP90 α expression levels of *P. borchgrevinki* found in Bilyk and Cheng (2014) where HSP90 α was found to be down-regulated 3.2-3.9-fold. Given the differences in treatment (single vs. multiple stressors), acclimation time (4d vs 7d) and tissue (liver vs gill); it is difficult to postulate what underlies these contrasting expression results. Furthermore, HSP90 is

thought to support the proper folding of large protein complexes primarily involved in signal transduction (Young *et al.*, 2001). Thus, its up-regulation at 7 days may be indicative of its role in cellular remodeling, a hallmark of the transition from the CSR to the CHR, as opposed to an initial heat shock response that may occur in a 2-4 day time period.

Cell proliferation and death

Under severe stress, a slowing of cell proliferation can frequently be observed, presumably to ensure sufficient time for DNA repair to proceed and potentially conserve cellular resources. Such a slowing, in addition to a reduction in translation, was observed in *P. borchgrevinki* after 4d of thermal stress (Bilyk & Cheng, 2014). Upon extending the acclimation period to 7d, we observed signs that this slowdown had persisted in *P. borchgrevinki*. Several suppressors of cytokine signaling (SOCS), which inhibit the JAK/STAT and growth factor signaling pathways (Cooney, 2002), are up-regulated (+3.3-fold, +3.0-fold, + 3.3-fold) in the 7d multi-stressor treatment. This trend is not found in the 28d time-point, and then experiences a reversal in the 56d time-point with all three SOCS genes being down-regulated (-2.4-fold, -2.3-fold, -2.1-fold).

Additionally, fish acclimated to the multi-stressor treatment for 7d demonstrated a strong up-regulation of genes regulating cell death (10) that continued to be elevated into the 28d time-point (4) before reversing at 56d (5) (Figure 5). By 28d *P. borchgrevinki* appears to be undergoing elevated rates of apoptosis (GO:0008219) with the up-regulation of a number of genes encoding caspase-8 (+20.6-fold, +3.8-fold, +2.5-fold, +2.0-fold), which is thought to be a cellular tipping point in apoptosis initiation (Kruidering & Evan, 2000).

With the initial inhibition of the JAK-STAT pathways, we see *P. borchgrevinki* arresting the cell cycle during its initial (CSR) response to the multi-stressor condition at day 7 and peak activation of apoptotic pathways by day 28. Yet, by day 56 there is no up-regulation of caspases, and the previously up-regulated SOCS genes are now strongly down-regulated, potentially indicating the completion of cellular remodeling and transition to a more stable, long-term homeostatic state consistent with the CHR.

Carbohydrate and lipid metabolism

Given the significant energetic costs often associated with the CSR, increased metabolic capacity and mobilization of energy stores frequently accompanies the up-regulation of stress response genes (Buckley et al., 2006; Gracey et al., 2001; Hennet et al., 1993; Jeffries et al., 2014; Logan & Somero, 2011; Podrabsky & Somero, 2004; K Schulze-Osthoff et al., 1993; Klaus Schulze-Osthoff et al., 1992; Tomalty et al., 2015). Nevertheless, *P. borchgrevinki* displayed little change in metabolic pathways despite displaying elevated rates of oxygen consumption after acclimation for 28d (Enzor et al., 2013). The analysis of significant changes in mRNA expression for genes associated with the GO Slim category lipid metabolic process (GO: 0006629) (Fig. 3.7) yielded a total of 589 genes associated with this term, 13 of which were significantly differentially expressed ($FDR \leq 0.05$) at one or more time-points. The 7d multi-stressor time-point showed the up-regulation of 4 genes involved in lipid metabolism (cis-aconitate decarboxylase, +5.0-fold; endothelial lipase, LIPG, +1.9-fold; cholesterol 25-hydroxylase, CH25H, +1.8-fold; long-chain acyl- synthetase, ACSL, +1.4-fold). Aside from ACSL, which continues to be up-regulated into the 28d time-point (+2.3-fold), the

majority of the changes in lipid metabolism are reversed in the 28d or 56d acclimation groups, suggesting an early energetic cost that quickly returns to basal levels (Fig, 5).

As seen with lipid metabolism, only 14 of the 546 genes associated with the GO Slim category carbohydrate metabolic process (GO:0005975) were found to be DE (FDR ≤ 0.05) at one or more time-points (Figure 5). Most notably was the observed up-regulation of enzymes involved in simple sugar metabolism (phosphomannomutase, PMM2, +2.0-fold; fructose-bisphosphate aldolase, ALDOA, +3.1-fold; acetyl-coA, +2.1-fold) at the 28d time-point. At 56d glycolytic pathways still demonstrate some signs of increased activity with the 9-fold up-regulation of beta-enolase-like isoform 1 (ENO1).

3.5 CONCLUSION

In line with previous single stressor studies, we have demonstrated that despite lacking a fully functional heat shock response, *P. borchgrevinki* does demonstrate a coordinated and consistent response to multiple-stressors. Although exhibiting many of the hallmarks of the classical cellular stress response, this response appears to be diminished in magnitude compared to other species. We further noted that while previous studies indicated that the short term effects of heat stress in *P. borchgrevinki* resulted in the general slowing of cell cycle progression and protein biosynthesis, the longer time scales observed in this study indicated that this is likely just a temporary effect. Even though the muted response to elevated temperature and ocean acidification could be viewed as a reduced capacity to respond, the whole of the data presented here, along with several earlier studies investigating individual biochemical and physiological metrics, suggests *P. borchgrevinki* may simply exhibit a lower sensitivity to environmental

variation. Our finding that *P. borchgrevinki* appears capable of up-regulating one of the major HSP protein families further supports this idea. Interestingly, to our knowledge, this is the first study to observe elevated expression of any of the major HSPs in an archetypal notothenioid and highlights the importance of using long-term acclimations in combination with co-variation of multiple stressors in studies assessing the physiological plasticity of polar organisms.

3.6 METHODS

Collection of fish

Specimens of *P. borchgrevinki* were collected in McMurdo Sound, Antarctica from September through December, 2012. Fish were caught using hook and line through 10-inch holes drilled through the sea ice and transported back to McMurdo Station in aerated coolers where they were housed in a flow-through aquaria maintained at ambient seawater temperature (-1.5°C). Fish were then tank-acclimated under ambient conditions for one week prior to being placed in experimental tanks. All procedures were conducted in accordance with the Animal Welfare Act and were approved by the University of South Carolina Institutional Animal Care and Use Committee (ACUP protocol # 100377).

Experimental design

We used four, 1240 L experimental tanks to assess the combined effects of elevated temperature and $p\text{CO}_2$ on *P. borchgrevinki*. Our two experimental treatments consisted of a control tank which was held near ambient conditions (-1°C and 430 μatm) and a high temperature + high $p\text{CO}_2$ treatment (+4°C/ 1000 μatm). Fish were placed in

experimental tanks and acclimated for a total of 56 days. Five fish per treatment were removed at 7d, 28d, and 56d time-points, after which fish were sacrificed and gill tissues were collected and immediately flash-frozen in liquid nitrogen. Although we recognize a fully replicated experimental design is ideal to exclude tank effects as a possible confounding factor, the constraints of working in Antarctica prevented us from using this approach. However, our previous analyses show no tank effect when treatments were alternated between tanks across multiple seasons (Enzor & Place, 2014; Enzor *et al.*, 2013).

Manipulation of seawater conditions

Temperature and $p\text{CO}_2$ levels were manipulated within the experimental treatment tanks using a $p\text{CO}_2$ generation system first described by Fanguie *et al.* (2010) and adapted for use with large-scale applications and combined with thermostated titanium heaters [Process Technology, Brookfield CT, USA] (Enzor *et al.*, 2013). Atmospheric air was pumped through drying columns (filled with drierite) to remove moisture, and air was scrubbed of CO_2 using columns filled with Sodasorb. Pure CO_2 and CO_2 -free air were then blended using digital mass flow controllers and bubbled into header tanks that were continuously replenished with ambient seawater using venturri injectors, which in turn fed into experimental treatment tanks.

Temperature, pH (total scale), salinity, total alkalinity (TA) and oxygen saturation were measured daily from both incoming seawater as well as experimental treatment tanks. For $p\text{CO}_2$ analysis, we followed the SOP as described in the Best Practices Guide (Jean-Pierre Gattuso, Kunshan Gao, Kitack Lee, 2010) for the spectrophotometric determination of pH using m-cresol purple and measurement of total alkalinity via acid

titration using a computer-controlled T50 Titrator (Mettler Toledo, Columbus, OH, USA). Temperature was measured with a calibrated digital thermocouple (Omega Engineering Inc., Stamford, CT, USA) and salinity was measured using a YSI 3100 Conductivity meter (Yellow Springs, OH, USA). CO₂ calc (Robbins *et al.*, 2010), using the constants of Mehrbach *et al.* (1973) as refit by Dickson & Millero (1987), was used to calculate all other carbonate parameters. Oxygen saturation was recorded using a galvanic oxygen probe (Loligo Systems, Denmark). Mean values (\pm s.d.) of temperature ($^{\circ}$ C) and p CO₂ (μ atm) over the course of the experiment were first reported in Enzor and Place (2014). Additionally, treatment tanks were sampled daily for the presence of ammonia, nitrite and nitrates, with no significant increase in waste products noted over the course of the experiment (data not shown).

Tissue collection and RNA extraction

To obtain individual gill-specific expression profiles, we separately indexed and sequenced RNA samples from gill tissue that had been collected from fish acclimated to the two experimental treatments described above (n=5 fish per treatment, n=3 in one group due to sample constraints) for 7 days, 28 days and 56 days. Immediately after euthanizing the fish, tissues were excised in a -2 $^{\circ}$ C environmental chamber, flash frozen in liquid nitrogen, and shipped back to our home institution on dry ice where they were stored at -80 $^{\circ}$ C until used. Total RNA from approximately 100 mg of frozen tissue was extracted using TRIzol (Invitrogen) following the manufacturer's recommendations. The RNA was further cleaned by re-suspending in 0.1 ml of RNase/ DNase-free water and adding 0.3 ml of 6 M guanidine HCl and 0.2 ml of 100% ethylalcohol (EtOH). The entire volume was loaded onto a spin column (Ambion) and centrifuged for 1 min at 12,000 \times g

at 4 °C. Flow-through was discarded, and filters were washed twice with 0.2 ml 80% EtOH. RNA was eluted off of the filters twice with 0.1 ml of DEPC-treated water. RNA was precipitated by the addition of 0.1 vol of 3 M sodium acetate (pH 5.0) and 2.5 vol of 100% EtOH, mixed by inversion of tubes and placed at -80 °C for 1 h. After this period, tubes were centrifuged at $12,000 \times g$ for 20 min at 4 °C. Pellets were washed twice with 80% EtOH and re-suspended in 30 μ l of RNase/ DNase-free water. Lastly, RNA was DNase treated at 30 °C for 10 min.

Total RNA from n=5 fish (n=3 in one group due to sample constraints) within an acclimation treatment was submitted to the Vaccine and Gene Therapy Institute (VGTI) Florida for quality assessment and determination of specific concentration using an Agilent 2100 BioAnalyzer. From the original samples, the 4 highest quality replicates (in 1 group 3 replicates were utilized due to limited specimen availability) from each treatment and time point were selected for cluster generation using the Illumina® TruSeq RNA Sample Prep v2 Hs protocol and sequencing via an Illumina® HiSeq 2500 Rapid Run initialized for both paired-end 150bp reads and single-end 100bp reads.

Quality control - Raw reads from each of the twenty-three samples were processed using Trimmomatic (version Trimmomatic-0.32) (Bolger *et al.*, 2014). For both paired-end and single-end reads Illumina® TruSeq RNA Sample Prep v2 HS adapters were removed as well as any bases on the end of the reads with a PHRED33 score of < 20 or any portion of the read that did not average at least a PHRED33 score of > 20 across a minimum span of 4bp. Paired-end reads with a length < 100 were removed, as well as any reads that were orphaned during the quality control process; whereas single-end reads with a length < 75 were removed (paired-end Trimmomatic parameter input: VGTI_Adapters_Trueq2-

PEMultiplex.fa:2:30:10 LEADING:20 TRAILING:20 SLIDINGWINDOW:4:20
MINLEN:100; single-end Trimmomatic parameter input: VGTI_Adapters_Truseq2-
PEMultiplex.fa:2:30:10 LEADING:20 TRAILING:20 SLIDINGWINDOW:4:20
MINLEN:75).

Reference transcriptome assembly, annotation and comparison

All paired-end reads surviving quality control were used as input in the Trinity *de novo* assembly utility (version trinityrnaseq-2.0.3) (Grabherr et al., 2011). The Trinity package efficiently recovers full-length transcripts and spliced isoforms across a range of expression levels, with less artificially constructed transcripts than other assembly utilities (Zhao et al., 2011). Assembly was conducted utilizing the Trinity's default parameters with read normalization (N=50). Following assembly raw transcripts were compacted using CD-HIT-EST (version cd-hit-v4.6.1-2012-08-27) (Fu *et al.*, 2012) with a sequence similarity requirement of 95% to eliminate redundant transcript sequences. Then the single ends reads were mapped to the compacted transcripts utilizing Bowtie2 (Langmead & Salzberg, 2012) with default parameters; after which RNA-Seq by Expectation-Maximization ("RSEM" version 1.2.18) (Li & Dewey, 2011) was conducted to generate calculated fragments per kilobase million (FPKM) values for each compacted transcript. Compacted transcripts were then filtered with only those possessing FPKM \geq 1 being retained for the final reference transcriptome.

Transcripts from the final reference transcriptome were used as query sequences in BLASTx (version: ncbi-blast-2.2.25+) (Camacho et al., 2009) searches with a minimum confidence value of 1E-6 required for annotation against the NCBI nr (non-redundant) database (version May 2015). BLASTx was implemented in a massively

parallel manner utilizing the resources of the Data Intensive Academic Grid (DIAG). After BLASTx results were obtained, the transcript sequences and the corresponding BLASTx results were input into the BLAST2GO utility (Conesa et al., 2005) for further annotation including GO Mapping, GO Annotation, Enzyme Code Annotation, and InterproScan (Jones et al., 2014). GO Slim (Gene Consortium, 2014) annotations were further generated for broad transcriptome wide comparisons.

Comparisons to an existing *P. borchgrevinki* transcriptome were conducted utilizing the transcripts of the current transcriptome as query sequences in BLASTn against the transcripts of the transcriptome from Bilyk and Cheng (2013) as the database with a threshold cutoff of 1E-3.

Differential Gene Expression Analysis

Using raw mapping counts from Bowtie2 (Langmead & Salzberg, 2012), RSEM (Li & Dewey, 2011) analyses were conducted to generate estimated read-count (count) and FPKM counts for each sample at the transcript and gene level. The Trinity pipeline (Trinity version trinityrnaseq-2.0.3) (Broad Institute and the Hebrew University of Jerusalem, 2014) was used to aggregate these counts into master matrices for import into the *R* statistical package (R Core Team, 2013). Before import, the samples were grouped by time-point and treatment similarity to conduct pairwise analyses of the effect of the multi-stressor treatment over time as compared to the control. Empirical analysis of digital gene expression data in *R* (“edgeR” version 3.4.2) was implemented to conduct differential gene expression analyses (Robinson *et al.*, 2010); dispersion values were calculated using the replicate groups; and exact tests utilizing a negative binomial

distribution with a cutoff false discovery rate (FDR) of 0.05 were used to identify differentially expressed transcripts and genes.

A sample-level differential expression heat map was generated from the differential gene expression analyses resulting from edgeR using the Trinity pipeline. Within the BLAST2GO graphical interface package (Conesa et al., 2005) Fisher's Exact tests ($FDR \leq 0.05$) were conducted for differentially expressed transcripts of the multi-stressor treatment to identify over-represented gene ontology terms within the up- and down-regulated transcripts within each treatment group in general. Using custom Python scripts: GO Slim, BLAST annotation and expression data files were combined, and GO categories and genes of interest were extracted for further analysis.

Table 3.1: *Pagothenia borchgrevinki* transcriptome assembly statistics.

	Transcript Level	Gene Level
# Sequences	83,869	46,176
N50 (bp)	2,590	2,771
Median Length (bp)	1,002	998
Mean Length (bp)	1,533	1,589
Total Transcriptome Length (bp)	128,610,174	73,397,004

Table 3.2: *Pagothenia borchgrevinki* transcriptome annotation statistics.

	Transcript Level	Gene Level
Total	83,869	46,176
GO Annotation	38,497	19,577
Blast Only	20,515	9,152
No Annotation Result	24,857	17,447

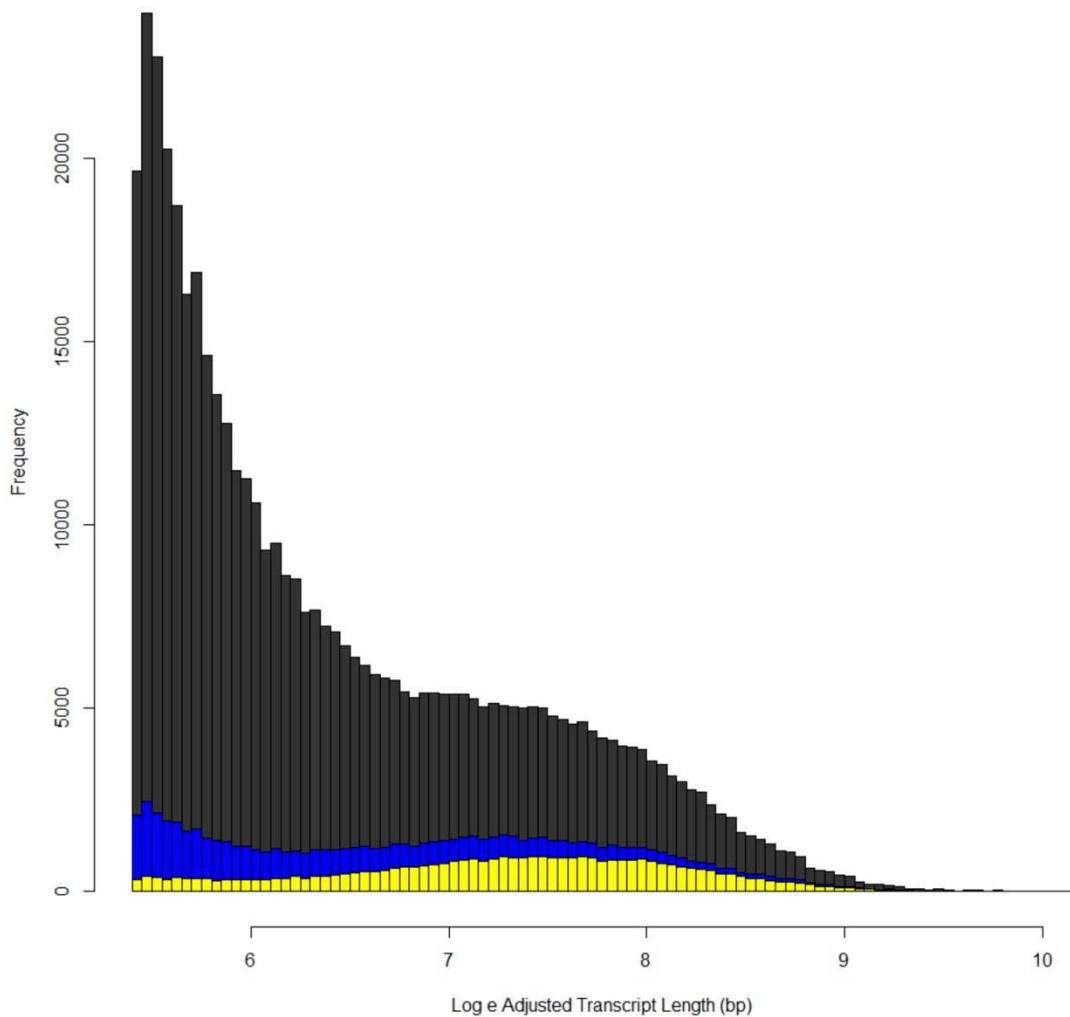


Figure 3.1 – Transcriptome transcript size distribution: The length distribution (log_e adjusted) of transcripts with a minimum length of 200bp resulting from de novo assembly (grey), following CD-HIT-EST transcript clustering with a percent identity requirement of 95% (blue) and transcript filtering after RSEM requiring an expression level of at least 1.0 FPKM (yellow).

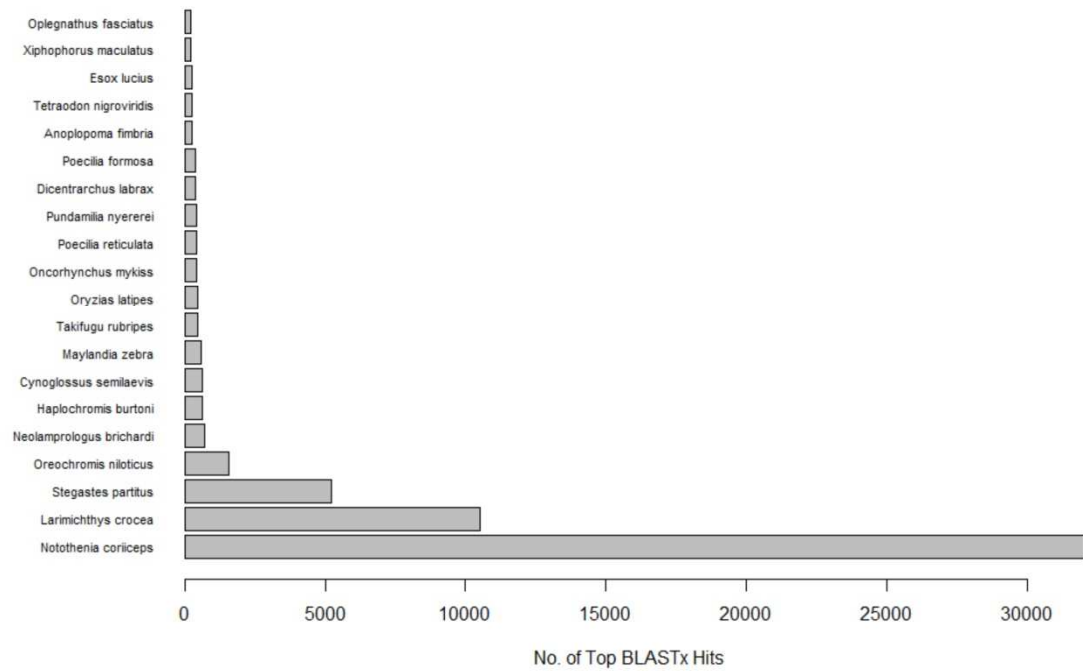


Figure 3.2 – Top BLAST result species: Following BLASTx searches of the transcripts of the reference transcriptome against the NCBI nr database, up to 10 BLAST hits were obtained for each transcript. The BLAST hit for each sequence with the lowest e-value was designated as the top hit and the species which the result match originated was recorded. The graph represents the total number of BLAST hits out of all top BLAST hits mapped to each particular species.

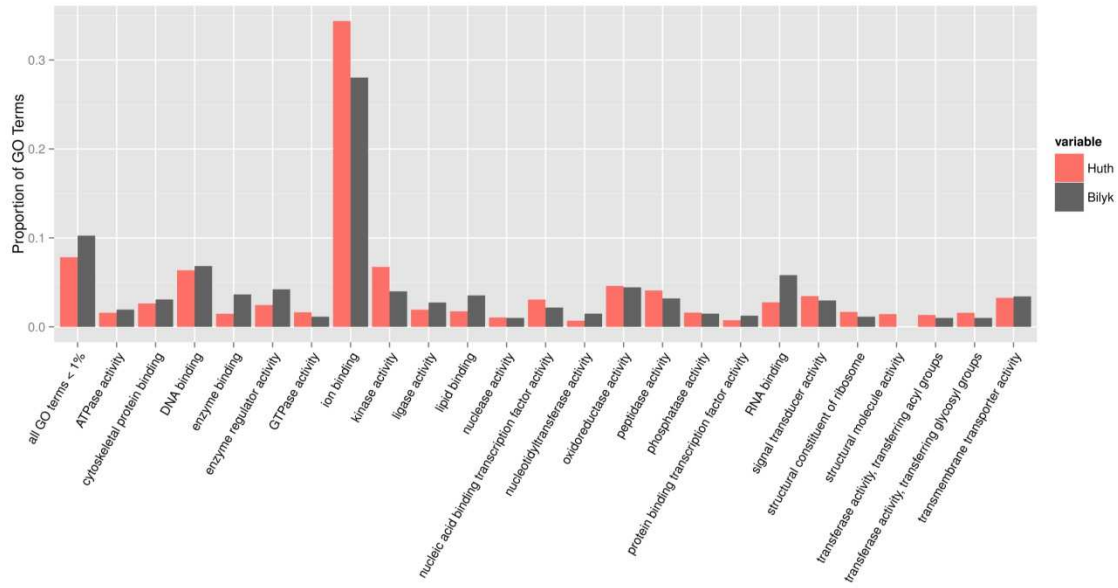


Figure 3.3 – *P. borchgrevinki* transcriptome level GO comparison: A comparison of the GO term distribution for the broad category of molecular function is provided for the previous *P. borchgrevinki* transcriptome assembly and annotation conducted by Bilyk and Cheng (2014) and the current transcriptome assembly and annotation. To provide a more direct comparison, the data bars represent the proportion of terms assigned to the specific GO term listed along the x-axis out of all GO terms within that broad category.

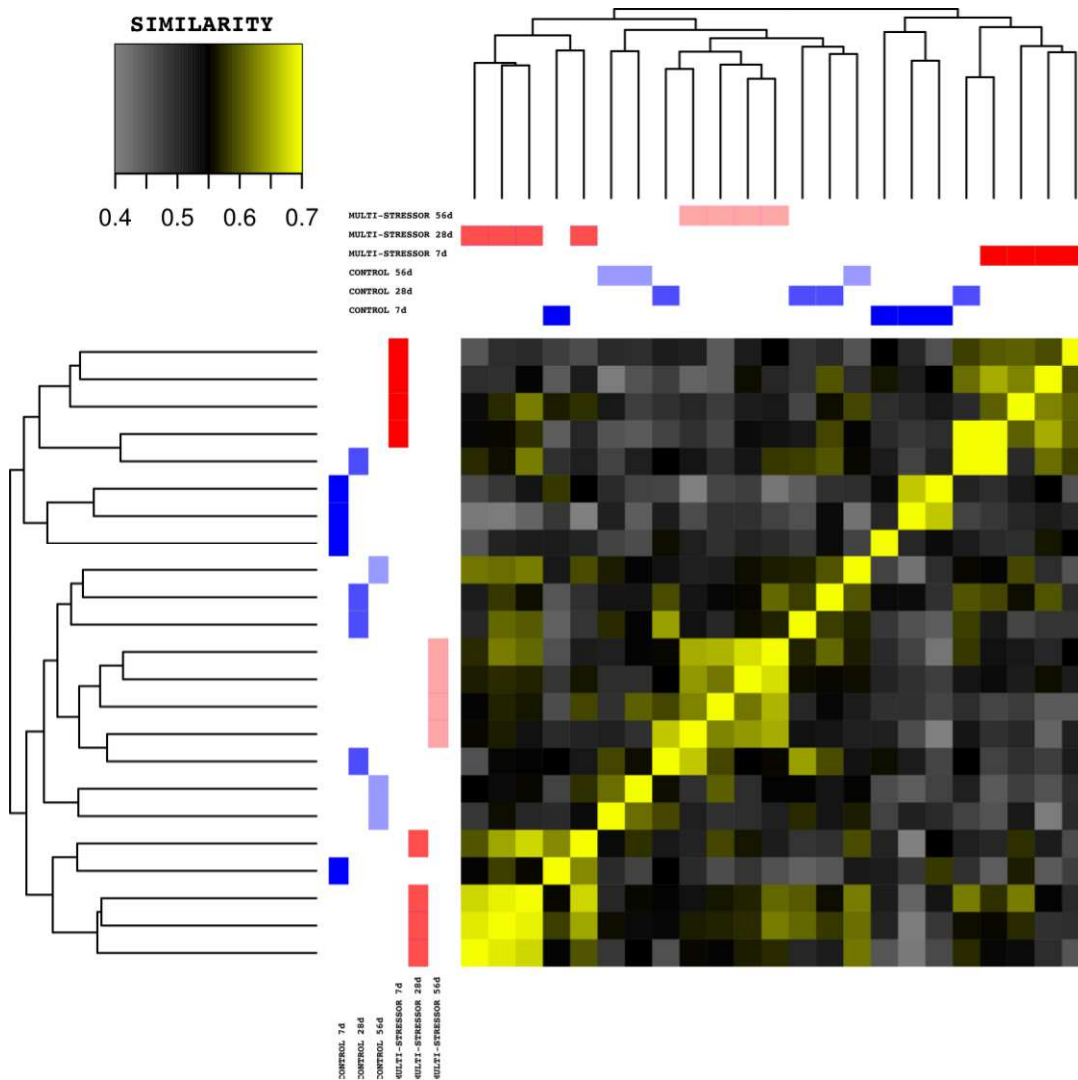


Figure 3.4 – Sample level gene expression correlation matrix: The correlation matrix demonstrates the level of transcriptome wide gene expression correlation from 0-1, with 0 indicating no correlation and 1 indicating an identical expression profile. The current correlation matrix is indexed between 0.5 and 0.9 with black representing a correlation of 0.5 and yellow representing a correlation of 0.9. Cluster dendrograms are provided to demonstrate the relationships between the expression profiles of each individual sample.

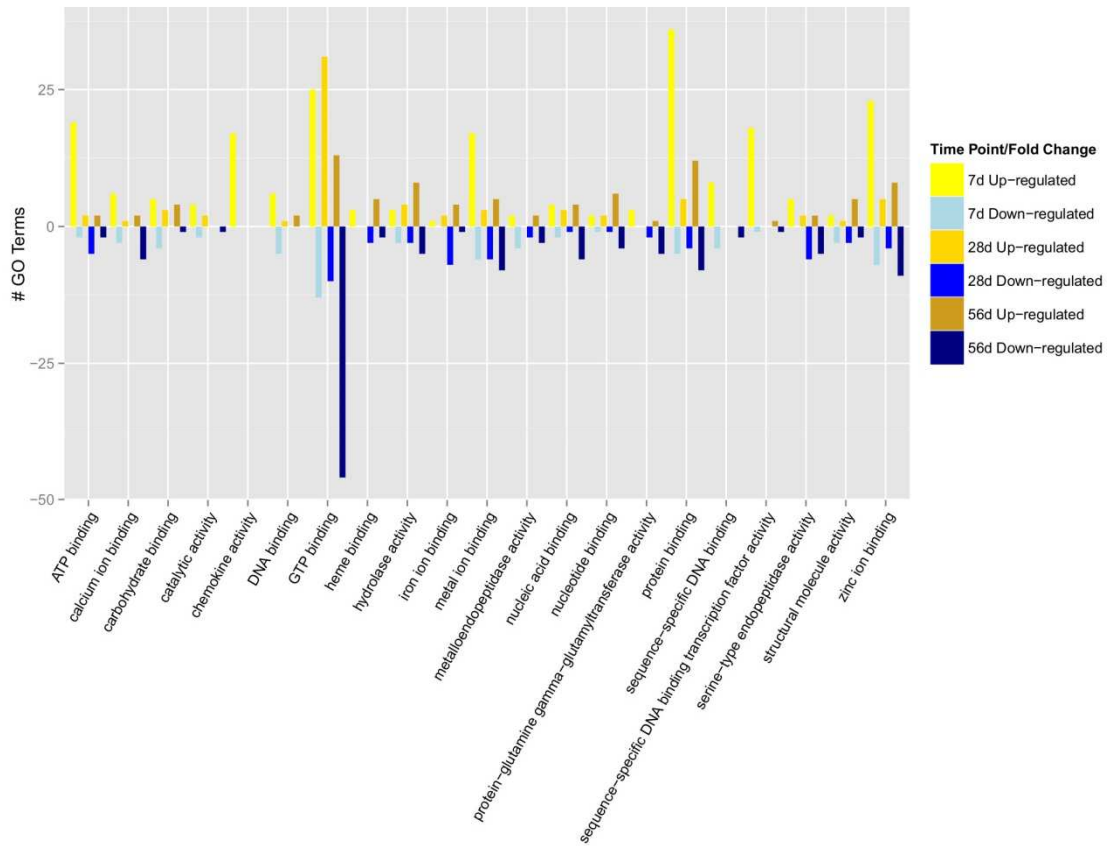


Figure 3.5 – GO molecular function expression: Molecular function gene ontology terms with more than 5 differentially expressed genes per category ($FDR \leq 0.05$) across all time-points are shown for each time-point. Yellow bars indicate the number of up-regulated genes associated with that GO term and blue bars indicate the number of down-regulated genes associated with that GO term.

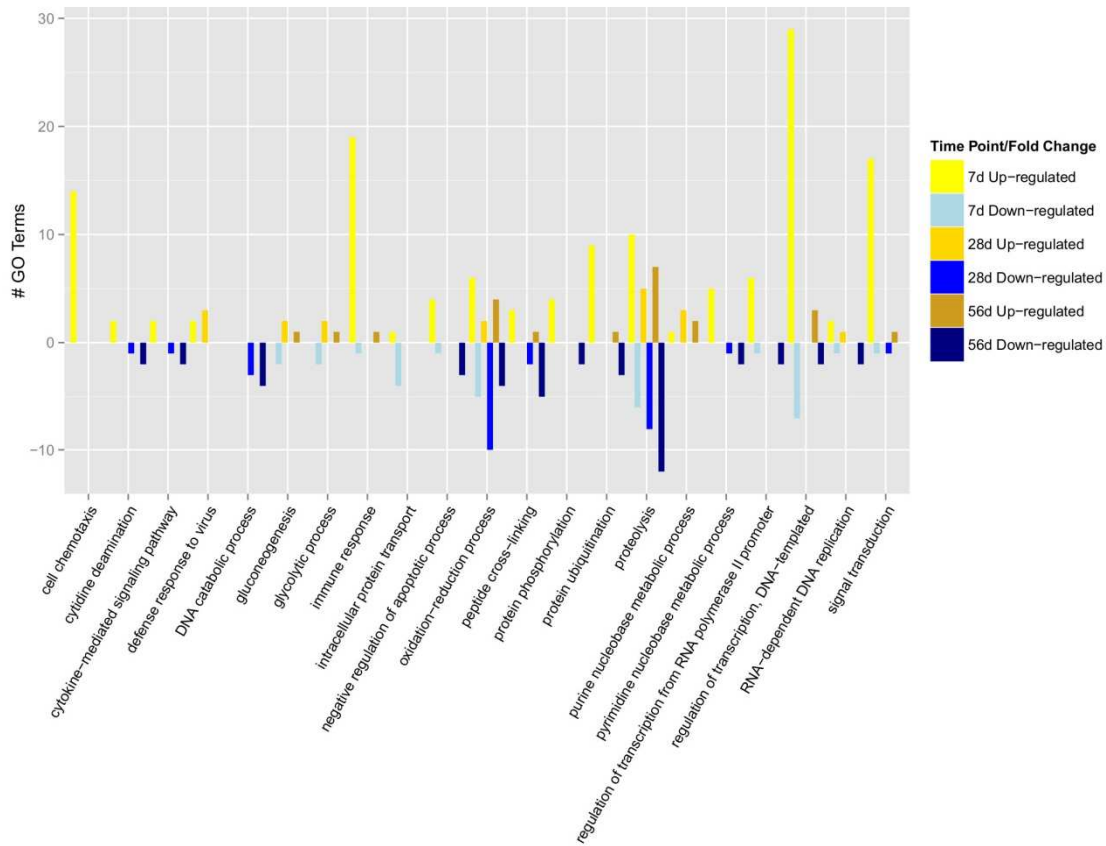


Figure 3.6 – GO biological process expression: Biological process gene ontology terms with more than 5 differentially expressed genes per category ($FDR \leq 0.05$) across all time-points are shown for each time-point. Yellow bars indicate the number of up-regulated genes associated with that GO term and blue bars indicate the number of down-regulated genes associated with that GO term.

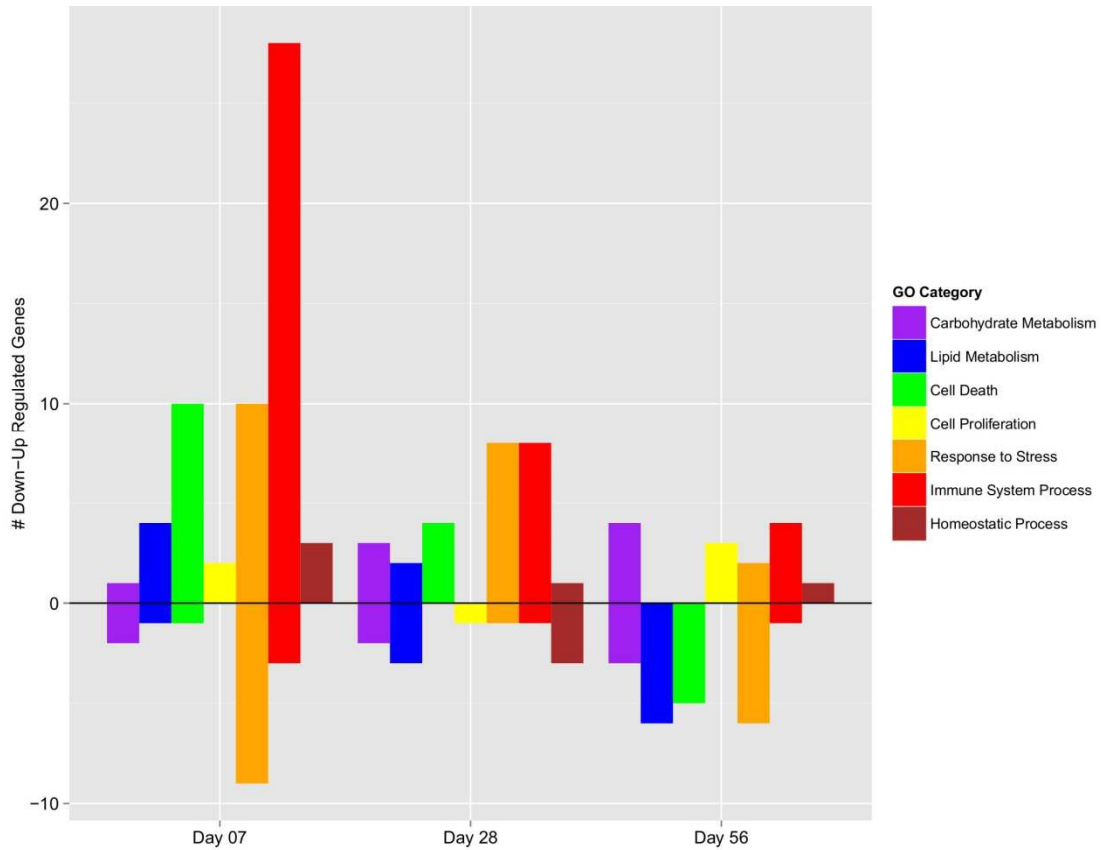


Figure 3.7 – Pathway expression summary: The number of differentially expressed genes ($FDR \leq 0.05$) for the biological process gene ontology categories: response to stress (GO:0006950), immune system process (GO:0002376), homeostatic process (GO:0042592), carbohydrate metabolic process (GO:0005975), lipid metabolic process (GO:0006629), cell proliferation (GO:0008283) and cell death (GO:0008219) are shown for each multi-stressor treatment as compared to the control for the 7d, 28d and 56d time-points. A bar above the black line indicates the number of up-regulated genes within that GO category, whereas the bar below the black lines indicates the number of down-regulated gene within that GO category.

CHAPTER 4

GENOME WIDE EXPRESSION ANALYSIS OF THE DUSKY ROCKCOD,
TREMATOMUS NEWNESI, DEMONSTRATES A PARADOXICAL RESPONSE TO
OCEAN ACIDIFICATION AND INCREASING SEA SURFACE TEMPERATURES.⁴

⁴ Huth, T. J., & Place, S. P. To be submitted to *G3: Genes Genomes Genetics*

4.1 INTRODUCTION

The Antarctic notothenioid fish of the Southern Ocean have long drawn the attention of polar researchers due to their dominance of the Southern Ocean fauna (J. T. Eastman, 2005; J. Eastman, 1993; Gon & Heemstra, 1990) and their unique cold adapted physiology (Bilyk et al., 2012; Chen et al., 2008; Crockett & Sidell, 1990; G E Hofmann et al., 2000; Place et al., 2004; Q. Xu et al., 2008). For these same reasons they have recently become a focus for researchers seeking to ascertain the potential ramifications of climate change on the species of the Southern Ocean. As global climate change accelerates and exerts a strong influence on high latitude regions, the waters of the Southern Ocean are likely to see a sustained and relatively rapid increase in temperature and $p\text{CO}_2$ (Pachauri et al., 2014). With their adaptation to the extreme and stable cold of the Southern Ocean, (Coppes Petricorena & Somero, 2007) notothenioids may be particularly susceptible to environmental perturbations while also finding that there is no similar alternative habitats available for migration.

A number of studies have identified the loss of an inducible heat shock response as one of the unique physiological alterations exhibited by notothenioids (G E Hofmann et al., 2000; Huth & Place, 2013, 2015b; Place et al., 2004). In addition, a number of physiological studies performed on these fish have broadened our scope of understanding with respect to the impacts of heat stress. These studies have found notothenioids to exhibit elevated oxidative damage (Carney Almroth et al., 2015), modulated oxygen consumption and metabolism (Jayasundara et al., 2013; Esme Robinson & Davison, 2008), and signs of increased apoptosis (Sleadd et al., 2014) when under short and long term heat stress. Genomic based studies have furthered this knowledge by examining

changes in gene expression under heat stress and identifying many of the molecular pathways involved in the notothenioid cellular stress response (CSR) (Bilyk et al., 2012; Buckley & Somero, 2009; Huth & Place, 2013).

Recognizing that the cumulative effect of multiple stressors may result in significant variation in stress responses (O'Donnell et al., 2009; Rosa & Seibel, 2008; Schulte, 2007) and in an attempt to more accurately represent potential future conditions of the Southern Ocean, recent studies have focused upon the effects of increasing temperature and $p\text{CO}_2$. These physiological studies provide a survey of three distinct notothenioid species *Pagothenia borchgrevinki*, *Trematomus bernacchii*, and *Trematomus newnesi*; indicating that all three species do exhibit some level of acclamatory response to the this multi-stressor condition and that the response varies between species (Enzor & Place, 2014, 2015; Enzor et al., 2013). In order to assess the difference between these three species, recent efforts have been undertaken to analyze the transcriptomic response of *T. bernacchii* (Huth & Place, 2015b) and *P. borchgrevinki* (Huth & Place, 2015a) under these same multi-stressor conditions, with the further goal of assessing the physiological plasticity possessed by these species to adapt to a changing Southern Ocean. The results of these studies confirm that the adaptive response of these notothenioids does vary considerably between species, and this variation may lead to impacts on the fitness of some notothenioid species in a changing environment.

The focus of the current study is to examine the genomic response of the third notothenioid, *T. newnesi*, under the multi-stressor condition of increased temperature and $p\text{CO}_2$. With little sequence data currently available for *T. newnesi* this study will greatly increase the genomic resources available for this notothenioid species. By gaining further

insight into the adaptive response of this notothenioid we aim to not only assess its physiological plasticity in light of a changing climate, but also to provide another point of reference that can be used to assess the susceptibility of the sub-order Notothenioidie as a whole. In this investigation we analyze *T. newnesi* on multiple levels from transcriptome-wide to gene specific changes in expression level, to assess its molecular response to conditions approximating those of a changing Southern Ocean(Pachauri et al., 2014) while providing broad comparisons of multiple notothenioid species under these same conditions.

4.2 RESULTS

Sequencing and quality control

Paired end sequencing of 150bp paired-end reads of all 24 individual samples derived from a single lane on an Illumina HiSeq 2500 Rapid Run yielded a total of 309,423,940 paired-end reads of raw sequencing data. Following aggressive quality control to eliminate reads of low quality, including any reads orphaned during the trimming process, 86.36% of these initial reads remained. The 267,215,937 paired-end reads surviving quality control were retained as high quality sequencing data for *de novo* assembly input.

Single end sequencing of 100bp paired-end reads of all 24 individual samples on two Illumina HiSeq 2500 Rapid Run lanes yielded an average of 24,666,422 single reads (s.d. = 2,293,013). Quality control removed single reads that exhibited overall low quality, however read quality proved to be excellent with an average of 94.2% of reads

surviving quality control screening (s.d. = 0.1%). Following quality control the individual samples possessed an average of 23,247,355 single end reads (s.d. = 2,172,968).

Reference transcriptome assembly, annotation

Following a normalized *de novo* assembly the transcriptome consisted of 728,129 transcripts and 462,993 ‘genes’ (unique gene products including all related transcripts); with a median transcript length of 444bp, mean transcript length of 924bp and N50 of 1748bp (Figure X). Following transcript compacting to eliminate redundant sequences; 421,169 transcripts and 315,483 genes remained (median = 413bp, mean = 819bp, N50 = 1448bp). Lastly, RSEM filtering at FPKM ≥ 1 to remove transcripts with little expression, and thus of potentially dubious value, produced a final reference transcriptome containing 95,561 transcripts and 53,587 genes; with a median transcript length of 893bp, mean transcript length of 1454bp and N50 of 2516bp (Table 1).

BLASTx searches yielded hits for 64,940 transcripts, which represented 30,374 hits on the gene level (Table 2); a success rate of 68.0% at the transcript level and 56.7% at the gene level. An analyses of the Top BLAST hit per transcript reveals the high degree of similarity between notothenioids and distinctiveness from non-polar species with 36,670 of the 64,940 BLAST top-hits to *Notothenia coriiceps*, which is over 3 times as many as the next nearest species, a non-notothenioid fish. GO annotation yielded a total of 32,277 transcripts with assigned GO Terms, represented 15,420 GO annotated genes (Table 2); or 48.9% of transcripts and 50.8% genes with a BLAST result being GO annotated.

Sample level differential gene expression analysis

Mapping of the 24 SE 100bp trimmed samples to the reference transcriptome yielded an average of 23,247,356 reads mapped to the reference transcriptome (s.d. = 2,127,217) an average mapping rate of 92.2% (s.d. = 0.9%).

Applying a 2-fold minimum change in expression to the gene level differential expression results uncovered 846 differentially expressed genes between the 7d control and the 7d multi-stressor treatments; of these 607 were up-regulated and 239 were down-regulated. Between the 28d control and multi-stressor treatments there were 949 differentially expressed genes exhibiting at least 2-fold changes, with 510 up-regulated and 439 down-regulated. The 42d time-point exhibited the lowest number of differentially expressed genes with a 2-fold or greater change with 451, of which 270 were up-regulated and 181 were down-regulated.

Differential expression patterns at the sample level indicate a general correlation in expression profiles between all samples of 71% (Figure 1). The sample correlation analysis further confirms the expected strong correlation in expression profiles between samples within both the same treatment and time-point with the correlations levels being: 7d control = 76%, 28d control = 78%, 42d control = 74%, 7d multi-stressor = 81%, 28d multi-stressor = 79%, and 42d multi-stressor 77% (Figure 1). Interestingly, despite individuals within the same time-point possessing a substantially higher correlation than that observed for all samples, we do not see a strong correlation between different time-points of the multi-stressor treatment with 70% correlation between the 7d/28d time-points, 72% correlation between the 7d/42d time-points, and 73% between the 28d/42d time-points (Figure 1).

Gene ontology over-representation

Utilizing GOSlim annotation in conjunction with Fisher's Exact Tests of GO over-representation ($p \leq 0.05$) to elucidate major cellular trends indicated an evolving cellular stress response to the multi-stressor treatment as time progressed. Biological processes found to be over-represented in genes up-regulated 2-fold or greater at the 7d multi-stressor time-point included tRNA metabolic process (61), cellular amino acid metabolic process (106), translation (61), and DNA metabolic process (17); which were complemented by a number of molecular functions including nuclease activity (11) and ligase activity (83). These processes are indicative of a large scale genomic response to the multi-stressor condition with a significant amount of new gene expression occurring. Significantly over-represented biological processes in the 7d down-regulated sub-group included response to stimuli (28) and protein folding (7), with corresponding molecular functions including helicase activity (9) and unfolded protein binding (7). Strikingly, these categories are often associated with molecular chaperone activity and proteins synthesis/ protein rescue.

Biological process significantly over-represented in the 2-fold up-regulated group of the multi-stressor condition at 28 days included immune system process (26), locomotion (15) and protein maturation (6). In the 28d multi-stressor sub-group both the up- and down-regulated subgroups exhibited the over-representation of the biological process nucleobase-containing compound catabolic process (9 and 12 respectively) and the molecular function nuclease activity (12 in both sub-groups). The 42 day multi-stressor time-point exhibit the over-representation of the biological processes sulfur compound metabolic process (8) and tRNA metabolic process (5) in the 2-fold up-

regulated sub-group, with the additional over-representation of the molecular function methyltransferase activity (8). The down-regulated sub-group exhibited over-representation in the biological processes system process (5) and growth (6).

An inverse heat-shock response

As anticipated, *T. newnesi* does not exhibit an up-regulation of inducible heat shock proteins in the 7d multi-stressor treatment. Conversely, we observed a strong and consistent down-regulation of a number of heat shock proteins ($FDR \leq 0.05$). The inducible isoform of the heat shock protein 90 family of chaperones (HSP90 α) experiences the down-regulation of 5 separate contigs ranging from 2.6-fold down-regulation to a 4.4-fold down-regulation (Figure 2, Supplementary Table 3). Additionally, the heat stress inducible HSP70 also experiences down-regulation in the 7d multi-stressor treatment, with two HSP70 isoforms both down-regulated 1.6-fold (Figure 2). This response continues into the 28d multi-stressor treatment with 4 HSP90 α isoforms continuing to exhibit a strong trend of down-regulation (-3.1-fold to -3.4-fold); and one HSP70 isoform down-regulated 1.7-fold (Figure 2). By the 42d multi-stressor treatment there is no differential regulation of heat shock proteins.

The cellular stress response

Although acclimation to the multi-stressor treatment for 7d elicits a strong cellular response in *T. newnesi* that involves many of the same pathways previously associated with the CSR, analysis of the direction of change in this species revealed a paradoxical response. A close analysis of a number of the over-represented GO terms above, in addition to several other biological processes including response to stress, cell proliferation, and transcription, indicates a number of the pathways associated with the

CSR in fish appeared to be strongly down-regulated at the 7d time-point in the multi-stressor condition (Table 3).

In addition to the down-regulation of HSP genes discussed above, other down-regulated genes associated with a response to stress include a number of PPIs, which assist in protein folding and are involved in oxidation related cellular necrosis (Supplementary Table 3). We did observe a number genes associated with Go category, response to stress, and were differentially up-regulated in at least one time point (FDR<0.005). However, the up-regulated genes associated with response to stress generally experience less dramatic changes in expression (average fold change = 0.88) than the down-regulated genes whose average magnitude of fold-change was over double that (Figure 2).

Despite the contradictory changes in gene expression of genes associated with the GO category response to stress, there was an up-regulation of genes associated with the maintenance of homeostasis (4 up-regulated, 0 down-regulated) and immune system processes (6 up-regulated and 3 down-regulated), which were more consistent with previous observations of gene expression patterns in notothenioid fish. (Table 3, Figure 2). Of particular note is the up-regulation (+2.0-fold, +1.8-fold) of thioredoxin TXNDC12.

Especially noteworthy at the 7d multi-stressor time-point is the strong and consistent up-regulation of genes related to transcription and translation with 13 genes associated with transcription up-regulated (and none down-regulated), and 38 genes associated with translation up-regulated (with only 1 down regulated) (Table 3, Figure 3). These trends also conflict with previous observations in other notothenioid fish that

appear to experience a decline in the early stages of acclimation to stressful conditions (Bilyk & Cheng, 2014; Huth & Place, 2015a, 2015b). Several of these genes are involved in the initiation of transcription in response to cellular stress including DDIT3 (+4.0-fold, +3.4-fold) and IRF3 (+2.5-fold). Relating to translation, a large number of these differentially expressed genes encode tRNA ligases, which are up-regulated anywhere from +1.6-fold to +4.8-fold (Supplementary Table 4). Additionally there are a number of up-regulated genes associated with translation elongation (EEF1A1, +1.7-fold; EEF1E1, +1.9-fold and +2.3-fold).

Corresponding with an increase in transcription and translation, we see the up-regulation of genes associated with cell proliferation (6 up-regulated, 2 down-regulated) (Table 3, Figure 4). The up-regulated genes include GDF15 (+3.4-fold, +3.5-fold) which inhibits macrophage activation and suppress apoptosis (Kadara, Schroeder, Lotan, Pisano, & Lotan, 2006) and IGF1 (+2.0-fold) (Supplementary Table 5) which promotes cell differentiation and growth (Kiepe, Ciarmatori, Hoeflich, Wolf, & Tönshoff, 2005). Conversely, genes associated with cellular death experience relatively muted expression, with only 2 significantly up-regulated and 1 significantly down-regulated (Table 3, Figure 4, Supplementary Table 5). Again, these results differ substantially from previous transcriptomic analyses that found evidence of reduced cell growth and proliferation combined with higher levels of apoptosis conditions (Bilyk & Cheng, 2014; Huth & Place, 2015a, 2015b).

Similar to trends observed in *P. borchgrevinki* held under the same acclimation conditions, we observed little impact on the metabolic pathways of *T. newnesi*. The 7d day multi-stressor treatment had little effect on carbohydrate metabolism, with only 3

total differentially expressed genes (1 up-regulated, 2 down-regulated) (Table 3, Figure 4). Lipid metabolism experiences more significant changes (9 up-regulated, 4 down-regulated) (Table 3, Figure 4); and there is some indication of the increased utilization of lipids as an energy source with the up-regulation of endothelial lipase (+2.1-fold) and PDC (+1.8-fold), but this trend was not overwhelming, especially when compared to the dramatic shifts in energy utilization observed in *T. bernacchii* when acclimated to the same multi-stressor conditions (Huth & Place, 2015b).

The cellular homeostatic response

The 28d multi-stressor treatment demonstrates a significant shift in expression from the 7d time-point (Figures 2-4). While pathways related to cellular stress continue to exhibit a robust, albeit changing, response; other pathways such as transcription and translation undergo significant reductions in differential gene expression.

Genes associated with response to stress continue a largely balanced expression pattern, with 8 up-regulated and 11 down-regulated (Table 3). However, the specific genes that experience differential regulation at this time-point are considerably different from those seen in the 7d multi-stressor treatment. At 28d there is a strong down-regulation of multiple variants of the pro-inflammatory gene, SAMHD1 (-3.8, -3.7, -2.7, and -1.6-fold) (Figure 2), in addition to the continued down-regulation of HSP90 isoforms discussed above. Meanwhile other pro-inflammatory genes are up-regulated for the first time including CatB (two variants both at +1.7-fold) and EPX (+1.8-fold) (Figure 2). An increasing inflammatory response is further supported by the up-regulation of 18 genes associated with immune system processes, as opposed to only 4 down-regulated (Table 3). Among the up-regulated genes are a large number of chemokine and major

histocompatibility complex related genes experience consistent and significant up-regulation from +1.9-fold to +27.3-fold (Figure 2). The homeostatic processes observed in 7d acclimated fish, however, have largely dissipated their differential regulation with only 1 up-regulated and 1 down-regulated gene (Table 3, Figure 2).

Fish acclimated to the 28d multi-stressor time-point also exhibited a substantial shift in the direction of the DE genes related to transcription with 10 up-regulated and 7 down-regulated (Table 3, Figure 3). This decline in protein turnover is further reflected in a decrease in the DE genes associated with translation, with only 1 gene up-regulated and 4 down-regulated (Table 3, Figure 3). Similarly, there is a drop in the differential expression of genes associated with cell proliferation with only 3 up-regulated and 1 down-regulated in the 28d multi-stressor treatment (Table 3, Figure 3). Cell death also experiences a similar dearth of differential gene expression (2 up-regulated, 2 down-regulated) (Table 3, Figure 3). The 28d multi-stressor also exhibits little change in energy metabolism with lipid metabolism experiencing only 3 up-regulated and 2 down-regulated genes, and carbohydrate metabolism experiencing only 6 up-regulated and no down-regulated genes (Table 3, Figure 3).

By the 42d multi-stressor treatment there is very little differential expression observed. Immune system processes, homeostatic processes and response to stress only exhibit 3, 0, and 1 differentially expressed genes respectively (Table 3, Figure 2). Transcription exhibits only 3 differentially expressed genes, with translation only demonstrating 4 (Table 3, Figure 3). This lack of a response is further seen in the metabolic pathways with only 2 differentially expressed genes in carbohydrate

metabolism and 1 in lipid metabolism; and cell death and proliferation also exhibiting only 1 and 2 differentially expressed genes a piece (Table 3, Figure 4).

4.3 DISCUSSION

It is clear that *T. newnesi* possesses a coordinated and evolving response to the conditions of the multi-stressor treatment intended to mimic potential future conditions in the Southern Ocean. However, the question remains how does this response affect the fitness of *T. newnesi* and what are the long term implications of this response on this species' adaptability to a changing climate?

Past research has consistently supported the finding that notothenioids lack an inducible heat shock response when exposed to heat stress (Buckley et al., 2004; G E Hofmann et al., 2000; Huth & Place, 2013). It has been surmised that the lack of an inducible heat shock response in notothenioids is a result of the need to constantly express these genes to counter the denaturing effects of persistent cold (Place & Hofmann, 2005; Place et al., 2004). Our recent studies involving the closely related species *T. bernacchii* and *P. borchgrevinki* have further confirmed that this finding is supported under the multi-stressor conditions employed in the current study (Huth & Place, 2015a, 2015b). While the current findings do support that idea that HSPs are not up-regulated during stressor conditions, we do find a consistent down-regulation of multiple HSP90 and HSP70 related genes in the 7d and 28 multi-stressor treatments, which was not found in our previous efforts with *T. bernacchii* and *P. borchgrevinki* under identical conditions (Huth & Place, 2015a, 2015b). However, other research into *P. borchgrevinki* under heat-stress alone observed a wide-spread and consistent down-

regulation of HSPs at 4 days (Bilyk & Cheng, 2014). This decrease in HSP expression has been postulated as an indication that elevated temperatures may provide more favorable protein folding conditions, potentially increasing the stability of some proteins and thus reducing the need for chaperoning activity (Bilyk & Cheng, 2014; Huth & Place, 2013). Increased protein folding efficiency would also result in reduced rates of protein turnover and potentially explain the slow-down in protein synthesis previously observed in notothenioid fish (Bilyk & Cheng, 2014; Haschemeyer & Matthews, 1983; Haschemeyer, 1982). It is possible that *T. newnesi* is experiencing a decrease in protein stress with warming temperatures and thus does not need to persistently express these HSPs. If this were true it would seem to indicate that notothenioids in general remain capable of modulating the expression of HSPs.

However, we would expect that this change would persist throughout all time-points within the multi-stressor treatment, which it does not. Furthermore, the apparent increase in transcription/translation observed in *T. newnesi* is at odds with the concept of reduced protein turn-over as a consequence of more stable protein folding conditions. Consequently, an alternative explanation may be that HSP90 and HSP70 are being down-regulated in order to allow apoptosis to occur more readily, as HSPs have been demonstrated to inhibit apoptotic pathways (Kennedy, Jäger, Mosser, & Samali, 2014; Sreedhar & Csermely, 2004). Once cellular remodeling is largely completed by the 42 time-point, these HSPs return to normal expression levels. Furthermore, *T. newnesi* displayed extended bouts of oxidative damage under these same acclimation conditions. Previous research under these same conditions has indicated an increase in protein carbonyl concentrations in *T. newnesi* at the 7d time-point, but not to the same degree as

P. borchgrevinki or *T. bernacchii* (Enzor & Place, 2014). Moreover, the protein carbonyl levels were shown to decrease less rapidly over time in *T. newnesi* as compared to the other two notothenioids studied (Enzor & Place, 2014) indicating that protein damage continues to accumulate³¹. The accumulation of oxidatively damaged protein may play a role in maintaining the elevated rates of transcription and translation observed throughout day 28 in these fish. and suggests a possible explanation for the increased continued oxidative damage is prevalent. The most indicative response to oxidative damage found at 7 days in the current study is the up-regulation of TXN.

Apart from the differential expression in HSP related genes, *T. newnesi* demonstrates a muted initial stress response at the 7d time-point to the multi-stressor treatment. There are a handful of up-regulated genes related to stress and inflammation including chemokines and MHC genes, but the initial cellular stress response in these molecular pathways does not demonstrate the robust nature previously seen in *T. bernacchii* under these same conditions at the 7d time-point¹³. By the 28d multi-stressor time-point we observe a robust cellular stress response in *T. newnesi* involving a large number of chemokine and major histocompatibility complex related genes, in conjunction with CatB. This response then diminishes rapidly at 42d time-point, potentially indicating the transition of these pathways into a more permanent CHR state. Both the peak CSR, and the apparent transition to the long-term acclimation state appear to be delayed in *T. newnesi* compared to other notothenioid species^{13,25}. It may be that *T. newnesi* is initially over-whelmed by the multi-stressor condition and cannot mount a more significant response, or alternatively that cellular resources are being allocated to other processes as part of an initial response.

While the initial cellular stress response demonstrated by *T. newnesi* is not nearly as robust as some other notothenioids, *T. newnesi* does exhibit a broad and relatively sustained up-regulation of both transcriptional and translational gene products with the most marked response in the 7d multi-stressor treatment. The analysis of over-represented gene ontology terms supports this idea of large scale cellular remodeling with the over-expression of transcription/translation-related GO terms such as tRNA metabolic process, cellular amino acid metabolic process, translation, and DNA metabolic process in the up-regulated sub-group. Previous studies of notothenioids have not established a clear consensus on the effect of stressors on transcriptional and translational activity; *P. borchgrevinki* has been demonstrated to down-regulate genes associated with transcription and translation after 4 days of heat stress alone in liver tissue (Bilyk & Cheng, 2014), whereas *T. bernacchii* has been shown up-regulate genes associated with transcription after 4 hours of heat stress in gill tissue (Buckley & Somero, 2009). These studies and others indicate that these results are not only time and species dependent, they are also tissue specific (Buckley et al., 2006; Prunet, Cairns, Winberg, & Pottinger, 2008). Our previous efforts involving *T. bernacchii* and *P. borchgrevinki* under the same multi-stressor conditions and in the same tissue of the current study have indicated that *T. bernacchii* demonstrates a sizable increase in genes related to transcription and translation at 7 days (Huth & Place, 2015b), whereas *P. borchgrevinki* does not (Huth & Place, 2015a). These results seem to indicate that the genus *Trematomus* initiates a much more robust CSR that involves a considerable amount of cellular remodeling, whereas the genus *Pagothenia* does not.

Two peculiar aspects of the CSR/CHR response of *T. newnesi* is the dearth of differential expression in carbohydrate or lipid metabolic processes and in genes related to cell death and proliferation, that contrasts with the response of other closely related notothenioids (Bilyk & Cheng, 2014; Buckley & Somero, 2009; Huth & Place, 2015a, 2015b). A lack of metabolic adaptation to the multi-stressor conditions does however correlate with other findings of *T. newnesi* under identical conditions, where *T. newnesi* unlike other notothenioids continued to experience increased resting metabolic rates throughout the multi-stressor treatment that did not return to basal levels (Enzor et al., 2013). It may be that *T. newnesi* either modifies its metabolic capacity more slowly than other notothenioids, or perhaps lacks the capacity to do so altogether, requiring continued increased levels of oxygen consumption to offset the energy expenditures necessary to cope with the multi-stressor condition. Additionally, the lack of differential expression in cell death and proliferation indicates that the remodeling response in *T. newnesi* may not be as robust and dramatic as other notothenioids, with almost no indication of cell proliferation throughout all time-periods. While other notothenioids may retain the capability of remodeling gill tissues to cope with the challenges of the multi-stressor environment as has been seen in other teleosts (Nilsson, 2007), *T. newnesi* may not possess the energy reserves for large scale remodeling.

Our findings indicate that *T. newnesi* does exhibit a coordinated response to the multi-stressor conditions intended to mimic future changes to the Southern Ocean. The initial CSR is relatively robust and provides evidence of some cellular remodeling in an attempt to cope with the stressor conditions, however not at the same scale observed in closely related species. However, the lack of significant changes in metabolism or

renewal of damaged tissues through cell proliferation may have important long-term implications for *T. newnesi*'s ability to cope with permanent changes in its environment. These aspects raise questions about *T. newnesi*'s fitness under changing conditions over an extended period of time and may reveal it to be one of the more susceptible notothenioids to global climate change impacts. With that said, however, this study focused upon the gill tissue of adult *T. newnesi* over a relatively short period of time due to experimental constraints. In order to obtain a firmer grasp of *T. newnesi*'s ability to adapt to a changing Southern Ocean further studies should be conducted involving additional tissue types over longer periods of time, as well as other phases of the reproductive cycle. The information obtained from such studies when combined with the present findings would likely present a much clearer picture of *T. newnesi*'s role in the ecosystem of a changing Southern Ocean.

4.4 METHODS

Collection of fish

Specimens of *T. newnesi* were collected in McMurdo Sound, Antarctica from September through December, 2012. Fish were caught using hook and line through 10-inch holes drilled through the sea ice and transported back to McMurdo Station in aerated coolers where they were housed in a flow-through aquaria maintained at ambient seawater temperature (-1.5°C). Fish were then tank-acclimated under ambient conditions for one week prior to being placed in experimental tanks. All procedures were conducted in accordance with the Animal Welfare Act and were approved by the University of

South Carolina Institutional Animal Care and Use Committee (ACUP protocol # 100377).

Experimental Design

We used four, 1240 L experimental tanks to assess the combined effects of elevated temperature and $p\text{CO}_2$ on *T. newnesi*. Our two experimental treatments consisted of a control tank which was held near ambient conditions (-1°C and $430\ \mu\text{atm}$) and a high temperature + high $p\text{CO}_2$ treatment ($+4^\circ\text{C}$ / $1000\ \mu\text{atm}$). Fish were placed in experimental tanks and acclimated for a total of 42 days. Five fish per treatment were removed at 7d, 28d, and 42d time-points, after which fish were sacrificed and gill tissues were collected and immediately flash-frozen in liquid nitrogen. Although we recognize a fully replicated experimental design is ideal to exclude tank effects as a possible confounding factor, the constraints of working in Antarctica prevented us from using this approach. However, our previous analyses show no tank effect when treatments were alternated between tanks across multiple seasons (Enzor & Place, 2014; Enzor et al., 2013).

Manipulation of seawater conditions

Temperature and $p\text{CO}_2$ levels were manipulated within the experimental treatment tanks using a $p\text{CO}_2$ generation system first described by Fanguie et al. (2010) (Fanguie et al., 2010) and adapted for use with large-scale applications and combined with thermostated titanium heaters (Process Technology, Brookfield CT, USA; Enzor et al. (2013) (Enzor et al., 2013)). Atmospheric air was pumped through drying columns (filled with drierite) to remove moisture, and air was scrubbed of CO_2 using columns filled with Sodasorb. Pure CO_2 and CO_2 -free air were then blended using digital mass flow controllers and bubbled into header tanks that were continuously replenished with

ambient seawater using venturri injectors, which in turn fed into experimental treatment tanks.

Temperature, pH (total scale), salinity, total alkalinity (TA) and oxygen saturation were measured daily from both incoming seawater as well as experimental treatment tanks. For $p\text{CO}_2$ analysis, we followed the SOP as described in the Best Practices Guide (Jean-Pierre Gattuso, Kunshan Gao, Kitack Lee, 2010) for the spectrophotometric determination of pH using m-cresol purple and measurement of total alkalinity via acid titration using a computer-controlled T50 Titrator (Mettler Toledo, Columbus, OH, USA). Temperature was measured with a calibrated digital thermocouple (Omega Engineering Inc., Stamford, CT, USA) and salinity was measured using a YSI 3100 Conductivity meter (Yellow Springs, OH, USA). CO_2 calc (Robbins et al., 2010), using the constants of Mehrbach et al. (1973) (Mehrbach et al., 1973) as refit by Dickson & Millero (1987) (Dickson & Millero, 1987), was used to calculate all other carbonate parameters. Oxygen saturation was recorded using a galvanic oxygen probe (Loligo Systems, Denmark). Mean values (\pm s.d.) of temperature ($^{\circ}\text{C}$) and $p\text{CO}_2$ (μatm) over the course of the experiment were first reported in Enzor and Place (2014) (Enzor & Place, 2014). Additionally, treatment tanks were sampled daily for the presence of ammonia, nitrite and nitrates, with no significant increase in waste products noted over the course of the experiment (data not shown).

Tissue collection and RNA extraction

To obtain individual gill-specific expression profiles, we separately indexed and sequenced RNA samples from gill tissue that had been collected from fish acclimated to the two experimental treatments described above ($n=5$ fish per treatment) for 7 days, 28

days and 42 days. Immediately after euthanizing the fish, tissues were excised in a -2 °C environmental chamber, flash frozen in liquid nitrogen, and shipped back to our home institution on dry ice where they were stored at -80 °C until used. Total RNA from approximately 100 mg of frozen tissue was extracted using TRIzol (Invitrogen) following the manufacturer's recommendations. The RNA was further cleaned by re-suspending in 0.1 ml of RNase/ DNase-free water and adding 0.3 ml of 6 M guanidine HCl and 0.2 ml of 100% ethylalcohol (EtOH). The entire volume was loaded onto a spin column (Ambion) and centrifuged for 1 min at $12,000 \times g$ at 4 °C. Flow-through was discarded, and filters were washed twice with 0.2 ml 80% EtOH. RNA was eluted off of the filters twice with 0.1 ml of DEPC-treated water. RNA was precipitated by the addition of 0.1 vol of 3 M sodium acetate (pH 5.0) and 2.5 vol of 100% EtOH, mixed by inversion of tubes and placed at -80 °C for 1 h. After this period, tubes were centrifuged at $12,000 \times g$ for 20 min at 4° C. Pellets were washed twice with 80% EtOH and re-suspended in 30 µl of RNase/ DNase-free water. Lastly, RNA was DNase treated at 30 °C for 10 min.

Total RNA from n=5 fish within an acclimation treatment was submitted to the Vaccine and Gene Therapy Institute (VGTI) Florida for quality assessment and determination of specific concentration using an Agilent 2100 BioAnalyzer. From the original samples, the 4 highest quality replicates from each treatment and time point were selected for cluster generation using the Illumina® TruSeq RNA Sample Prep v2 Hs Protocol and sequencing via an Illumina® HiSeq 2500 Rapid Run initialized for both paired-end 150bp reads and single-end 100bp reads.

Quality control

Raw reads from each of the twenty-three samples were processed using Trimmomatic (version Trimmomatic-0.33) (Bolger et al., 2014). For both paired-end and single-end reads Illumina® TruSeq RNA Sample Prep v2 HS adapters were removed as well as any bases on the end of the reads with a PHRED33 score of < 20 or any portion of the read that did not average at least a PHRED33 score of > 20 across a minimum span of 4bp. Paired-end reads with a length < 100 were removed, as well as any reads that were orphaned during the quality control process; whereas single-end reads with a length < 75 were removed (paired-end Trimmomatic parameter input: VGTI_Adapters_Trueq2-PEMultiplex.fa:2:30:10 LEADING:20 TRAILING:20 SLIDINGWINDOW:4:20 MINLEN:100; single-end Trimmomatic parameter input: VGTI_Adapters_Trueq2-PEMultiplex.fa:2:30:10 LEADING:20 TRAILING:20 SLIDINGWINDOW:4:20 MINLEN:75).

Reference transcriptome assembly, annotation and comparison

All paired-end reads surviving quality control were used as input in the Trinity *de novo* assembly utility (version trinityrnaseq-2.0.3) (Grabherr et al., 2011). The Trinity package efficiently recovers full-length transcripts and spliced isoforms across a range of expression levels, with less artificially constructed transcripts than other assembly utilities (Zhao et al., 2011). Assembly was conducted utilizing the Trinity's default parameters with read normalization (N=50). Following assembly raw transcripts were compacted using CD-HIT-EST (version cd-hit-v4.6.1-2012-08-27) (Fu et al., 2012) with a sequence similarity requirement of 95% to eliminate redundant transcript sequences. Then the single ends reads were mapped to the compacted transcripts utilizing Bowtie2

(Langmead & Salzberg, 2012) with default parameters; after which RSEM (Li & Dewey, 2011) was conducted to generate calculated FPKM values for each compacted transcript. Compacted transcripts were then filtered with only those possessing $FPKM \geq 1$ being retained for the final reference transcriptome.

Transcripts from the final reference transcriptome were used as query sequences in BLASTx (version: ncbi-blast-2.2.25+) (Camacho et al., 2009) searches with a minimum confidence value of $1E-6$ required for annotation against the NCBI nr (non-redundant) database (version May 2015). BLASTx was implemented in a massively parallel manner utilizing the resources of the Data Intensive Academic Grid (DIAG) (“Data Intensive Academic Grid,” n.d.). After BLASTx results were obtained, the transcript sequences and the corresponding BLASTx results were input into the BLAST2GO utility (Conesa et al., 2005) for further annotation including GO Mapping, GO Annotation, and Enzyme Code Annotation (Jones et al., 2014). GO Slim (Gene et al., 2014) annotations were further generated for broad transcriptome wide comparisons and pathway analyses.

Differential Gene Expression Analysis

Using raw mapping counts from Bowtie2 (Langmead & Salzberg, 2012), RNA-Seq by Expectation-Maximization (“RSEM” version 1.2.18) (Li & Dewey, 2011) analyses were conducted to generate estimated read-count (count) and fragments per kilobase million (FPKM) counts for each sample at the transcript and gene level. The Trinity pipeline (Trinity version trinityrnaseq-2.0.3) (Broad Institute and the Hebrew University of Jerusalem, 2014) was used to aggregate these counts into master matrices for import into the *R* statistical package (R Core Team, 2013). Before import, the samples

were grouped by time-point and treatment similarity to conduct pairwise analyses of the effect of the multi-stressor treatment over time as compared to the control. Empirical analysis of digital gene expression data in *R* (“edgeR” version 3.4.2) was implemented to conduct differential gene expression analyses (M. D. Robinson et al., 2010); dispersion values were calculated using the replicate groups; and exact tests utilizing a negative binomial distribution with a cutoff false discovery rate of 0.05 were used to identify differentially expressed transcripts and genes.

A sample-level differential expression heat map was generated from the differential gene expression analyses resulting from edgeR using the Trinity pipeline. Within the BLAST2GO graphical interface package (Conesa et al., 2005) Fisher's Exact tests ($FDR \leq 0.05$) were conducted for differentially expressed transcripts of the multi-stressor treatment to identify over-expressed gene ontology terms within the up- and down- regulated transcripts within each treatment group in general. Using custom Python scripts GO Slim, BLAST annotation and expression data files were combined, and GO categories and genes of interest were extracted for further analysis.

Table 4.1: *Trematomus newnesi* transcriptome assembly statistics: Statistics for the filtered de novo assembly were computed on the transcript and gene level. The # of sequences of the transcript level represent all surviving contiguous sequences, the # of sequences on the gene level represent the number of putative genes surviving based upon groupings of homologous transcripts.

	Transcript Level	Gene Level
# Sequences	95,561	53,587
N50 (bp)	2,516	2,778
Median Length (bp)	893	734
Mean Length (bp)	1,454	1,434
Total Transcriptome Length (bp)	138,966,447	76,875,859

Table 4.2: *Trematomus newnesi* transcriptome annotation statistics: Statistics for the filtered de novo assembly were computed on the transcript and gene level. The # of sequences of the transcript level represent all surviving contiguous sequences, the # of sequences on the gene level represent the number of putative genes surviving based upon groupings of homologous transcripts.

	Transcript Level	Gene Level
Total	95,561	53,587
GO Annotation	32,277	15,420
BLAST Only	33,677	14,953
No Annotation Result	29,607	23,213

Table 4.3: Pathway up- and down-regulation at each time-point: The total number of genes expressed in the up- and down-regulated sub-groups for each multi-stressor time point ($FDR \leq 0.05$) including genes associated with the gene ontology terms carbohydrate metabolic process (GO:0005975), lipid metabolic process (GO:0006629), cell death (GO:0008219), cell proliferation (GO:0008283), response to stress (GO:0006950), immune system process (GO:0002376), homeostatic process (GO:0042592), transcription (GO:0006351), translation (GO:0006412), and genes with BLAST results including heat shock related proteins. Total indicates the total number of genes of that particular category found in the reference transcriptome library as a whole.

	Total	7d Multi-stressor		28d Multi-stressor		42d Multi-stressor	
		<i>Up</i>	<i>Down</i>	<i>Up</i>	<i>Down</i>	<i>Up</i>	<i>Down</i>
Carbohydrate Metabolic Process	466	1	2	6	0	1	1
Lipid Metabolic Process	501	9	4	3	2	1	0
Cell Death	254	1	2	2	2	0	2
Cell Proliferation	174	6	2	3	1	1	0
Response to Stress	543	10	10	8	11	0	1
Immune System Process	364	6	3	18	4	2	1
Homeostatic Process	262	4	0	1	1	0	0
Transcription	599	13	0	10	7	2	1
Translation	480	38	1	4	0	4	0
Heat Shock Related	57	0	8	0	5	0	0

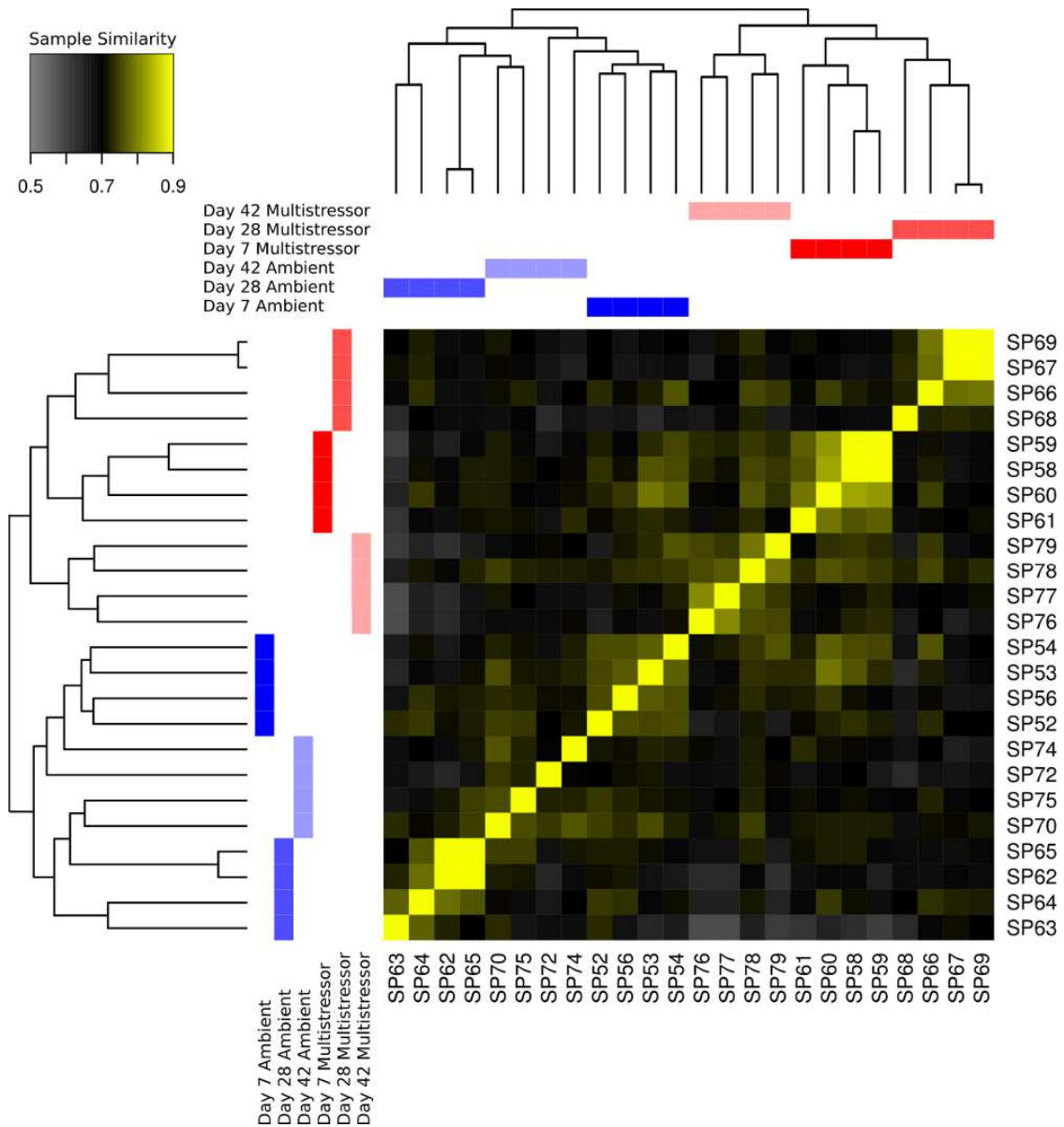


Figure 4.1 – Sample level gene-expression correlation matrix: The correlation matrix demonstrates the level of transcriptome wide gene expression correlation from 0-1, with 0 indicating no correlation and 1 indicating an identical expression profile. The current correlation matrix is indexed between 0.5 and 0.9 with black representing a correlation of 0.5 and yellow representing a correlation of 0.9. Cluster dendrograms are provided to demonstrate the relationships between the expression profiles of each individual sample.

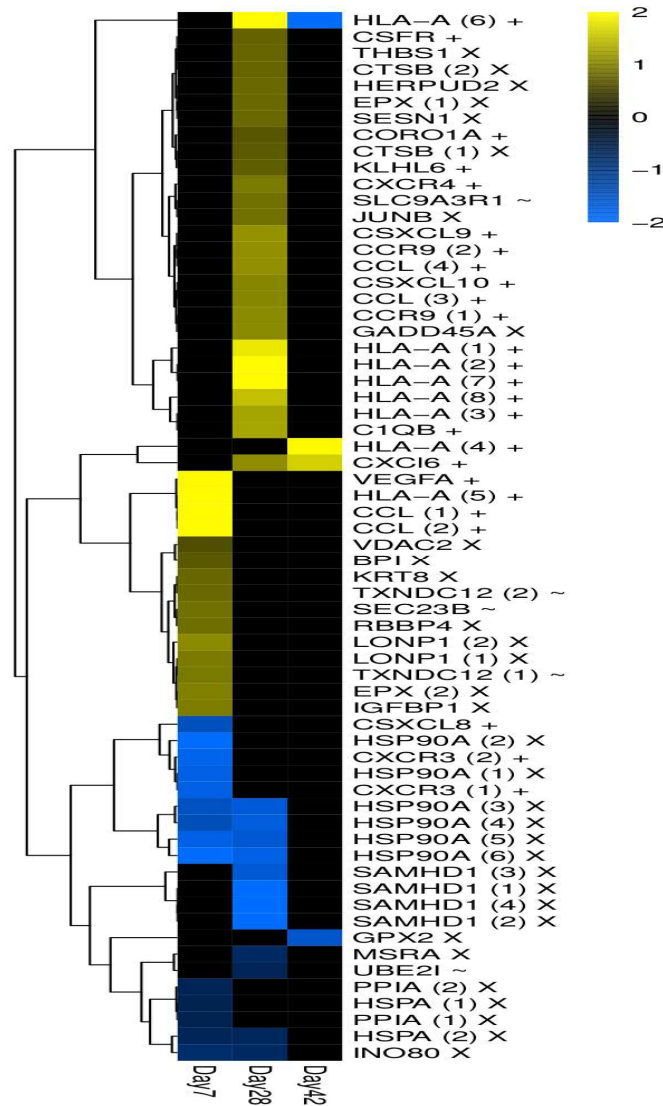


Figure 4.2 – The stress response heatmap: The heatmap displays all differentially regulated genes ($FDR \leq 0.05$) within the GO categories response to stress (GO:0006950), immune system process (GO:0002376), and homeostatic process (GO:0042592) for each multi-stressor time-point as compared to the control (7 days, 28 days, and 42 days). The fold change is \log_2 scaled with blue representing down-regulation, black indicating no significant regulation, and yellow representing up-regulation. Any changes with an absolute fold change greater than $\log_2(2)$ (abs 4X) are represented as the maximum. The gene symbol is included for each gene with a number within parentheses indicating an isoform of that gene. Each gene symbol also includes an additional symbol associating that gene with a GO category in the following manner: response to stress = “X”, immune system process = “+”, and homeostatic process = “~”.

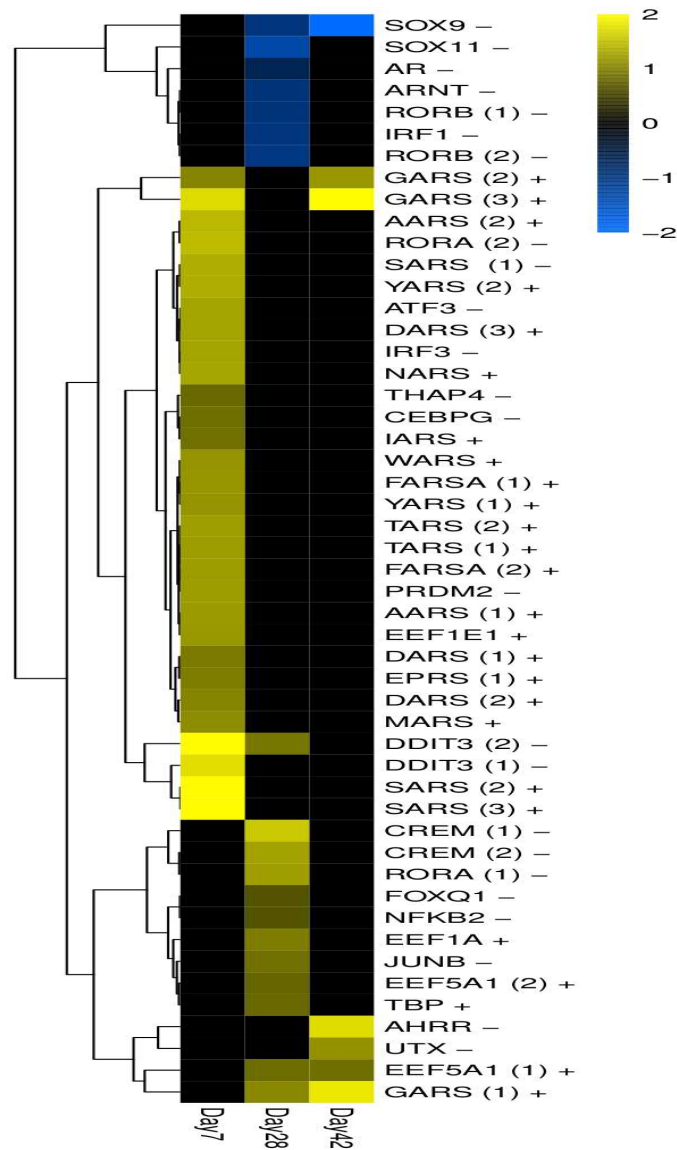


Figure 4.3 – Transcription and translation heatmap: The heatmap displays all differentially regulated genes (FDR ≤ 0.05) within the GO categories transcription (GO:0006351) and translation (GO:0006412) for each multi-stressor time-point as compared to the control (7 days, 28 days, and 42 days). The fold change is log₂ scaled with blue representing down-regulation, black indicating no significant regulation, and yellow representing up-regulation. Any changes with an absolute fold change greater than log₂(2) (abs 4X) are represented as the maximum. The gene symbol is included for each gene with a number within parentheses indicating an isoform of that gene. Each gene symbol also includes an additional symbol associating that gene with a GO category in the following manner: transcription = “-” and translation = “+”.

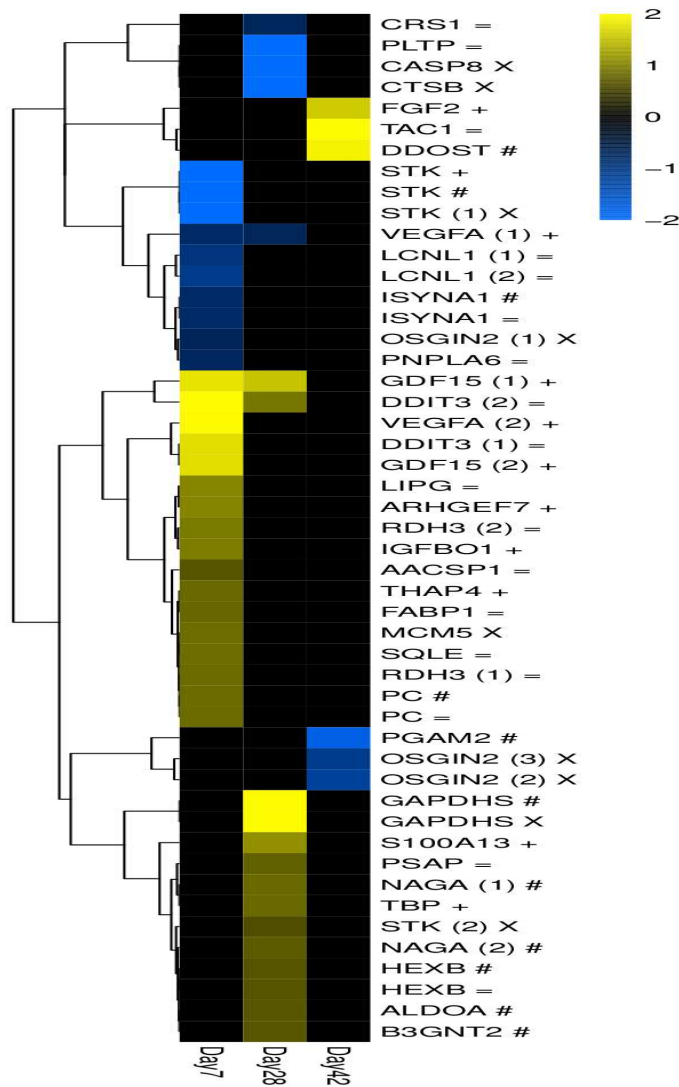


Figure 4.4 – Metabolism, proliferation and death heatmap: The heatmap displays all differentially regulated genes ($FDR \leq 0.05$) within the GO categories carbohydrate metabolic process (GO:0005975), lipid metabolic process (GO:0006629), cell proliferation (GO:0008283) cell death (GO:0008219), for each multi-stressor time-point as compared to the control (7 days, 28 days, and 42 days). The fold change is log₂ scaled with blue representing down-regulation, black indicating no significant regulation, and yellow representing up-regulation. Any changes with an absolute fold change greater than log₂(2) (abs 4X) are represented as the maximum. The gene symbol is included for each gene with a number within parentheses indicating an isoform of that gene. Each gene symbol also includes an additional symbol associating that gene with a GO category in the following manner: carbohydrate metabolic process = “#”, lipid metabolic process = “=”, cell proliferation = “+”, and cell death = “X”.

CHAPTER 5

A BRIEF COMPARATIVE ANALYSIS OF THE DIFFERENTIAL GENE
EXPRESSION OF *T. BERNACCHII*, *P. BORGREVINKI* AND *T. NEWNESI* UNDER
THE MULTI-STRESSOR CONDITION.

5.1 CONCLUSORY REMARKS

The Notothenioid species investigated throughout this research all demonstrate some form of cellular stress and cellular homeostatic response when exposed to a multi-stressor condition of increased temperature and $p\text{CO}_2$. Yet despite sharing a common phylogenetic lineage in an environment that necessitates the adaptation to extreme and stable cold (Chen et al., 2008; J. T. Eastman, 2005; J. Eastman, 1991, 1993; Ritchie et al., 1997), we observed considerable variation between the response of these three species. These variations are exhibited not only in the timing, duration and intensity of response; but also in the biological pathways that drive this response.

These responses are employed as representative of the physiological plasticity of these species when confronting a changing Southern Ocean, and thus provide insight into the adaptive ability of these species to changing conditions. The differential response of a particular species may indicate the impact of climate change on that species energetic costs, growth, and reproduction. To more comprehensively understand the long term ramifications of the conditions that notothenioids will face as climate change continues (Pachauri et al., 2014) the scope of tissues sampled, the life stages of samples collected, and the duration of exposure to the multi-stressor conditions will all need to be expanded and further analyzed.

Bearing in mind these limitations, the responses of the three notothenioids studied: *Trematomus bernacchii*, *Pagothenia borchgrevinki*, and *Trematomus newnesi*, are compared below to assess the variation in the cellular stress and homeostatic responses between these fish and how it may affect their success in a changing Southern Ocean.

5.2 OVERALL DIFFERENTIAL GENE EXPRESSION

An analysis of the overall differential expression at each time-point demonstrates drastic differences in the timing of differential expression between these species (Fig. 5.1). *T. bernacchii* and *P. borchgrevinki* demonstrate a robust initial response at 7 days; of the total 43,094 genes within the *T. bernacchii* reference transcriptome, 924 are differentially regulated (753 up- and 171 down-regulated; $FDR \leq 0.05$, $FC \geq 2$); and of the 46,176 genes within the *P. borchgrevinki* transcriptome 923 genes are differentially regulated (665 up- and 258 down-regulated; $FDR \leq 0.05$, $FC \geq 2$). On the other hand, *T. newnesi* exhibits 846 differentially expressed genes (607 up- and 239 down-regulated; $FDR \leq 0.05$, $FC \geq 2$) within its larger transcriptomic library of 53,587 genes.

However, the most drastic differences are seen after the initial cellular stress response as the transition to a long term cellular homeostatic response begins (Fig. 5.1). *T. bernacchii* exhibits almost no further response to the multi-stressor condition at 28 days and 56 days, with only 13 and 27 differentially expressed genes total found at each time-point respectively. This is in stark contrast to *T. newnesi* which experiences an increase in differential expression at 28 days (949 differentially expressed genes; 510 up- and 439 down-regulated; $FDR \leq 0.05$, $FC \geq 2$) that remains robust into the 42 day time-point days (451 differentially expressed genes; 270 up- and 181 down-regulated; $FDR \leq 0.05$, $FC \geq 2$). *P. borchgrevinki* demonstrates a decrease in differential expression at 28 days (372 differentially expressed genes; 221 up- and 151 down-regulated; $FDR \leq 0.05$, $FC \geq 2$), that then increases at 56 days (606 differentially expressed genes; 220 up- and 386 down-regulated; $FDR \leq 0.05$, $FC \geq 2$). To further grasp the significance of these

variations in differential expression a more detailed pathway based analysis at each time-point is conducted below.

5.3 THE INITIAL CELLULAR STRESS RESPONSE

All three species demonstrate a relatively robust differential gene expression response at 7 days to the multi-stressor treatment, but a closer examination reveals significant deviations in the pathways involved in this response (Fig. 5.2). *P. borchgrevinki* demonstrates a very robust up-regulation of immune system processes (28 genes, $FDR \leq 0.05$, $FC \geq 2$), with *T. bernacchii* not far behind (18 genes, $FDR \leq 0.05$, $FC \geq 2$); whereas as *T. newnesi* has a much more diminished response (6 genes, $FDR \leq 0.05$, $FC \geq 2$) (Fig. 5.2). The strong up-regulation of genes associated with the immune system is a common characteristic of the teleost stress response (Wendelaar Bonga, 1997). It is possible that this up-regulation of the immune system is to compensate for the overall lack of an inducible heat shock response in notothenioids (Place & Hofmann, 2005).

By lacking a robust heat shock response *bernacchii* (Buckley et al., 2004; G E Hofmann et al., 2000; Huth & Place, 2013), the up-regulation of immune system processes in conjunction with up-regulation of genes associated with response to stress may represent the primary mechanisms of the notothenioid cellular stress response. Among these species *T. bernacchii* exhibits the strongest up-regulation genes associated with response to stress (21 genes, $FDR \leq 0.05$, $FC \geq 2$) whereas *P. borchgrevinki* and *T. newnesi* both up-regulate 10 such genes. In that frame of mind *P. borchgrevinki* and *T. bernacchii* demonstrate a robust capability to respond to the multi-stressor condition, whereas *T. newnesi* does not (Fig. 5.2). This is further reinforced by the number of genes

associated with cell death that are up-regulated in *P. borchgrevinki* (10) and *T. bernacchii* (14) which is in stark contrast to *T. newnesi* (6) (Fig 5.2). Stressor conditions, such as the multi-stressor condition utilized in this study, are known to induce large scale cellular reorganization of gill tissue in teleosts via apoptosis (Nilsson, 2007); as such the cellular death observed may be indicative of reorganizational efforts.

5.4 A RESPONSE IN TRANSITION

Following the initial cellular stress response is a transition to a long term cellular homeostatic response (Kültz, 2005). The most immediately striking discovery at 28 days is that *T. bernacchii* demonstrates no differential expression in any of the six pathways analyzed, potentially indicating that this species has already reached a state of homeostasis under the multi-stressor conditions and requires no further differential regulation. *T. newnesi* appears to be in the midst of its cellular stress response with strong differential regulation of genes associated with response to stress (19 differentially expressed genes; 8 up- and 11 down-regulated; $FDR \leq 0.05$, $FC \geq 2$), immune system process (19 differentially expressed genes; 8 up- and 11 down-regulated; $FDR \leq 0.05$, $FC \geq 2$), cell death (4 differentially expressed genes; 2 up- and 2 down-regulated; $FDR \leq 0.05$, $FC \geq 2$), and cell growth (4 differentially expressed genes; 3 up- and 1 down-regulated; $FDR \leq 0.05$, $FC \geq 2$). Meanwhile, *P. borchgrevinki* is still up-regulating genes associated with response to stress (9) immune system process (9), and cell death (4); albeit at a lower level than at 7 days, which may be indicative of a winding down of the cellular stress response in preparation to transition to a more stable cellular homeostatic response.

5.5 THE CELLULAR HOMEOSTATIC RESPONSE

By the last time-point, 56 days for *P. borchgrevinki* and *T. bernacchii*, and 42 days for *T. newnesi*; the shift to a longer term state of cellular homeostasis is well underway. *T. bernacchii* exhibits a slight amount of differential expression, but at levels that continue to indicate that this species has likely acclimated to the multi-stressor condition (Fig. 5.4). This supports prior research that found that under these same conditions by the 56 day time-point *T. bernacchii* experienced a significant decrease in protein damage (Enzor & Place, 2014). While subtle changes in biological pathways and metabolism may influence *T. bernacchii*'s success over many generations, this fish exhibits an adaptive response that may well be superior to other notothenioid species and indicating that *T. bernacchii* may potentially benefit from slightly warmer temperatures.

In contrast to *T. bernacchii*, *P. borchgrevinki* continues to exhibit a robust response to the multi-stressor condition even at 56 days, although a shift from the up-regulation of genes associated with response to stress (2) and immune system processes (4) to the up-regulation of genes associated with metabolism (lipid 6, carbohydrate 4) has begun (Fig. 5.4). Furthermore, relatively substantial gene regulation is occurring in pathways associated with cell death and cell proliferation (Fig. 5.4). As a degree of acclimation to heat stressor conditions has been observed in this species (Bilyk et al., 2012; Enzor et al., 2013; Franklin et al., 2007; Esme Robinson & Davison, 2008), we may be observing *P. borchgrevinki* shifting its metabolism while continuing a robust cellular remodeling response in order to acclimate to the multi-stressor condition.

Of the three notothenioid species *T. newnesi* may be the least capable of acclimating to the multi-stressor condition and thus possible future conditions in the

Southern Ocean. *T. newnesi* has previously been shown to be the only fish among the three studied that still exhibits an increased resting metabolic rate over a longer time frame (Enzor et al., 2013), which may have significant effects on its fitness. Throughout this study *T. newnesi* has exhibited the most meager response and maintained that general level of response into the 42 day time-point. Furthermore, unlike *T. bernacchii* who exhibited a very robust initial response that rapidly diminishes, it appears less likely that the diminished response in *T. newnesi* is not a return to cellular homeostasis but rather evidence that *T. newnesi* is overwhelmed by the multi-stressor condition and unable to adequately respond.

It is clear that these three species *T. bernacchii*, *P. borchgrevinki* and *T. newnesi* exhibit variable responses to the multi-stressor condition of increased temperature and $p\text{CO}_2$ intended to simulate predicted future conditions in the Southern Ocean. The efforts herein have provided a basis from which others may continue this investigation to better determine how the fauna of the Southern Ocean will change as we confront global climate change.

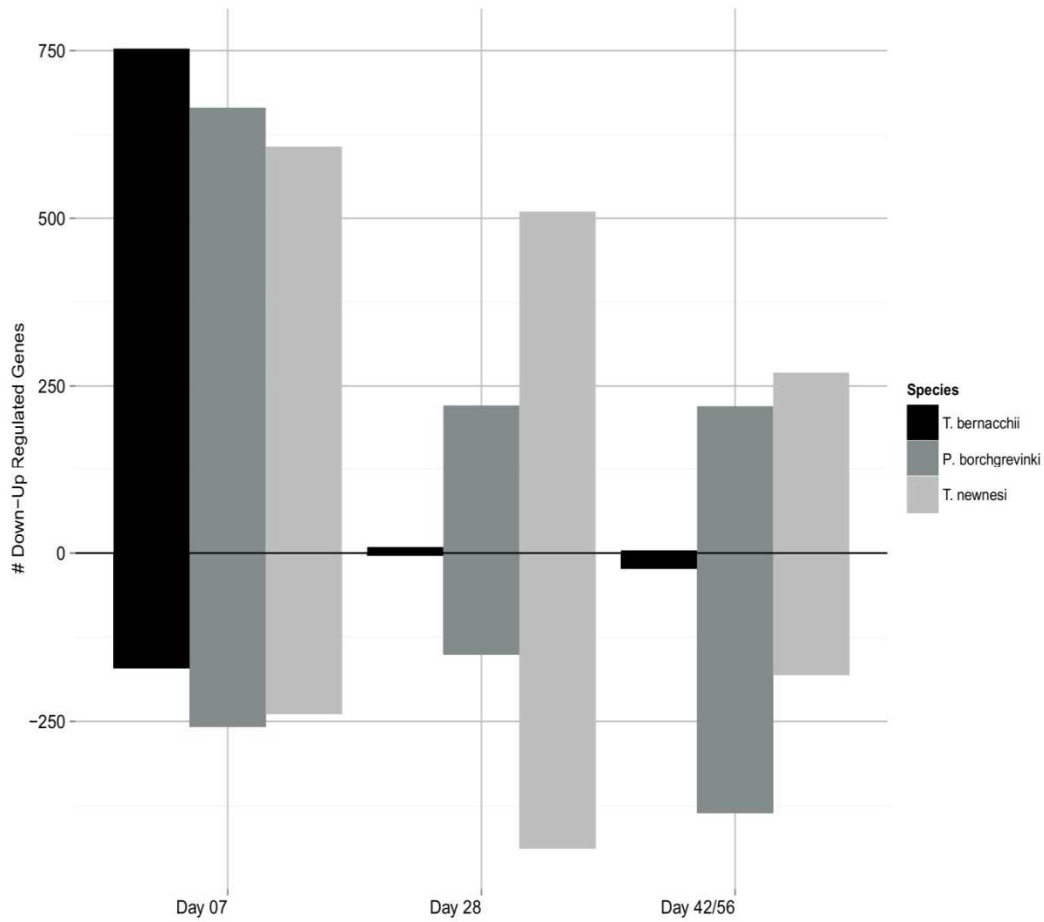


Figure 5.1. The total number of differentially expressed genes (FDR ≤ 0.05 , fold change ≥ 2) for *T. bernacchii* (black), *P. borchgrevinki* (dark grey), and *T. newnesi* (light grey) in the multi-stressor treatment as compared to the control at each time-point 7 days, 28 days and 42/56 days for *T. newnesi* and *T. bernacchii*/*P. borchgrevinki*, respectively. Bars above the x-axis indicate up-regulated genes; bars below the x-axis indicate down-regulated genes.

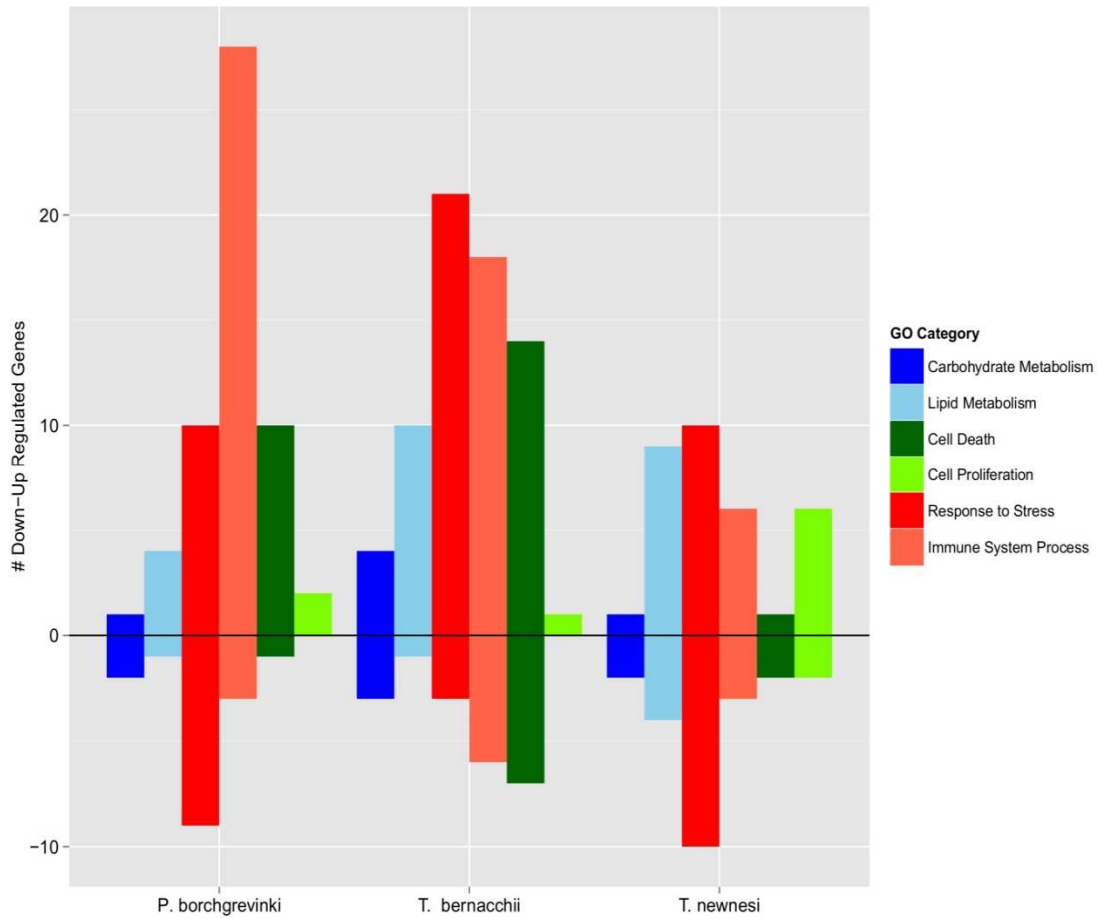


Figure 5.2. The total number of differentially expressed genes ($FDR \leq 0.05$, fold change ≥ 2) for *T. bernacchii*, *P. borchgrevinki*, and *T. newnesi* in the multi-stressor treatment as compared to the control at 7 days for the biological processes: carbohydrate metabolism (blue), lipid metabolism (light blue), cell death (dark green), cell proliferation (light green), response to stress (red), and immune system process (light red). Bars above the x-axis indicate up-regulated genes; bars below the x-axis indicate down-regulated genes.

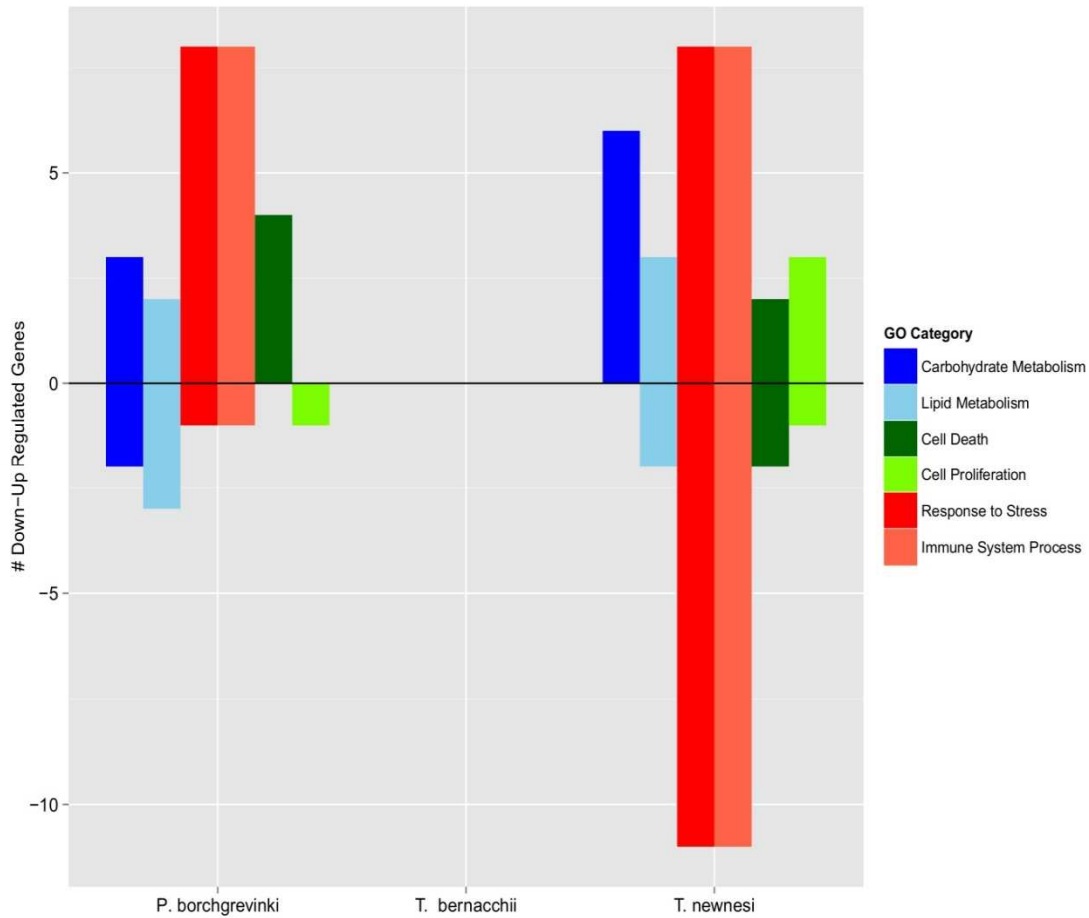


Figure 5.3. The total number of differentially expressed genes ($FDR \leq 0.05$, fold change ≥ 2) for *T. bernacchii*, *P. borchgrevinki*, and *T. newnesi* in the multi-stressor treatment as compared to the control at 28 days for the biological processes: carbohydrate metabolism (blue), lipid metabolism (light blue), cell death (dark green), cell proliferation (light green), response to stress (red), and immune system process (light red). Bars above the x-axis indicate up-regulated genes; bars below the x-axis indicate down-regulated genes.

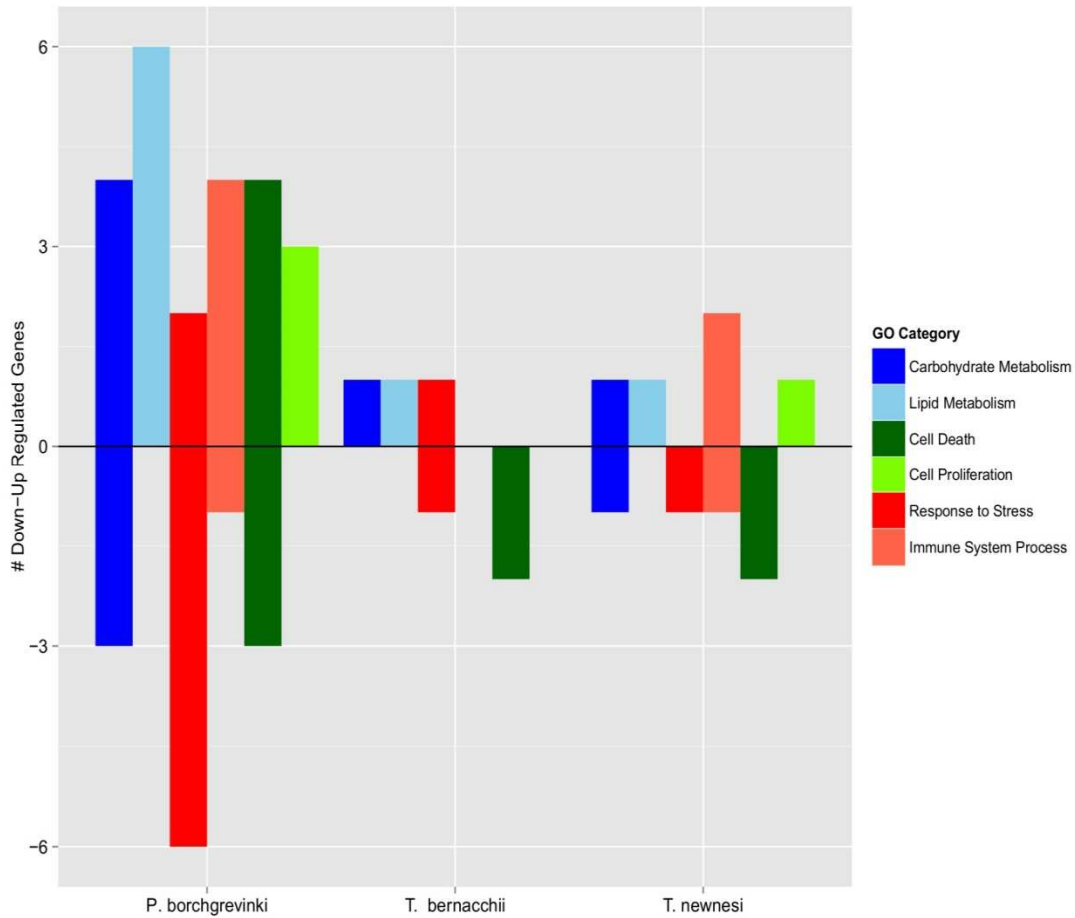


Figure 5.4. The total number of differentially expressed genes ($FDR \leq 0.05$, fold change ≥ 2) for *T. bernacchii*, *P. borchgrevinki*, and *T. newnesi* in the multi-stressor treatment as compared to the control at 42 (*T. newnesi*) or 56 (*T. bernacchii* and *P. borchgrevinki*) days for the biological processes: carbohydrate metabolism (blue), lipid metabolism (light blue), cell death (dark green), cell proliferation (light green), response to stress (red), and immune system process (light red). Bars above the x-axis indicate up-regulated genes; bars below the x-axis indicate down-regulated genes.

REFERENCES

- Adler, V., Yin, Z., Tew, K. D., & Ronai, Z. (1999). Role of redox potential and reactive oxygen species in stress signaling. *Oncogene*, *18*(45), 6104–6111. doi:10.1038/sj.onc.1203128
- Alexander, W. S., & Hilton, D. J. (2004). The role of suppressors of cytokine signaling (SOCS) proteins in regulation of the immune response. *Annual Review of Immunology*, *22*, 503–529. doi:10.1146/annurev.immunol.22.091003.090312
- Altschul, S., Gish, W., Miller, W., Myers, E., & Lipman, D. (1990). Basic local alignment search tool. *Journal of Molecular Biology*, *215*, 403–410.
- Andersson, U., Wang, H., Palmblad, K., Aveberger, a C., Bloom, O., Erlandsson-Harris, H., ... Tracey, K. J. (2000). High mobility group 1 protein (HMG-1) stimulates proinflammatory cytokine synthesis in human monocytes. *The Journal of Experimental Medicine*, *192*(4), 565–570. doi:10.1084/jem.192.4.565
- Arntz, W. E., Brey, T., & Gallardo, V. a. (1994). Antarctic zoobenthos. *Oceanography and Marine Biology, Vol 32: An Annual Review*, *32*(JANUARY), 241–304. Retrieved from <Go to ISI>://WOS:A1994BB49M00005
- Bae, J.-S., & Rezaie, a. R. (2011). Activated protein C inhibits high mobility group box 1 signaling in endothelial cells. *Blood*, *118*(14), 3952–3959. doi:10.1182/blood-2011-06-360701
- Bartelt-Kirbach, B., & Golenhofen, N. (2014). Reaction of small heat-shock proteins to different kinds of cellular stress in cultured rat hippocampal neurons. *Cell Stress & Chaperones*, *19*(1), 145–53. doi:10.1007/s12192-013-0452-9
- Basler, M., Kirk, C. J., & Groettrup, M. (2013). The immunoproteasome in antigen processing and other immunological functions. *Current Opinion in Immunology*, *25*(1), 74–80. doi:10.1016/j.coi.2012.11.004
- Basu, N., Todgham, a. E., Ackerman, P. a., Bibeau, M. R., Nakano, K., Schulte, P. M., & Iwama, G. K. (2002). Heat shock protein genes and their functional significance in fish. *Gene*, *295*(2), 173–183. doi:10.1016/S0378-1119(02)00687-X
- Ben-Zvi, T., Yaron, A., Gertler, A., & Monsonego-Ornan, E. (2006). Suppressors of cytokine signaling (SOCS) 1 and SOCS3 interact with and modulate fibroblast

growth factor receptor signaling. *Journal of Cell Science*, 119(Pt 2), 380–387.
doi:10.1242/jcs.02740

Bilyk, K. T., & Cheng, C. H. C. (2013). Model of gene expression in extreme cold - reference transcriptome for the high-Antarctic cryopelagic notothenioid fish *Pagothenia borchgrevinki*. *BMC Genomics*, 14(1), 634. doi:10.1186/1471-2164-14-634

Bilyk, K. T., & Cheng, C. H. C. (2014). RNA-seq analyses of cellular responses to elevated body temperature in the high Antarctic cryopelagic nototheniid fish *Pagothenia borchgrevinki*. *Marine Genomics*, 18, 163–171.
doi:10.1016/j.margen.2014.06.006

Bilyk, K. T., & DeVries, A. L. (2011). Heat tolerance and its plasticity in Antarctic fishes. *Comparative Biochemistry and Physiology - A Molecular and Integrative Physiology*, 158(4), 382–390. doi:10.1016/j.cbpa.2010.12.010

Bilyk, K. T., Evans, C. W., & DeVries, A. L. (2012). Heat hardening in Antarctic notothenioid fishes. *Polar Biology*, 35(9), 1447–1451. doi:10.1007/s00300-012-1189-0

BLAST2GO Command Line. (2014). Blast2GO Command Line (CLI) Please choose among the following options : Main Command Line Features. Retrieved from <http://www.blast2go.com/blast2gocli>

Bobulescu, I. A., & Moe, O. W. (2006). Na⁺/H⁺ Exchangers in Renal Regulation of Acid-Base Balance. *Seminars in Nephrology*, 26(5), 334–344.
doi:10.1016/j.semnephrol.2006.07.001

Bolger, A. M., Lohse, M., & Usadel, B. (2014). Trimmomatic: a flexible trimmer for Illumina sequence data. *Bioinformatics (Oxford, England)*.
doi:10.1093/bioinformatics/btu170

Broad Institute and the Hebrew University of Jerusalem. (2014). Identification and Analysis of Differentially Expressed Trinity Genes and Transcripts. Retrieved from http://trinityrnaseq.sourceforge.net/analysis/diff_expression_analysis.html

Buckley, B. a, Gracey, A. Y., & Somero, G. N. (2006). The cellular response to heat stress in the goby *Gillichthys mirabilis*: a cDNA microarray and protein-level analysis. *The Journal of Experimental Biology*, 209(Pt 14), 2660–2677.
doi:10.1242/jeb.02292

Buckley, B. a, Place, S. P., & Hofmann, G. E. (2004). Regulation of heat shock genes in isolated hepatocytes from an Antarctic fish, *Trematomus bernacchii*. *The Journal of Experimental Biology*, 207(Pt 21), 3649–3656. doi:10.1242/jeb.01219

- Buckley, B. a., & Somero, G. N. (2009). CDNA microarray analysis reveals the capacity of the cold-adapted Antarctic fish *Trematomus bernacchii* to alter gene expression in response to heat stress. *Polar Biology*, *32*(3), 403–415. doi:10.1007/s00300-008-0533-x
- Camacho, C., Coulouris, G., Avagyan, V., Ma, N., Papadopoulos, J., Bealer, K., & Madden, T. L. (2009). BLAST+: architecture and applications. *BMC Bioinformatics*, *10*, 421. doi:10.1186/1471-2105-10-421
- Carney Almroth, B., Asker, N., Wassmur, B., Rosengren, M., Jutfelt, F., Gräns, A., ... Sturve, J. (2015). Warmer water temperature results in oxidative damage in an Antarctic fish, the bald notothen. *Journal of Experimental Marine Biology and Ecology*, *468*, 130–137. doi:10.1016/j.jembe.2015.02.018
- Chen, Z., Cheng, C.-H. C., Zhang, J., Cao, L., Chen, L., Zhou, L., ... Chen, L. (2008). Transcriptomic and genomic evolution under constant cold in Antarctic notothenioid fish. *Proceedings of the National Academy of Sciences of the United States of America*, *105*(35), 12944–9. doi:10.1073/pnas.0802432105
- Cheng, C.-H. C., Cziko, P. a., & Evans, C. W. (2006). Nonhepatic origin of notothenioid antifreeze reveals pancreatic synthesis as common mechanism in polar fish freezing avoidance. *Proceedings of the National Academy of Sciences of the United States of America*, *103*(27), 10491–10496. doi:10.1073/pnas.0603796103
- Claiborne, J. B., Edwards, S. L., & Morrison-Shetlar, A. I. (2002). Acid-base regulation in fishes: Cellular and molecular mechanisms. *Journal of Experimental Zoology*, *293*(3), 302–319. doi:10.1002/jez.10125
- Clarke, A. (2011). Reproduction in the cold: Thorson revisited. *Invertebrate Reproduction & Development*, *1-3*, 175–183.
- Clarke, A., Johnston, N., Murphy, E., & Rogers, A. (2007). Introduction, Antarctic ecology from genes to ecosystems: the impact of climate change and the importance of scale. *Phil Trans R Soc B*, *362*(1477), 5–9.
- CLC Bio. (2012a). CLC Genomics Workbench: Version 5.1.5. CLC bio A/S Science Park Aarhus Finlandsgade 10–12 8200. Denmark: Aarhus N.
- CLC Bio. (2012b). *White paper on de novo assembly in CLC Assembly Cell 4.0. CLC bio Finlandsgade 10–12, 8200. Denmark: Aarhus N.*
- Cole, K. E., Strick, C. a, Paradis, T. J., Osborne, K. T., Loetscher, M., Gladue, R. P., ... Neote, K. (1998). Interferon-inducible T cell alpha chemoattractant (I-TAC): a novel non-ELR CXC chemokine with potent activity on activated T cells through selective high affinity binding to CXCR3. *The Journal of Experimental Medicine*, *187*(12), 2009–2021. doi:10.1084/jem.187.12.2009

- Conesa, A., Götz, S., García-Gómez, J. M., Terol, J., Talón, M., & Robles, M. (2005). Blast2GO: a universal tool for annotation, visualization and analysis in functional genomics research. *Bioinformatics (Oxford, England)*, *21*(18), 3674–6. doi:10.1093/bioinformatics/bti610
- Cooney, R. N. (2002). JAK / STAT PATHWAY, *17*(2), 83–90.
- Coppe, A., Agostini, C., Marino, I. a M., Zane, L., Bargelloni, L., Bortoluzzi, S., & Patarnello, T. (2013). Genome evolution in the cold: Antarctic icefish muscle transcriptome reveals selective duplications increasing mitochondrial function. *Genome Biology and Evolution*, *5*(1), 45–60. doi:10.1093/gbe/evs108
- Coppes Petricorena, Z. L., & Somero, G. N. (2007). Biochemical adaptations of notothenioid fishes: Comparisons between cold temperate South American and New Zealand species and Antarctic species. *Comparative Biochemistry and Physiology - A Molecular and Integrative Physiology*, *147*(3), 799–807. doi:10.1016/j.cbpa.2006.09.028
- Crockett, E. L., & Sidell, B. D. (1990). Some pathways of energy metabolism are cold adapted in Antarctic fishes. *Physiological Zoology*, *63*(3), 472–488. Retrieved from <Go to ISI>://ZOOREC:ZOOR12700014138
- D'Amico, S., Claverie, P., Collins, T., Georlett, e D., Gratia, E., Hoyoux, A., ... Gerday, C. (2002). Molecular basis of cold adaptation. *Phil Trans R Soc B*, (357), 917–925.
- Data Intensive Academic Grid. (n.d.). University of Maryland School of Medicine. Retrieved from <http://diagcomputing.org/>
- Davison, W., Axelsson, M., Forster, M., & Nilsson, S. (1995). Cardiovascular responses to acute handling stress in the Antarctic fish *Trematomus bernacchii* are not mediated by circulatory catecholamines. *Fish Physiology and Biochemistry*, *14*(3), 253–257.
- Davison, W., Franklin, C. E., & Carey, P. W. (1990). Oxygen uptake in the Antarctic teleost *Pagothenia borchgrevinki* . Limitations imposed by X-cell gill disease. *Fish Physiology and Biochemistry*, *8*(1), 69–77.
- Davison, W., Franklin, C. E., & McKenzie, J. C. (1994). Hematological-Changes in an Antarctic Teleost, *Trematomus-Bernacchii*, Following Stress. *Polar Biology*, *14*(7), 463–466.
- Detrich, H. W., Parker, S. K., Williams, J., Nogales, E., & Downing, K. H. (2000). Cold adaptation of microtubule assembly and dynamics. Structural interpretation of primary sequence changes present in the ??- and ??-tubulins of antarctic fishes. *Journal of Biological Chemistry*, *275*(47), 37038–37047. doi:10.1074/jbc.M005699200

- DeVries, a L., & Wohlschlag, D. E. (1969). Freezing resistance in some Antarctic fishes. *Science (New York, N.Y.)*, *163*(871), 1073–1075. doi:10.1126/science.163.3871.1073
- DeVries, A. L., & Cheng, C. C. (2005). Antifreeze proteins and organismal freezing avoidance in polar fishes. *Fish Physiology*, *22*, 155–201.
- Dickson, A. G., & Millero, F. J. (1987). A comparison of the equilibrium constants for the dissociation of carbonic acid in seawater media. *Deep Sea Research Part A. Oceanographic Research Papers*, *34*(10), 1733–1743.
- Eastman, J. (1991). Evolution and Diversification of Antarctic Notothenioid Fishes. *American Zoologist*, *31*(1), 93–109.
- Eastman, J. (1993). *Antarctic fish biology: evolution in a unique environment*. Academic Press, Inc.
- Eastman, J. T. (2005). The nature of the diversity of Antarctic fishes. *Polar Biology*, *28*(2), 93–107. doi:10.1007/s00300-004-0667-4
- Egginton, S. (1997). A comparison of the response to induced exercise in red- and white-blooded Antarctic fishes. *Journal of Comparative Physiology - B Biochemical, Systemic, and Environmental Physiology*, *167*(2), 129–134. doi:10.1007/s003600050056
- Egginton, S. (1998). CONTROL OF TISSUE BLOOD FLOW AT VERY LOW TEMPERATURES. *Journal of Thermal Biology*, *22*(6), 403–407.
- Ensembl: (n.d.). Zebrafish assembly and gene annotation. Retrieved from http://useast.ensembl.org/Danio_rerio/Info/Annotation#assembly
- Enzor, L. A., & Place, S. P. (2014). Is warmer better? Decreased oxidative damage in notothenioid fish after long-term acclimation to multiple stressors. *Journal of Experimental Biology*, *217*(18), 3301–3310. doi:10.1242/jeb.108431
- Enzor, L. A., & Place, S. P. (2015). In Review.
- Enzor, L. A., Zippay, M. L., & Place, S. P. (2013). High latitude fish in a high CO₂ world: Synergistic effects of elevated temperature and carbon dioxide on the metabolic rates of Antarctic notothenioids. *Comparative Biochemistry and Physiology. Part A, Molecular & Integrative Physiology*, *164*(1), 154–61. doi:10.1016/j.cbpa.2012.07.016
- Evans, D. H., Piermarini, P. M., & Choe, K. P. (2005). The Multifunctional Fish Gill : Dominant Site of Gas Exchange , Osmoregulation , Acid-Base Regulation , and Excretion of Nitrogenous Waste, 97–177. doi:10.1152/physrev.00050.2003.

- Fangue, N. a., O'Donnell, M. J., Sewell, M. a., Matson, P. G., MacPherson, A. C., & Hofmann, G. E. (2010). A laboratory-based, experimental system for the study of ocean acidification effects on marine invertebrate larvae. *Limnology and Oceanography: Methods*, 8, 441–452. doi:10.4319/lom.2010.8.441
- Feder, M. E., & Hofmann, G. E. (1999). HEAT-SHOCK PROTEINS, MOLECULAR CHAPERONES, AND THE STRESS RESPONSE: Evolutionary and Ecological Physiology. *Annual Review of Physiology*, 61(1), 243–282. doi:10.1146/annurev.physiol.61.1.243
- Ferreira de Carvalho, J., Poulain, J., Da Silva, C., Wincker, P., Michon-Coudouel, S., Dheilly, a, ... Ainouche, M. (2013). Transcriptome de novo assembly from next-generation sequencing and comparative analyses in the hexaploid salt marsh species *Spartina maritima* and *Spartina alterniflora* (Poaceae). *Heredity*, 110(2), 181–93. doi:10.1038/hdy.2012.76
- Fiuza, C., Bustin, M., Talwar, S., Tropea, M., Gerstenberger, E., Shelhamer, J. H., & Suffredini, A. F. (2003). Inflammation-promoting activity of HMGB1 on human microvascular endothelial cells. *Blood*, 101(7), 2652–2660. doi:10.1182/blood-2002-05-1300
- Forester, M. E., Franklin, C. E., H, T. H., & Daviso, W. (1987). The aerobic scope of Antarctic fish. *Pagothenia borchgrevinki* and its significance for metabolic cold adaptation. *Polar Biology*, 8, 155–159.
- Franklin, C. E., Davison, W., & Seebacher, F. (2007). Antarctic fish can compensate for rising temperatures: thermal acclimation of cardiac performance in *Pagothenia borchgrevinki*. *The Journal of Experimental Biology*, 210(Pt 17), 3068–3074. doi:10.1242/jeb.003137
- Fu, L., Niu, B., Zhu, Z., Wu, S., & Li, W. (2012). CD-HIT: accelerated for clustering the next-generation sequencing data. *Bioinformatics (Oxford, England)*, 28(23), 3150–2. doi:10.1093/bioinformatics/bts565
- Gattuso, J.-P., Bijma, J., Gehlen, M., Riebesell, U., & Turley, C. (2011). Ocean acidification: knowns, unknowns and perspectives. *Ocean Acidification*.
- Gene, T., Consortium, O., Gene, T., & Go, O. (2014). Gene Ontology Consortium: going forward. *Nucleic Acids Research*, 43(D1), D1049–D1056. doi:10.1093/nar/gku1179
- Gerdol, M., Buonocore, F., Scapigliati, G., & Pallavicini, A. (2015). Marine Genomics Analysis and characterization of the head kidney transcriptome from the Antarctic fish *Trematomus bernacchii* (Teleostea, Notothenioidea): A source for immune relevant genes. *Marine Genomics*, 2014–2016. doi:10.1016/j.margen.2014.12.005

- Gille, S. T. (2002). Warming of the Southern Ocean since the 1950s. *Science (New York, N.Y.)*, 295(5558), 1275–1277. doi:10.1126/science.1065863
- Gilmour, K. M., & Perry, S. F. (2009). Carbonic anhydrase and acid-base regulation in fish. *The Journal of Experimental Biology*, 212(Pt 11), 1647–1661. doi:10.1242/jeb.029181
- Gon, O., & Heemstra, P. (1990). *Fishes of the Southern Ocean*. Grahamstown, South Africa: J L B Smith Institute of Ichthyology.
- Grabherr, M. G., Haas, B. J., Yassour, M., Levin, J. Z., Thompson, D. a, Amit, I., ... Regev, A. (2011). Full-length transcriptome assembly from RNA-Seq data without a reference genome. *Nature Biotechnology*, 29(7), 644–52. doi:10.1038/nbt.1883
- Gracey, a Y., Troll, J. V, & Somero, G. N. (2001). Hypoxia-induced gene expression profiling in the euryoxic fish *Gillichthys mirabilis*. *Proceedings of the National Academy of Sciences of the United States of America*, 98(4), 1993–1998. doi:10.1073/pnas.98.4.1993
- Gutt, J., Bertler, N., Bracegirdle, T. J., Buschmann, A., Comiso, J., Hosie, G., ... Xavier, J. C. (2014). The Southern Ocean ecosystem under multiple climate change stresses - an integrated circumpolar assessment. *Global Change Biology*, n/a–n/a. doi:10.1111/gcb.12794
- Haas, B., Papanicolaou, A., Yassour, M., Grabherr, M., Blood, P., Bowden, J., ... Regev, A. (2013). De novo transcript sequence reconstruction from RNA-seq using the Trinity platform for reference generation and analysis. *Nat Protoc.*, Aug;8(8), 1494–412.
- Hara, T., & Tanegashima, K. (2014). CXCL14 antagonizes the CXCL12-CXCR4 signaling axis. *Biomolecular Concepts*, 5(2), 167–173. doi:10.1515/bmc-2014-0007
- Haschemeyer, A. E. V. (1982). L-leucine transport in liver of Antarctic fish in vivo at 0 degrees C. *American Journal of Physiology - Regulatory, Integrative and Comparative Physiology*, 242(3), 280–284.
- Haschemeyer, A. E. V., & Matthews, R. (1983). Temperature dependency of protein synthesis in isolated hepatocytes of Antarctic fish. *Physiol. Zool.*, 56, 78–87.
- Hatahet, F., & Ruddock, L. W. (2009). Protein disulfide isomerase: a critical evaluation of its function in disulfide bond formation. *Antioxidants & Redox Signaling*, 11(11), 2807–2850. doi:10.1089/ars.2009.2466
- Heisler, N. (1989). Parameters and methods in acid–base physiology. In C. R. Bridges & P. J. Butler (Eds.), *Techniques in Comparative Respiratory Physiology: an Environmental Approach* (pp. 305–332). Cambridge: Cambridge University Press.

- Hennet, T., Richter, C., & Peterhans, E. (1993). Tumour necrosis factor-alpha induces superoxide anion generation in mitochondria of L929 cells. *The Biochemical Journal*, 289 (Pt 2(1 993), 587–592.
- Hoegh-guldberg, O., & Bruno, J. F. (2010). The Impact of Climate Change on the World's Marine Ecosystems. *Science*, 328, 1523–1528. doi:10.1126/science.1189930
- Hofmann, G. E., Buckley, B. a, Airaksinen, S., Keen, J. E., & Somero, G. N. (2000). Heat-shock protein expression is absent in the antarctic fish *Trematomus bernacchii* (family Nototheniidae). *The Journal of Experimental Biology*, 203(Pt 15), 2331–2339.
- Hofmann, G. E., & Todgham, A. E. (2010). Living in the now: physiological mechanisms to tolerate a rapidly changing environment. *Annual Review of Physiology*, 72, 127–145. doi:10.1146/annurev-physiol-021909-135900
- Huth, T. J., & Place, S. P. (2013). De novo assembly and characterization of tissue specific transcriptomes in the emerald notothen, *Trematomus bernacchii*. *BMC Genomics*, 14, 805. doi:10.1186/1471-2164-14-805
- Huth, T. J., & Place, S. P. (2015a). *Pagothenia borchgrevinki* under multi-stressor conditions. *In Review*.
- Huth, T. J., & Place, S. P. (2015b). Transcriptome wide analyses reveal a sustained cellular stress response in the gill tissue of *Trematomus bernacchii* after long-term acclimation to multiple stressors. *In Review*.
- Jayasundara, N., Healy, T. M., & Somero, G. N. (2013). Effects of temperature acclimation on cardiorespiratory performance of the Antarctic notothenioid *Trematomus bernacchii*. *Polar Biology*, 36(7), 1047–1057. doi:10.1007/s00300-013-1327-3
- Jean-Pierre Gattuso, Kunshan Gao, Kitack Lee, B. R. and K. G. S. (2010). Guide to best practices for ocean acidification research and data reporting. *Sciences-New York*. Retrieved from http://epic.awi.de/epic/Main?ui_parameter=Export&page=abstract&action=export&entry_dn=LaR2009c&lang=en
- Jeffries, K. M., Hinch, S. G., Sierocinski, T., Pavlidis, P., & Miller, K. M. (2014). Transcriptomic responses to high water temperature in two species of Pacific salmon. *Evolutionary Applications*, 7(2), 286–300. doi:10.1111/eva.12119
- Ji, P., Liu, G., Xu, J., Wang, X., Li, J., Zhao, Z., ... Sun, X. (2012). Characterization of common carp transcriptome: Sequencing, de novo assembly, annotation and comparative genomics. *PLoS ONE*, 7(4), 9–11. doi:10.1371/journal.pone.0035152

- Jia, D., Jurkowska, R. Z., Zhang, X., Jeltsch, A., & Cheng, X. (2007). Structure of Dnmt3a bound to Dnmt3L suggests a model for de novo DNA methylation. *Nature*, *449*(7159), 248–51. doi:10.1038/nature06146
- Johnston, I., Calvo, J., Guderley, H., & D. (1998). Latitudinal variation in the abundance and oxidative capacities of muscle mitochondria in perciform fishes. *The Journal of Experimental Biology*, *201* (Pt 1), 1–12. Retrieved from <http://www.ncbi.nlm.nih.gov/pubmed/9390931>
- Jones, P., Binns, D., Chang, H.-Y., Fraser, M., Li, W., McAnulla, C., ... Hunter, S. (2014). InterProScan 5: genome-scale protein function classification. *Bioinformatics* (Oxford, England), *30*(9), 1236–40. doi:10.1093/bioinformatics/btu031
- Kadara, H., Schroeder, C. P., Lotan, D., Pisano, C., & Lotan, R. (2006). Induction of GDF-15/NAG-1/MIC-1 in human lung carcinoma cells by retinoid-related molecules and assessment of its role in apoptosis. *Cancer Biology and Therapy*, *5*(5), 518–522. doi:10.4161/cbt.5.5.2602
- Kanehisa, M., & Goto, S. (2000). KEGG: kyoto encyclopedia of genes and genomes. *Nucleic Acids Research*, *28*(1), 27–30. Retrieved from <http://www.pubmedcentral.nih.gov/articlerender.fcgi?artid=102409&tool=pmcentrez&rendertype=abstract>
- Karnaky, K. J. (1986). Structure and function of the chloride cell of *Fundulus heteroclitus* and other teleosts. *Integrative and Comparative Biology*, *26*(1), 209–224. doi:10.1093/icb/26.1.209
- Kennedy, D., Jäger, R., Mosser, D. D., & Samali, A. (2014). Regulation of apoptosis by heat shock proteins. *IUBMB Life*, *66*(5), 327–338. doi:10.1002/iub.1274
- Kiepe, D., Ciarmatori, S., Hoeflich, A., Wolf, E., & Tönshoff, B. (2005). Insulin-like growth factor (IGF)-I stimulates cell proliferation and induces IGF binding protein (IGFBP)-3 and IGFBP-5 gene expression in cultured growth plate chondrocytes via distinct signaling pathways. *Endocrinology*, *146*(7), 3096–3104. doi:10.1210/en.2005-0324
- Kriegenburg, F. (2012). Quality control of protein folding : an overview, *279*, 8457. doi:10.1111/j.1742-4658.2011.08457.x
- Kruidering, M., & Evan, G. I. (2000). Caspase-8 in apoptosis: the beginning of “the end”? *IUBMB Life*, *50*(2), 85–90. doi:10.1080/713803693
- Kültz, D. (2005). Molecular and evolutionary basis of the cellular stress response. *Annual Review of Physiology*, *67*(1), 225–257. doi:10.1146/annurev.physiol.67.040403.103635

- Langmead, B., & Salzberg, S. L. (2012). Fast gapped-read alignment with Bowtie 2. *Nature Methods*, 9(4), 357–9. doi:10.1038/nmeth.1923
- Lee, S.-O., Cho, K., Cho, S., Kim, I., Oh, C., & Ahn, K. (2010). Protein disulphide isomerase is required for signal peptide peptidase-mediated protein degradation. *The EMBO Journal*, 29(2), 363–375. doi:10.1038/emboj.2009.359
- Li, B., & Dewey, C. N. (2011). RSEM: accurate transcript quantification from RNA-Seq data with or without a reference genome. *BMC Bioinformatics*, 12, 323. doi:10.1186/1471-2105-12-323
- Liebermann, D. a., & Hoffman, B. (2008). Gadd45 in stress signaling. *Journal of Molecular Signaling*, 3, 15. doi:10.1186/1750-2187-3-15
- Livermore, R., Nankivell, A., Eagles, G., & Morris, P. (2005). Paleogene opening of Drake Passage. *Earth and Planetary Science Letters*, 236(1-2), 459–470. doi:10.1016/j.epsl.2005.03.027
- Logacheva, M. D., Kasianov, A. S., Vinogradov, D. V, Samigullin, T. H., Gelfand, M. S., Makeev, V. J., & Penin, A. a. (2011). De novo sequencing and characterization of floral transcriptome in two species of buckwheat (*Fagopyrum*). *BMC Genomics*, 12(1), 30. doi:10.1186/1471-2164-12-30
- Logan, C. a., & Somero, G. N. (2011). Effects of thermal acclimation on transcriptional responses to acute heat stress in the eurythermal fish *Gillichthys mirabilis* (Cooper). *American Journal of Physiology. Regulatory, Integrative and Comparative Physiology*, 300(6), R1373–R1383. doi:10.1152/ajpregu.00689.2010
- Lucassen, M., Schmidt, a, Eckerle, L. G., & Pörtner, H.-O. (2003). Mitochondrial proliferation in the permanent vs. temporary cold: enzyme activities and mRNA levels in Antarctic and temperate zoarcid fish. *American Journal of Physiology. Regulatory, Integrative and Comparative Physiology*, 285(6), R1410–R1420. doi:10.1152/ajpregu.00111.2003
- Lushchak, V. I. (2011). Environmentally induced oxidative stress in aquatic animals. *Aquatic Toxicology*, 101(1), 13–30. doi:10.1016/j.aquatox.2010.10.006
- MacRae, T. H. (2000). Structure and function of small heat shock/alpha-crystallin proteins: established concepts and emerging ideas. *Cellular and Molecular Life Sciences : CMLS*, 57(6), 899–913.
- Mehrbach, C., Culberson, C. H., Hawley, J. E., & Pytkowicz, R. M. (1973). Measurement of the apparent dissociation constants of carbonic acid in seawater at atmospheric pressure. *Limnology and Oceanography*, 18(6), 897–907. doi:10.4319/lo.1973.18.6.0897

- Miyazaki, E., Sakaguchi, M., Wakabayashi, S., Shigekawa, M., & Mihara, K. (2001). NHE6 Protein Possesses a Signal Peptide Destined for Endoplasmic Reticulum Membrane and Localizes in Secretory Organelles of the Cell. *Journal of Biological Chemistry*, 276(52), 49221–49227. doi:10.1074/jbc.M106267200
- Mortazavi, A., Williams, B. a, McCue, K., Schaeffer, L., & Wold, B. (2008). Mapping and quantifying mammalian transcriptomes by RNA-Seq. *Nature Methods*, 5(7), 621–628. doi:10.1038/nmeth.1226
- Narberhaus, F. (2002). α -Crystallin-Type Heat Shock Proteins : Socializing Minichaperones in the Context of a Multichaperone Network α -Crystallin-Type Heat Shock Proteins : Socializing Minichaperones in the Context of a Multichaperone Network. *Society*, 66(1), 64–93. doi:10.1128/MMBR.66.1.64
- Nilsson, G. E. (2007). Gill remodeling in fish--a new fashion or an ancient secret? *The Journal of Experimental Biology*, 210(Pt 14), 2403–2409. doi:10.1242/jeb.000281
- Novak, A. E., Jost, M. C., Lu, Y., Taylor, A. D., Zakon, H. H., & Ribera, A. B. (2006). Gene duplications and evolution of vertebrate voltage-gated sodium channels. *Journal of Molecular Evolution*, 63(2), 208–221. doi:10.1007/s00239-005-0287-9
- O'Brien, K. M., & Sidell, B. D. (2000). The interplay among cardiac ultrastructure, metabolism and the expression of oxygen-binding proteins in Antarctic fishes. *The Journal of Experimental Biology*, 203(Pt 8), 1287–1297.
- O'Donnell, M. J., Hammond, L. M., & Hofmann, G. E. (2009). Predicted impact of ocean acidification on a marine invertebrate: Elevated CO₂ alters response to thermal stress in sea urchin larvae. *Marine Biology*, 156(3), 439–446. doi:10.1007/s00227-008-1097-6
- Pachauri, R. K., Meyer, L., Van Ypersele, J.-P., Brinkman, S., Van Kesteren, L., Leprince-Ringuet, N., & Van Boxmeer, F. (2014). *Climate Change 2014 Synthesis Report The Core Writing Team Core Writing Team Technical Support Unit for the Synthesis Report. Russian Federation), Hoesung Lee (Republic of Korea) Scott B. Power (Australia) N.H. Ravindranath (India).*
- Peck, L. S., Barnes, D. K. a., & Willmott, J. (2005). Responses to extreme seasonality in food supply: diet plasticity in Antarctic brachiopods. *Marine Biology*, 147(2), 453–463. doi:10.1007/s00227-005-1591-z
- Peck, L. S., Clark, M. S., Morley, S. a., Massey, A., & Rossetti, H. (2009). Animal temperature limits and ecological relevance: Effects of size, activity and rates of change. *Functional Ecology*, 23(2), 248–256. doi:10.1111/j.1365-2435.2008.01537.x

- Peck, L. S., Webb, K. E., & Bailey, D. M. (2004). Extreme sensitivity of biological function to temperature in Antarctic marine species, 625–630. doi:10.1111/j.0269-8463.2004.00903.x
- Perry, S. F., & Gilmour, K. M. (2006). Acid-base balance and CO₂ excretion in fish: Unanswered questions and emerging models. *Respiratory Physiology and Neurobiology*, 154(1-2), 199–215. doi:10.1016/j.resp.2006.04.010
- Pierson, P. M., Lamers, a., Flik, G., & Mayer-Gostan, N. (2004). The stress axis, stanniocalcin, and ion balance in rainbow trout. *General and Comparative Endocrinology*, 137, 263–271. doi:10.1016/j.ygcen.2004.03.010
- Pittsburgh Supercomputing Center - Blacklight Supercomputer. (2014). Blacklight Pittsburgh Supercomputing Center - Blacklight System Configuration. Retrieved from <https://www.psc.edu/index.php/computing-resources/blacklight#arch>
- Place, S. P., & Hofmann, G. E. (2005). Constitutive expression of a stress-inducible heat shock protein gene, hsp70, in phylogenetically distant Antarctic fish. *Polar Biology*, 28(4), 261–267. doi:10.1007/s00300-004-0697-y
- Place, S. P., O'Donnell, M. J., & Hofmann, G. E. (2008). Gene expression in the intertidal mussel *Mytilus californianus*: Physiological response to environmental factors on a biogeographic scale. *Marine Ecology Progress Series*, 356, 1–14. doi:10.3354/meps07354
- Place, S. P., Zippay, M. L., & Hofmann, G. E. (2004). Constitutive roles for inducible genes: evidence for the alteration in expression of the inducible hsp70 gene in Antarctic notothenioid fishes. *American Journal of Physiology. Regulatory, Integrative and Comparative Physiology*, 287(2), R429–R436. doi:10.1152/ajpregu.00223.2004
- Podrabsky, J. E., & Somero, G. N. (2004). Changes in gene expression associated with acclimation to constant temperatures and fluctuating daily temperatures in an annual killifish *Austrofundulus limnaeus*. *The Journal of Experimental Biology*, 207(Pt 13), 2237–2254. doi:10.1242/jeb.01016
- Pörtner, H. O., Lucassen, M., & Storch, D. (2005). Metabolic Biochemistry: Its Role in Thermal Tolerance and in the Capacities of Physiological and Ecological Function. *Fish Physiology*. doi:10.1016/S1546-5098(04)22003-9
- Pörtner, H., Peck, L., & Somero, G. (2006). Thermal limits and adaptation in marine Antarctic ectotherms: an integrative view. *Phil Trans R Soc B*, (362), 2233.
- Portner, H.-O., & Knust, R. (2007). Climate Change Affects Marine Fishes Through the Oxygen Limitation of Thermal Tolerance. *Science*, 315, 95–97.

- Prunet, P., Cairns, M. T., Winberg, S., & Pottinger, T. G. (2008). Functional genomics of stress responses in fish, (September 2015). doi:10.1080/10641260802341838
- Pucciarelli, S., Parker, S. K., Detrich, H. W., & Melki, R. (2006). Characterization of the cytoplasmic chaperonin containing TCP-1 from the Antarctic fish *Notothenia coriiceps*. *Extremophiles*, *10*(6), 537–549. doi:10.1007/s00792-006-0528-x
- R Core Team. (2013). R: A language and environment for statistical computing. Vienna, Austria.: R Foundation for Statistical Computing,. Retrieved from URL <http://www.R-project.org/>
- Ritchie, P. a, Lavoué, S., & Lecointre, G. (1997). Molecular phylogenetics and the evolution of antarctic notothenioid fishes. *Comparative Biochemistry and Physiology. Part A, Physiology*, *118*(4), 1009–25. Retrieved from <http://www.ncbi.nlm.nih.gov/pubmed/9505416>
- Robbins, L. L., Hansen, M. E., Kleypas, J. a, & Meylan, S. C. (2010). CO2calc - a user-friendly seawater carbon calculator for Windows, Mac OS X and iOS (iPhone). *U.S. Geological Survey Open-File Report 2010-1280*, 17.
- Robertson, M. J. (2010). Role of chemokines in the biology of natural killer cells. *Current Topics in Microbiology and Immunology*, *341*(1), 37–58. doi:10.1007/82-2010-20
- Robinson, E., & Davison, W. (2008). Antarctic fish can survive prolonged exposure to elevated temperatures. *Journal of Fish Biology*, *73*(7), 1676–1689. doi:10.1111/j.1095-8649.2008.02041.x
- Robinson, E., & Davison, W. (2008). The Antarctic notothenioid fish *Pagothenia borchgrevinki* is thermally flexible: Acclimation changes oxygen consumption. *Polar Biology*, *31*(3), 317–326. doi:10.1007/s00300-007-0361-4
- Robinson, M. D., McCarthy, D. J., & Smyth, G. K. (2010). edgeR: a Bioconductor package for differential expression analysis of digital gene expression data. *Bioinformatics (Oxford, England)*, *26*(1), 139–40. doi:10.1093/bioinformatics/btp616
- Rogers, A. D., Murphy, E. J., Johnston, N. M., & Clarke, A. (2007). Introduction. Antarctic ecology: from genes to ecosystems. Part 2. Evolution, diversity and functional ecology. *Philosophical Transactions of the Royal Society of London. Series B, Biological Sciences*, *362*(1488), 2187–9. doi:10.1098/rstb.2007.2135
- Rosa, R., & Seibel, B. a. (2008). Synergistic effects of climate-related variables suggest future physiological impairment in a top oceanic predator. *Proceedings of the National Academy of Sciences of the United States of America*, *105*(52), 20776–20780. doi:10.1073/pnas.0806886105

- Saunders, L. R., & Barber, G. N. (2003). The dsRNA binding protein family: critical roles, diverse cellular functions. *The FASEB Journal : Official Publication of the Federation of American Societies for Experimental Biology*, *17*(9), 961–983. doi:10.1096/fj.02-0958rev
- Schulte, P. M. (2007). Responses to environmental stressors in an estuarine fish: Interacting stressors and the impacts of local adaptation. *Journal of Thermal Biology*, *32*(3), 152–161. doi:10.1016/j.jtherbio.2007.01.012
- Schulze-Osthoff, K., Bakker, A. C., Vanhaesebroeck, B., Beyaert, R., Jacob, W. a., & Fiers, W. (1992). Cytotoxic activity of tumor necrosis factor is mediated by early damage of mitochondrial functions: Evidence for the involvement of mitochondrial radical generation. *Journal of Biological Chemistry*, *267*(8), 5317–5323.
- Schulze-Osthoff, K., Beyaert, R., Vandevoorde, V., Haegeman, G., & Fiers, W. (1993). Depletion of the mitochondrial electron transport abrogates the cytotoxic and gene-inductive effects of TNF. *The EMBO Journal*, *12*(8), 3095–3104.
- Seebacher, F., Davison, W., Lowe, C. J., & Franklin, C. E. (2005). A falsification of the thermal specialization paradigm: compensation for elevated temperatures in Antarctic fishes. *Biology Letters*, *1*(2), 151–154. doi:10.1098/rsbl.2004.0280
- Shagin, D. a, Rebrikov, D. V, Kozhemyako, V. B., Altshuler, I. M., Shcheglov, A. S., Zhulidov, P. a, ... Lukyanov, S. (2002). A Novel Method for SNP Detection Using a New Duplex-Specific Nuclease From Crab Hepatopancreas A Novel Method for SNP Detection Using a New Duplex-Specific Nuclease From Crab Hepatopancreas, 1935–1942. doi:10.1101/gr.547002
- Shin, S. C., Kim, S. J., Lee, J. K., Ahn, D. H., Kim, M. G., Lee, H., ... Park, H. (2012). Transcriptomics and comparative analysis of three antarctic notothenioid fishes. *PloS One*, *7*(8), e43762. doi:10.1371/journal.pone.0043762
- Sidell, B. D., Crockett, E. L., & Driedzic, W. R. (1995). Antarctic fish tissues preferentially catabolize monoenoic fatty acids. *Journal of Experimental Zoology*, *271*(2), 73–81. doi:10.1002/jez.1402710202
- Skoko, D., Wong, B., Johnson, R. C., & Marko, J. F. (2004). Micromechanical analysis of the binding of DNA-bending proteins HMGB1, NHP6A, and HU reveals their ability to form highly stable DNA-protein complexes. *Biochemistry*, *43*(43), 13867–13874. doi:10.1021/bi048428o
- Sleadd, I. M., Lee, M., Hassumani, D. O., Stecyk, T. M. a, Zeitz, O. K., & Buckley, B. a. (2014). Sub-lethal heat stress causes apoptosis in an Antarctic fish that lacks an inducible heat shock response. *Journal of Thermal Biology*, *44*(1), 119–125. doi:10.1016/j.jtherbio.2014.06.007

- Solomon, S., Qin, D., Manning, M., Chen, Z., Marquis, M., Averyt, K. B., ... Miller, H. L. (2007). Contribution of Working Group III to the fourth assessment report of the Intergovernmental Panel on Climate Change. Climate Change 2007: The Physical Science Basis. Retrieved from <http://philpapers.org/rec/METCOW>
- Somero, G. N. (2010). The physiology of climate change: how potentials for acclimatization and genetic adaptation will determine “winners” and “losers”. *The Journal of Experimental Biology*, 213(6), 912–920. doi:10.1242/jeb.037473
- Somero, G. N., & DeVries, A. L. (1967). Temperature tolerance of some Antarctic fishes. *Science*, 156, 257–258.
- Sreedhar, A. S., & Csermely, P. (2004). Heat shock proteins in the regulation of apoptosis: new strategies in tumor therapy: a comprehensive review. *Pharmacology & Therapeutics*, 101(3), 227–257. doi:10.1016/j.pharmthera.2003.11.004
- Stenkamp, D. L., Cunningham, L. L., Raymond, P. a, & Gonzalez-Fernandez, F. (1998). Novel expression pattern of interphotoreceptor retinoid-binding protein (IRBP) in the adult and developing zebrafish retina and RPE. *Molecular Vision*, 4(July), 26.
- Texas Advanced Computing Center - Stampede Super Computer. (2014). System Overview. Retrieved from <https://www.tacc.utexas.edu/user-services/user-guides/stampede-user-guide>
- Tillmann, P. (2011). Climate Change Effects and Adaptation Approaches in Marine and Coastal Ecosystems of the North Pacific Landscape Conservation Cooperative Region, (August), 279. Retrieved from http://pajk.arh.noaa.gov/Articles/articles/NPLCC_MarineClimateEffects.pdf
- Tomalty, K. M. H., Meek, M. H., Stephens, M. R., Rincon, G., Fangue, N. a., May, B. P., & Baerwald, M. R. (2015). Transcriptional Response to Acute Thermal Exposure in Juvenile Chinook Salmon Determined by RNAseq. *G3: Genes|Genomes|Genetics*, 5(July), 1335–1349. doi:10.1534/g3.115.017699
- Walther, G., Post, E., Convey, P., Menzel, A., Parmesan, C., Beebee, T. J. C., ... Bairlein, F. (2002). Ecological responses to recent climate change. *Nature*, 416, 389–395.
- Weber, C., Weber, K. S. C., Klier, C., Gu, S., Wank, R., Horuk, R., ... Dc, W. (2011). Specialized roles of the chemokine receptors CCR1 and CCR5 in the recruitment of monocytes and T H 1-like / CD45RO + T cells Specialized roles of the chemokine receptors CCR1 and CCR5 in the recruitment of monocytes and T H 1-like / CD45RO 2 T cells, 97(4), 1144–1146. doi:10.1182/blood.V97.4.1144

- Wendelaar Bonga, S. E. (1997). The stress response in fish. *Physiological Reviews*, 77(3), 591–625. doi:stress physiologie comportement cortisol cerveau hypophyse catecholamine osmoregulation branchie
- Windisch, H. S., Kathover, R., Portner, H.-O., Frickenhaus, S., & Lucassen, M. (2011). Thermal acclimation in Antarctic fish: transcriptomic profiling of metabolic pathways. *AJP: Regulatory, Integrative and Comparative Physiology*, 301(5), R1453–R1466. doi:10.1152/ajpregu.00158.2011
- Windisch, H. S., Lucassen, M., & Frickenhaus, S. (2012). Evolutionary force in confamilial marine vertebrates of different temperature realms: adaptive trends in zoarcid fish transcriptomes. *BMC Genomics*, 13(1), 549. doi:10.1186/1471-2164-13-549
- Wuyts, A., Van Osselaer, N., Haelens, A., Samson, I., Herdewijn, P., Ben-Baruch, A., ... Van Damme, J. (1997). Characterization of synthetic human granulocyte chemotactic protein 2: Usage of chemokine receptors CXCR1 and CXCR2 and in vivo inflammatory properties. *Biochemistry*, 36(9), 2716–2723. doi:10.1021/bi961999z
- Xia, J. H., Liu, P., Liu, F., Lin, G., Sun, F., Tu, R., & Yue, G. H. (2013). Analysis of stress-responsive transcriptome in the intestine of Asian Seabass (*Lateolabrax japonicus*) using RNA-seq. *DNA Research*, 20(5), 449–460. doi:10.1093/dnares/dst022
- Xu, L., Chen, H., Hu, X., Zhang, R., Zhang, Z., & Luo, Z. W. (2006). Average gene length is highly conserved in prokaryotes and eukaryotes and diverges only between the two kingdoms. *Molecular Biology and Evolution*, 23(6), 1107–1108. doi:10.1093/molbev/msk019
- Xu, Q., Cheng, C. H. C., Hu, P., Ye, H., Chen, Z., Cao, L., ... Chen, L. (2008). Adaptive evolution of hepcidin genes in antarctic notothenioid fishes. *Molecular Biology and Evolution*, 25(6), 1099–1112. doi:10.1093/molbev/msn056
- Ye, J., Fang, L., Zheng, H., Zhang, Y., Chen, J., Zhang, Z., ... Wang, J. (2006). WEGO: a web tool for plotting GO annotations. *Nucleic Acids Research*, 34(Web Server issue), W293–7. doi:10.1093/nar/gkl031
- Young, J. C., Moarefi, I., & Ulrich Hartl, F. (2001). Hsp90: A specialized but essential protein-folding tool. *Journal of Cell Biology*, 154(2), 267–273. doi:10.1083/jcb.200104079
- Zhao, Q.-Y., Wang, Y., Kong, Y.-M., Luo, D., Li, X., & Hao, P. (2011). Optimizing de novo transcriptome assembly from short-read RNA-Seq data: a comparative study. *BMC Bioinformatics*, 12(Suppl 14), S2. doi:10.1186/1471-2105-12-S14-S2

Zhulidov, P. a, Bogdanova, E. a, Shcheglov, A. S., Vagner, L. L., Khaspekov, G. L., Kozhemyako, V. B., ... Shagin, D. a. (2004). Simple cDNA normalization using kamchatka crab duplex-specific nuclease. *Nucleic Acids Research*, 32(3), e37.
doi:10.1093/nar/gnh031

APPENDIX A: PERMISSION TO REPRINT CHAPTER 1

We hereby assert that the reprinting of this article is in compliance with the terms of the BioMed Central Open Access Charter as set forth below. The research article as included in Chapter 1 contains no substantive changes or errors and is properly attributed.

BioMed Central Open Access Charter

Every peer-reviewed research article appearing in any journal published by BioMed Central is 'open access', meaning that:

The article is universally and freely accessible via the Internet, in an easily readable format and deposited immediately upon publication, without embargo, in an agreed format - current preference is XML with a declared DTD - in at least one widely and internationally recognized open access repository (such as PubMed Central).

The author(s) or copyright owner(s) irrevocably grant(s) to any third party, in advance and in perpetuity, the right to use, reproduce or disseminate the research article in its entirety or in part, in any format or medium, provided that no substantive errors are introduced in the process, proper attribution of authorship and correct citation details are given, and that the bibliographic details are not changed. If the article is reproduced or disseminated in part, this must be clearly and unequivocally indicated.

URL: <http://www.biomedcentral.com/about/charter>